CEREBROVASCULAR INFLUENCE ON BRAIN AND COGNITIVE AGING

BY

CHIN HONG TAN

DISSERTATION

Submitted in partial fulfillment of the requirements
for the degree of Doctor of Philosophy in Psychology
in the Graduate College of the
University of Illinois at Urbana-Champaign, 2016

Urbana, Illinois

Doctoral Committee:

Professor Monica Fabiani, Chair & Director of Research
Professor Gabriele Gratton
Professor Arthur F. Kramer
Associate Professor Brad Sutton
Assistant Professor Florin Dolcos

ABSTRACT

A dysfunctional cerebrovascular system can result in severe adverse effects on brain health and cognitive aging. Recently, Fabiani et al., (2014) introduced a novel non-invasive approach of quantifying cerebrovascular health using diffuse optical imaging in a sample of older adults. This method is based on the estimation of the arterial pulse across the whole scalp. From these estimates, three indices reflecting arterial health can be extracted: pulse amplitude, arterial compliance and pulse transit time. In their initial paper, Fabiani et al. (2014) showed that, in older adults, these indices are correlated with important variables, including volumetric changes in the brain and in psychometric measures. In this thesis, Chapter 1 discusses the importance of cerebrovascular health in brain and cognitive aging followed by a brief introduction to diffusive optical methods and its advantages in quantifying cerebrovascular health.

Chapter 2 contains a series of two experiments examining how changes in pulse amplitude reflect changes in cerebrovascular tone (i.e. vasodilation and vasoconstriction) of cerebral blood vessels. We used both a physiological voluntary breath holding task to track generalized changes and a cognitive Sternberg task to track localized changes in cerebrovascular tone. Further, we found that an index of cerebrovascular reactivity derived from the breath holding task was associated with age and cognitive functioning. These results indicate that cerebral pulse amplitude works well as a proxy measure of blood pressure in the brain.

Chapter 3 contains a replication and extension of the work presented in Fabiani et al., (2014) to investigate changes in pulse amplitude and arterial compliance in a group of younger and older adults. The study also contains methodological improvements whereby we employed a denser optical recording array and increased data collection time substantially in order improve signal to noise ratio. The results indicate strong reliability for both pulse amplitude and arterial compliance measures. We replicated the initial findings, demonstrating that associations with age, cardiorespiratory fitness, brain anatomy and

cognition can also be found across the adult lifespan. Further, we found new evidence supporting the value of regional arterial compliance in predicting working memory performance on the operation word span (OSPAN) task.

Chapter 4 contains a study investigating the relationships of arterial compliance with measures of cerebral white matter lesion (manifested as white matter signal abnormalities (WMSA) on T1 weighted images) and white matter microstructure integrity (measured using DTI indices of fractional anisotropy and mean diffusivity). Using hierarchical regression, we found that arterial compliance predicts variance in WMSA over and above age and systemic pulse pressure (difference between systolic blood pressure and diastolic blood pressure), indicating that brain measures of arterial compliance have added predictive utility of WMSA volume over systemic measures of vascular health. Mediation analyses revealed that the relationship between greater age and poorer fluid intelligence (IQ) was mediated sequentially by a reduction in arterial compliance and greater WMSA volume. Additional mediation analyses involving switching the temporal sequence of arterial compliance and WMSA was not statistically significant. Further, substituting WMSA for DTI measures of FA and MD in the mediation analysis also did not reach statistical significance. These results suggest that the cerebrovascular pathway involved in age-related cognitive decline in fluid IQ are mediated primarily through arterial compliance and WMSA, but not changes in white matter microstructure measured by DTI. Tentative findings suggest that vascular damage manifested as poorer arterial compliance and WMSA volume, may converge with degradation to white matter microstructure in the fornix.

Acknowledgements

I would like to extend my deepest gratitude to my advisors Monica Fabiani and Gabriele Gratton, for their impeccable guidance and timely advice throughout graduate school. In addition, I would like to thank my committee members, Art Kramer, Brad Sutton and Florin Dolcos for their helpful feedback on my dissertation. I would not have been able to complete this journey without the support and encouragement of CNL members, friends, family and especially, Jacinth and Akachan. Lastly, to my parents, thank you both for giving me the best education that you can. For demanding nothing from me and believing that I can excel, even if left to my own devices.

TABLE OF CONTENTS

CHAPTER 1

GENERAL INTRODUCTION

"A man is as old as his arteries."
Thomas Sydenham, MD, English Physician, 1624-1689

The importance of a healthy cardiovascular system in healthy aging has been known for a long time. However, even though great strides have been made over the past centuries to reduce cardiovascular-related mortality rates, 611,105 deaths in 2013 can still be attributed to heart disease. Trailing not far behind are the 128,978 and 84,767 people who died of cerebrovascular and Alzheimer's disease (AD), respectively (Xu, Murphy, Kochanek & Bastian, 2016). The links between a poor cardiovascular system, decline in cerebrovascular health, and cognitive decline seen in AD has received more attention recently, with Torre (2013) suggesting that the accumulation of vascular risk factors are in effect, "ticking time bombs" predicting the onset of cognitive decline and dementia.

Studies conducted to examine these relationships have mostly focused on systemic measures of the cardiovascular system to predict cognitive decline in aging. Large-scale longitudinal studies have found that vascular risk factors such as elevated blood pressure and left ventricular hypertrophy are predictive of clinically significant cognitive decline (Unverzagt et al., 2011). A longitudinal study consisting of 7 waves of testing over 19 years also found *directional* evidence that lower pulmonary function causes declines in fluid cognition. Even though studies like these suggest that the remodelling of arteries due to accumulation of cardiovascular risk factors such as hypertension may result in end-organ damage in the brain (Jennings & Zanstra, 2009), they are merely using systemic measures of cardiovascular health as proxy measures for cerebrovascular health.

Efforts to circumvent these indirect measures of cerebrovascular health have mostly relied on using transcranial Doppler (TCD) ultrasound (e.g. Kassab et al., 2007) and arterial spin labelling (ASL; e.g. Zimmerman et al., 2014) techniques. In general, findings from TCD studies suggest that blood flow

velocity and pulsatility indices are predictive of cognitive decline associated with AD (see Tomek, Urbanoca & Hort, 2014 for a review) and findings from ASL studies suggest that cerebral hypoperfusion is a potential biomarker for neurodegenerative conditions (see Wolk & Detre, 2012 for a review). However, TCD methods only allow for the sonography of a few large arteries such as the middle cerebral artery (MCA) and ASL methods suffer from inherent limitations in signal-to-noise ratio. Although very useful for deriving global and generalized indices of cerebrovascular health, these methods are not particularly suited for investigation of regional cerebrovascular health. Given findings that brain atrophy as a function of aging does not occur at the same rate for all regions (e.g. Fletcher et al., 2016; Raz et al., 2005; Tan et al., 2016) and that the brain possesses some degree of functional specificity for different cognitive processes (e.g., Kanwisher, 2010), it is evident that we should look beyond generalized cerebrovascular health. In fact, both within- and between-subject variations in *regional* cerebrovascular health can allow us to better investigate the influence of cerebrovascular function on brain and cognitive aging.

To this end, this dissertation describes the novel use of diffuse optical imaging to extract indices of both generalized and regional cerebrovascular health. In brief, diffuse optical methods involve the transmission of near-infrared light through the surface of the head and into cortical structures (see, Gratton & Fabiani, 2010 for a review). The pulsation of cerebral arteries as a function of the cardiac cycle allows us to extract pulsatility indices due to changes in absorption and scattering properties (see Fabiani et al., 2014). In particular, the current thesis relies on two diffusive optical indices of cerebrovascular health, namely pulse amplitude and arterial compliance.

Pulse amplitude is quantified by the reduction in alternating current (AC) light intensity due to the temporary distension of the arteries in the brain during the systolic phase of the cardiac cycle (see Figure 1.1). The pulse waveform is time-locked to the electrocardiogram (EKG) and the measure is

extracted from 384–534 ms, the time window in which the peak systolic phase occurs for all regions of the brain.

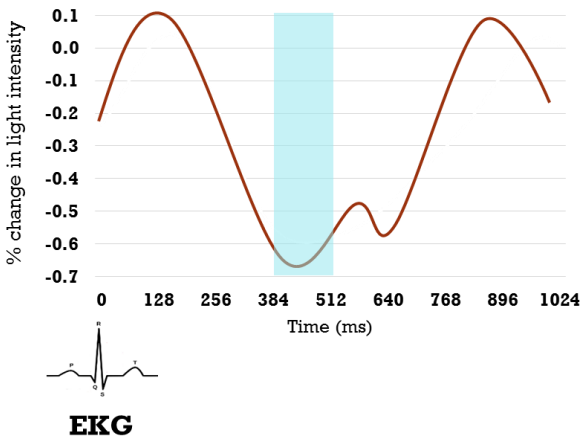

Figure 1.1. Pulse amplitude is quantified by averaging the reduction in light intensity from 384–534 ms (blue bar), a time period in which the peak systolic phase occurs for all regions of the brain.

Arterial compliance was defined as the area under the pulse between the peak systole and the peak diastole normalized by both time and amplitude and subtracted by a constant value of 0.5 (Fabiani et al., 2014). The constant value was subtracted to compare the area of the pulse response measured to an area of a hypothetical pulse presenting a linear decay of its amplitude after the systolic period. (see Figure 1.2.).

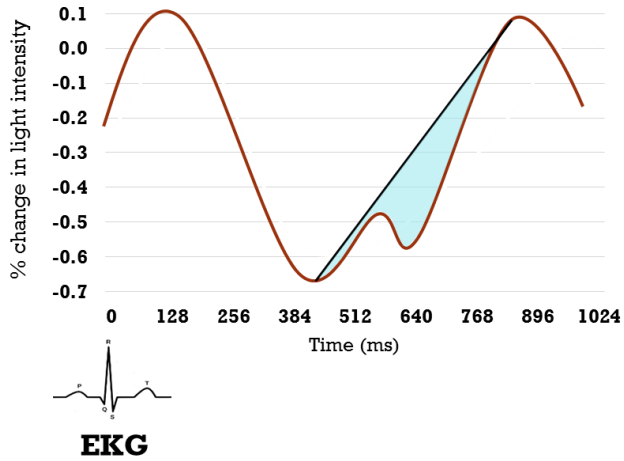

Figure 1.2. Arterial compliance is quantified by the region in blue. This value is normalized by both peak-to-peak time and amplitude for each individual subject.

The subsequent chapters focus on further explicating the relationship between both global and regional cerebrovascular health (as indexed by pulse amplitude and arterial compliance) and a variety of indices associated with aging, including blood pressure, brain volume, cardiorespiratory fitness, white matter health, and domain-general and domain-specific cognitive function. The data described in the dissertation come from 2 independent subject populations. Specifically, the data from Chapter 2 were collected from a sample of older adults ranging in age from 55 – 87 years and the data from Chapter 3 and 4 were collected from a sample of younger and older adults ranging in age from 18 – 75 years.

References

de la Torre, J. C. (2013). Vascular risk factors: a ticking time bomb to Alzheimer's disease. American *Journal of Alzheimer's Disease and Other Dementias, 28*(6), 551–559. http://doi.org/10.1177/1533317513494457

Fabiani, M., Low, K. A., Tan, C.-H., Zimmerman, B., Fletcher, M. A., Schneider-Garces, N., … Gratton, G. (2014). Taking the pulse of aging: mapping pulse pressure and elasticity in cerebral arteries with optical methods. *Psychophysiology, 51*(11), 1072–1088. http://doi.org/10.1111/psyp.12288

Fletcher, M., Low, K. A., Boyd, R., Zimmerman, B., Gordon, B., Tan, C.H., Schneider-Garces, N., Sutton, B. P., Gratton, G & Fabiani, M. (2016). Comparing aging and fitness effects on brain anatomy. *Frontiers in Human Neuroscience, 10* (286). doi:10.3389/fnhum.2016.00286

Gratton, G., & Fabiani, M. (2010). Fast optical imaging of human brain function. *Frontiers in Human Neuroscience, 4*, 52. http://doi.org/10.3389/fnhum.2010.00052

Jennings, J. R., & Zanstra, Y. (2009). Is the brain the essential in hypertension? *NeuroImage, 47*(3), 914–921. http://doi.org/10.1016/j.neuroimage.2009.04.072

Kanwisher, N. (2010). Functional specificity in the human brain: a window into the functional architecture of the mind. *Proceedings of the National Academy of Sciences of the United States of America, 107*(25), 11163–11170. http://doi.org/10.1073/pnas.1005062107

Kassab, M. Y., Majid, A., Farooq, M. U., Azhary, H., Hershey, L. A., Bednarczyk, E. M., … Johnson, M. D. (2007). Transcranial Doppler: An Introduction for Primary Care Physicians. *The Journal of the American Board of Family Medicine, 20*(1), 65–71. http://doi.org/10.3122/jabfm.2007.01.060128

Raz, N., Lindenberger, U., Rodrigue, K. M., Kennedy, K. M., Head, D., Williamson, A., … Acker, J. D. (2005). Regional brain changes in aging healthy adults: general trends, individual differences and modifiers. *Cerebral Cortex, 15*(11), 1676–1689. http://doi.org/10.1093/cercor/bhi044

Tan, C.H., Low, K. A., Schneider-Garces, N., Fletcher, M., Zimmerman, B., Maclin, E.L., Chiarelli, A. M., Gratton, G. & Fabiani, M. (2016). Optical measures of changes in cerebral vascular tone during voluntary breath holding and a Sternberg memory task. *Biological Psychology, 118.* doi:10.1016/j.biopsycho.2016.05.008

Tomek, A., Urbanová, B., & Hort, J. (2014). Utility of transcranial ultrasound in predicting Alzheimer's disease risk. *Journal of Alzheimer's Disease: JAD, 42* Suppl 4, S365-374. http://doi.org/10.3233/JAD-141803

Unverzagt, F. W., McClure, L. A., Wadley, V. G., Jenny, N. S., Go, R. C., Cushman, M., … Howard, G. (2011). Vascular risk factors and cognitive impairment in a stroke-free cohort. *Neurology, 77*(19), 1729–1736. http://doi.org/10.1212/WNL.0b013e318236ef23

Wolk, D. A., & Detre, J. A. (2012). Arterial Spin Labeling MRI: An Emerging Biomarker for Alzheimer's Disease and Other Neurodegenerative Conditions. *Current Opinion in Neurology, 25*(4), 421–428. http://doi.org/10.1097/WCO.0b013e328354ff0a

Xu, Murphy, Kochanek & Bastian (2016) Deaths: Final Data for 2013. http://www.cdc.gov/nchs/data/nvsr/nvsr64/nvsr64_02.pdf. Accessed May 1, 2016.

Zimmerman, B., Sutton, B. P., Low, K. A., Fletcher, M. A., Tan, C. H., Schneider-Garces, N., … Fabiani, M. (2014). Cardiorespiratory fitness mediates the effects of aging on cerebral blood flow. *Frontiers in Aging Neuroscience, 6*(59). doi:10.3389/fnagi.2014.00059

CHAPTER 2

OPTICAL MEASURES OF CHANGES IN CEREBRAL VASCULAR TONE DURING VOLUNTARY BREATH HOLDING AND A STERNBERG MEMORY TASK

The human cerebrovasculature is very adept at regulating blood flow in response to changes in blood pressure and/or oxygen demands induced by increased neuronal activity or other physiological challenges. The vascular system reacts to these departures from homeostasis via cerebral autoregulation (Cipolla, 2009; Iadecola, 2004; Van Beek, Claasen, Rikkert & Jensen, 2008). The efficacy of the vascular system in responding to these deviations is critical for normal physiological and cognitive function. Blood flow to the brain is regulated primarily by the vasodilation and vasoconstriction of cerebral arterioles. Changes in cerebrovascular tone (vasoconstriction and vasodilation) also mediate the changes in blood flow measured by the BOLD fMRI signal, whereby increased neuronal activity results in overall increases in tissue oxygenation, which are in turn reflected by a greater BOLD signal (Logothetis, 2002; Ogawa, Lee, Kay & Tank, 1990). The ability of the brain to react to challenges is also known to be affected by aging, due to a number of factors, including a reduced sensitivity of CO_2 receptors in small brain arteries (Brandes, Fleming & Busse, 2005). These issues may also be compounded by arterial stiffening and atherosclerosis, and overall decreases in brain blood flow with aging (e.g., Brown et al., 2010; Cantin et al., 2011; Choi et al., 2004; Fabiani et al., 2014a; 2014b; Riecker et al., 2003; Zimmerman et al., 2014).

Recently we have shown that it is possible to measure several indices of cerebrovascular function using parameters of the cerebral arterial pulse (amplitude, compliance and transit time) obtained by means of diffuse optical imaging methods (Fabiani et al., 2014b). Diffuse optical methods are based on measuring changes in the basic optical properties (absorption and scattering) of near-infrared light as it diffuses in brain (or other biological) tissue. A critical aspect of diffuse optical methods is the separation of sources and detectors (typically by a few centimetres) and the reliance on the highly scattering properties of most biological tissues, to allow for the measurement of relatively deep

structures from surface recordings. These methods (also referred to as diffuse optical tomography, or DOT, when reconstructed in 3D; e.g., Chiarelli et al., 2016) include functional near-infrared spectroscopy (fNIRS, Hoshi & Tamura, 1993; Villringer & Chance, 1997), and the event related optical signal (Gratton & Fabiani, 2010). The spectroscopic approach used by fNIRS involves estimating the relative absorption changes of oxy- and deoxy-haemoglobin during brain activity. However, fluctuations in these optical signals occur not only with variations in tissue oxygenation, but also with arterial pulsatility (Fabiani et al., 2014b). When the focus is on the (relatively small) activity-related changes, these (relatively large) pulsatility measures are treated as nuisance signals and corrected for (Gratton & Corballis, 1995). Here, instead, we focus on cerebral arterial pulsation parameters as our signals of interest.

Fabiani et al. (2014b) showed that these optical indices of cerebrovascular function are correlated with vascular tone *at rest*, as well as with age and cardiorespiratory fitness (CRF). Specifically, younger and/or highly fit adults have smaller peak pulse amplitudes, higher arterial compliance and slower pulse velocity in the brain. Here we expand on our initial findings by demonstrating that diffuse optical imaging measures of cerebrovascular pulse amplitude can also be used to track changes in vasodilation and vasoconstriction occurring in response to experimental manipulations, both globally and regionally in the brain.

When measured with diffuse optical methods, pulse amplitude refers to the amount of *reduction* in alternating current (AC) light intensity that happens during the systole due to the transient distension of the cerebral arteries. This distension is caused by the transit of the pulse pressure wave carrying a bolus of oxygenated blood, which results in greater absorption of near-infrared (NIR) light photons, and in a corresponding reduction in the light received by the detectors.

Vasodilation and vasoconstriction of intracranial (i.e., cerebral) and extracranial (i.e., scalp) arteries affect pulse amplitude in a consistent and opposing manner. During arterial vasodilation, cerebral pulse amplitude is reduced. Vasodilation of the arterioles causes a reduction in peripheral

resistance and allows blood to flow more easily into the tissue. This results in a reduction of cerebral blood pressure in (upstream) larger arteries. Given that the optical pulse signal originates predominately from the larger upstream intracranial arteries (Fabiani et al., 2014b), this reduction in blood pressure causes a reduction in the drop in light intensity occurring during systole. Conversely, vasoconstriction in the cerebral arterioles creates greater resistance for the blood flowing out of the larger upstream arteries, resulting in an increase in pressure. In other words, higher pulse pressure increases the light intensity drop during systole and is reflected by a corresponding increase in pulse amplitude (refer to Figure 2 for an example).

Here we present results from two studies, in which we measured changes in pulse amplitude by manipulating vascular tone in the brain. The first study involved a voluntary breath-holding task (BHT), which is expected to generate widespread effects on cerebral pulse amplitude. The second study used a Sternberg memory task, in which we expect to see regional vascular tone effects in task-relevant brain areas but not in other areas that are irrelevant for the task.

The BHT is commonly used to induce hypercapnic conditions in the brain (e.g. Bright & Murphy, 2013; Leoni et al., 2012; Markus & Culliane, 2001). During a BHT, increases in arterial carbon dioxide (CO_2) concentration cause a reduction in perivascular pH. This increase in acidity alters the cerebral vascular tone leading to the vasodilation of cerebral blood vessels, ultimately resulting in increased cerebral blood flow (CBF; Ainslie & Duffin, 2009; Cohen, Ugurbil & Kim, 2002) and reduced blood pressure. Upon resumption of breathing, the reverse happens: CO_2 concentration decreases, and blood vessels constrict. However, typically, for a brief period after breath holding, vasoconstriction exceeds the baseline value ("overshoot") and blood pressure is even greater than during the baseline period. Finally all the values return to normal. As a consequence, we hypothesized that, compared to resting conditions, changes in pulse amplitude should follow a quadratic trend whereby pulse amplitude decreases during the breath hold due to vasodilation, and then increases during the subsequent post-

hold period due to vasoconstriction. We expect changes in pulse amplitude to be globally distributed, in line with existing fMRI studies showing a generalized effect across most gray matter areas (Kastrup, Kruger, Neumann-Haefelin & Moseley, 2001; Kastrup, Tie, Atsuchi, Glover & Moseley, 1998; Thomason, Burrows, Gabrieli & Glover, 2005), although there may be some differences in sensitivity among regions (Kastrup, Kruger, Glover, Neumann-Haefelin & Moseley, 1999).

The breath-holding index (BHI), a measure of cerebrovascular reactivity (CVR) can also be derived from these changes in optical pulse amplitude. The cerebrovascular BHI is typically estimated using transcranial Doppler ultrasonography, which is based on measures of blood flow velocity. The BHI is derived by calculating the percent increase in blood flow velocity (typically in the middle cerebral artery) induced by breath holding compared to rest, and then dividing it by the duration of the breath hold (Markus & Harrison, 1992; Kassab et al., 2007; Silvestrini et al., 2000). Here we replace the measures of blood flow velocity with diffuse optical imaging measures of pulse amplitude. Note that pulse wave velocity is expected to increase with blood pressure, as the arterial walls become more rigid, thus transmitting the pulse wave faster, during vasoconstriction. Therefore, an increase in pulse wave velocity should be associated with an increase in blood pressure, and with an increase in pulse amplitude (and vice versa for a reduction in pulse wave velocity resulting from vasodilation).

Impairments of cerebral hemodynamics with increasing age are manifested by low cerebrovascular reactivity (Peisker, Bartos, Skoda, Ibrahim & Kalvach; 2010). For instance, decreasing BHI values as a function of age were found in a sample of 120 healthy adults aged 25 to 76 (Zavereo & Demarin 2010). Low CVR has also been shown to be associated with poorer performance on the Mini-Mental State Examination (MMSE) in older adults affected by Alzheimer's disease (AD), mixed dementia and also amnestic mild cognitive impairment (Richiardi et al., 2015; Stefani et al., 2009). In a 12-month longitudinal study, Silvestrini et al. (2006) also found that lower CVR predicts a greater drop in MMSE scores in an AD population. In the present study, participants ranged in age between 55 and 87 years

and performed the modified Mini-Mental Status Examination (mMMSE) as part of our screening process (see Methods). Specifically, we expected that, if optically-measured cerebral pulse amplitude is an index of CVR during the breath-holding task, it should be associated with both age and mMMSE.

An advantage of optical cerebral pulse measures is that, in addition to enabling the examination of generalized changes in pulse amplitude induced by breath holding, they also allow for the investigation of *regional* vasodilation effects produced by cerebral functional hyperaemia during a cognitive task. The Sternberg (1966) memory search task is especially suited for this purpose as it allows for the comparison of cognitive loads across different set sizes and has been extensively studied using fMRI (e.g., Altamura et al., 2007; D'Esposito, Postle, & Rypma, 2000; Schneider-Garces et al., 2010; Veltman, Rombouts, & Dolan, 2003; Zarahn et al., 2007). These studies typically find greater vasodilation - manifested by greater BOLD activation, in the medial and lateral prefrontal, parietal and also visual cortices as a function of increasing set sizes. As such, we should also expect that these task relevant regions – but not others that are irrelevant for the task (e.g., somatosensory and auditory cortex), would show a decrease in pulse amplitude from low to high set sizes.

The BHT and Sternberg task are commonly used to investigate physiological (BHT) and cognitive (Sternberg) changes as a function of experimental manipulations. These two particular tasks were chosen to provide effect that were either global (BHT) or engaging a reasonably large subset of brain areas (the Sternberg task), but would also differ in the mechanisms by which they induce vasodilation. Given the novel use of diffuse optical imaging methods to quantify changes in cerebrovascular tone, the main aim of the two studies presented here is to provide evidence demonstrating that the results derived with this approach align with those found in studies using other methodologies, such as Doppler ultrasound and fMRI. This will pave the way towards using optical methods to assess physiological and cognitive function in conjunction with these more traditional methods. In addition, because these new

optical methods potentially allow for regional specificity, they may also provide a window into the measurement of local cerebrovascular tone, and potentially enable new avenues for intervention.

Experiment 1: Breath Holding Task

We used a voluntary BHT to investigate global changes in pulse amplitude. We hypothesized that: a) the cerebral CVR function measured optically should show a quadratic trend, whereby we would observe a reduction in pulse amplitude during breath holding and an increase after breath holding; and b) the optical CVR measurements of pulse amplitudes during the BHT should correlate with age and general cognitive functioning as measured by the mMMSE.

Experiment 1: Methods

***Participants*.** Fifty-five older adults were recruited through advertisements in local newspapers, campus-wide e-mailings, and postings at area gyms, retirement homes and community centers. Four participants were excluded from subsequent analysis due to one participant dropping out of the experiment before the collection of optical data, and inability to reliably measure the pulse in three participants (because of errors in data collection and/or excessive movements by the subjects). The final sample comprised 51 older adults (age range = 55-87 years, mean age = 70.2 years, mean education level = 16.9 years, 26 males). The demographic characteristics of the participants are summarized in Table 2.1.

Table 2.1. ***Demographic characteristics of the participants***

Variable	Experiment 1 (N=51) Mean (SD)	Experiment 2 (N=52) Mean (SD)
Age (years)	70.2 (8.4)	69.8 (8.4)
Education (years)	16.9 (2.8)	16.8 (2.9)
Modified Mini-Mental Status Examination	55.3 (1.4)	55.3 (1.4)
Shipley's Vocabulary Test	35.9 (2.6)	36 (2.6)
Beck's Depression Index	2.8 (3.4)	2.9 (3.4)

Screening procedures. Participants were screened based on a number of health and cognitive criteria. Subjects with serious or chronic medical conditions or a history of major neurological or psychiatric disease or drug abuse were excluded from this study. Seventeen subjects who reported

taking blood pressure medications were not excluded because these conditions are pervasive in our age range, and we were interested in vascular risk factors. Additionally, to be included in the study subjects had to score at least 51 on the mMMSE (Mayeux, Stern, Rosen & Leventhal, 1981) and no more than 14 on Beck's Depression Inventory (Beck, Steer & Brown, 1996). Subjects who smoked more than half a pack of cigarettes and/or consumed more than two alcoholic drinks per day were also excluded. All participants were right-handed (as assessed by the Edinburgh Handedness Inventory; Oldfield, 1971), had normal or corrected-to-normal vision, and were native speakers of English.

***Breath-holding paradigm*.** Participants underwent six breath-holding trials, grouped in two blocks of three trials each, with a break between blocks. Given that the BHT is a voluntary task, visual cues and feedback mechanisms were used to reduce inter-subject adherence variability (see Thomason & Glover, 2008). All on-screen prompts (timing the subject's task) were presented using E-Prime 2.0 (Schneider, Eschman, & Zuccolotto, 2002) on a grey screen with black letters. First participants were presented with on-screen instruction prompts, designed to guide them to perform the breath-hold task in a time-consistent manner: (a) a prompt to *breathe normally* (29 s); (b) a *get ready* prompt (2 seconds), (c) instructions to *breathe in* (2 s), (d) instructions to *breathe out* (4 s) and finally (e) instructions to *hold their breath* (14 s). During the hold interval participants were shown a concentric circle at fixation, which became smaller in six visual steps to indicate how much longer they needed to hold their breath.

Participants were given a practice trial to familiarize themselves with the task before moving on to the 6 actual trials, and to decrease any anxiety that could be associated with the breath hold[1]. In addition, a breathing belt that measured chest expansion was used to monitor task compliance, and

[1] Hypercapnia can potentially induce anxiety (Eifert, Zvolensky, Sorrell, Hopko, & Lejuez, 1999). However a few things should be considered here: (1) none of our participants reported anxiety or had to interrupt the task due to anxiety; (2) subjects practiced the task 3 times before the optical recordings on which this paper is based (in addition to the practice trial reported here there was another session involving breath-holding within a mock scanner and within an MR scanner, Zimmerman et al., 2014). This should help habituate any eventual anxiety response; (3) the voluntary nature of the breath-holding should diminish anxiety, compared to hypercapnia generated by breathing CO_2 enriched air, as the participants maintain control on their breathing at all times.

experimental blocks in which deviance from the protocol was detected were excluded from subsequent analysis. It is important to note that breath holds as short as 3 s have been found to elicit a measurable BOLD signal change, although longer breath holds can result in more robust effects (Abbott, Opdam, Briellmann, & Jackson, 2005). Comparing between breath holds of 9, 15 and 20 s after inspiration, Magon and colleagues (2009) concluded that breath holds of 15 s are sufficient to capture differences in the cerebrovascular response to hypercapnia due to good stability and reproducibility across trials. Further, given our sample of older adults, we did not want to require a longer breath-holding period, due to concerns that harder challenges may not be tolerable for our oldest or less fit participants (see also Bright & Murphy, 2013, Chang et al., 2009).

Data Acquisition

***Electrocardiogram*.** Lead I of an electrocardiogram (EKG, left wrist referenced to right wrist) was recorded using a Grass Model 12 amplifier with a sampling rate of 200 Hz and a band-pass filter of 0.1 to 100 Hz. The R-wave of the EKG was used to determine the beginning of each cardiac systole.

***Optical recording*.** The optical data were recorded with six integrated frequency domain oximeters (Imagent; ISS, Inc., Champaign, IL). Data were collected from 24 detectors and 16 time-multiplexed sources (384 channels). Laser diodes generated light at wavelengths of 830 and 690 nm (max amplitude: 10 mW, mean amplitude after multiplexing: 1 mW), modulated at 110 MHz. The light from the diodes was transmitted to the surface of the head using optic fibers (one per emitter; diameter = 400 μm). Light was collected from the surface of the head using detectors (fiber optic bundles, diameter = 3 mm) connected to photomultiplier tubes (PMTs). Sources and detectors were held flush to the participants' scalp using a modified motorcycle helmet. We used an extended optical montage consisting of 128 source and 24 detectors that covered the whole outer cortical surface (see figure 1). A fast Fourier transform of the output data from the PMTs was used to calculate direct current (DC; average) intensity, AC (amplitude), and relative phase delay (in picoseconds). Since the focus of the

current study is on the cardiac pulse, we report AC intensity values only, where the pulse is most easily detected (see Fabiani et al., 2014b, supplementary materials, for the same measures taken with the phase parameter). Optical parameters were sampled at 39.0625 Hz (25.6ms per sampling point). The arterial pulse is the largest phenomenon that can be measured using AC intensity, being typically easily visible on single trials.

Structural MRI acquisition and co-registration with optical data. Although in this study we are investigating widespread hypercapnia effects, which do not necessitate co-registration with brain anatomy, this step is necessary for experiment 2 in which we are evaluating regional changes. As data for the two experiments were recorded in the same session and participants, we implemented the co-registration procedures for both to ensure consistency and precision. Each subject's optical pulse data was coregistered with the person's structural MRI to allow for alignment of functional and anatomical images. First, using nasion and pre-auricular points as references, the locations of individual optical sources and detectors were digitized using a Polhemus "3Space" FASTRAK 3D digitizer (Polhemus, Colchester, VT). T1 weighted structural magnetic resonance images were obtained for each subject using a Siemens TRIO 3-T full body scanner using a 3D MPRAGE protocol. The MPRAGE parameters were: flip angle = 9◦, TR = 1900 ms, TE = 2.32 ms 186 and inversion time = 900 ms. Slices were acquired in the sagittal plane (192 slices, .9 mm slice thickness, 187 voxel size .9 x .9 x .9 mm) with matrix dimensions of 192 x 256 x 256 (in-plane interpolated at 188 acquisition to 192 x 512 x 512) and field of view of 172.8 x 230 x 230 mm. These MPRAGE images were ac-pc (anterior commissure, posterior commissure) aligned using AFNI (Cox, 1996). The Polhemus digitization points were then co-registered with the transformed MR images first using the three fiducial markers and then surface-fitting the entire set of digitized points to the estimated scalp surface based on a Levenberg-Marquardt algorithm (least-squares fit), which has been shown to have errors of less than 4 mm (Whalen, Maclin, Fabiani, & Gratton, 2008; see also Chiarelli et al., 2015). Figure 2.1 depicts the recording montage (together with

the additional digitized points defining the head's surface) superimposed on the structural MRI of one representative participant.

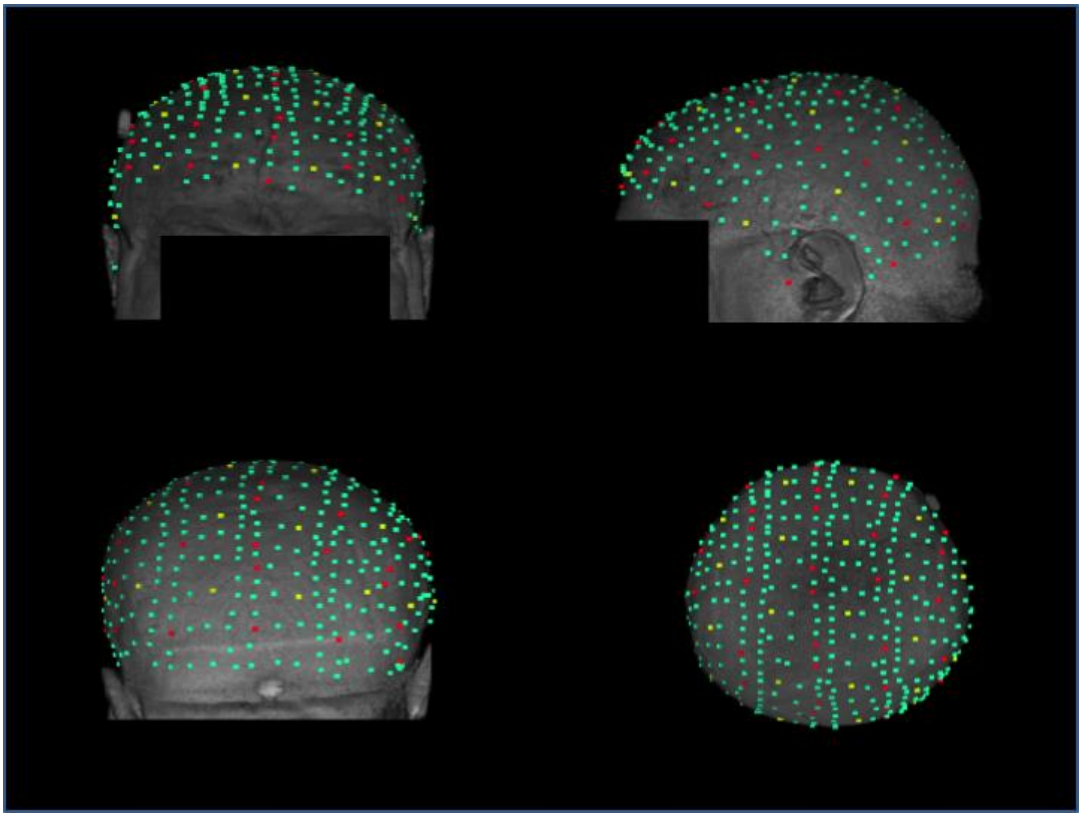

Figure 2.1. Example of co-registration of the full-head optical montage with the structural magnetic resonance image of an individual subject. Red squares on the scalp indicate light sources, yellow squares indicate light detectors and teal squares indicate additional digitized points used for co-registration with the MRI. Nasion and preauricular fiducial points are also in red. From top left going clockwise, front view, side view, back view and top view.

Data Analysis.

***Optical Processing*.** The optical data were first normalized and band-pass filtered between 0.5 and 5.0 Hz. The data were then divided into 2048 ms epochs starting with the peak of each R-wave, obtained from the simultaneously recorded EKG. Each breath-hold period was divided into 3 separate phases: *Rest* (4 seconds before the subjects were asked to breathe out and hold), *breath-hold* (last 10 seconds) and *post-hold* (4 seconds). The choice of these intervals was motivated by previous studies: Abbott et al. (2005) showed measureable BOLD signal changes after 3 seconds of breath holding, and

also suggested that the 4-seconds measurement interval used in the current study after breath holding begins, and the 4 seconds after breath holding ends are sufficient to generate significant effects. The selection of a 4-seconds measurement period after breath hold was also motivated by Doppler studies investigating the BHI, by comparing mean flow velocity between rest and the average of a 4s-period immediately following the breath hold (Markus & Harrisson, 1992; Silvestrini et al., 2000; Vernieri et al., 2001).

Pulse epochs occurring during each phase of the BHT were then averaged together and baselined to the first peak diastole period occurring between 128 ms and 256 ms after the R-wave of the EKG. Note that the cerebral pulse is delayed with respect to the EKG R-wave, by approximately 200 to 400 ms (see Fabiani et al., 2014b). Therefore the peak diastole of the previous cerebral pulse cycle typically occurs well after (i.e., more than 100 ms) the EKG R-wave of the following cycle. The duration of the breath hold measurement period was chosen to maximize the effects of breath holding given that the relationship between $PaCO_2$ and blood flow is known to be sigmoidal (Harper & Glass, 1965; Madden, 1993).

In-house software "Opt-3d" (Gratton, Sarno, Maclin, Corballis & Fabiani, 2000) was utilized to merge channels whose mean diffusion paths (modeled as a curved ellipsoid) intersected for a given brain volume (Wolf et al., 2000). Only source-detector distances between 35 and 55 mm were used in the analysis in order to bias signal extraction from deeper brain regions as opposed to superficial skin effects, visible with shorter source-detector distances (channels with source-detector distances exceeding 55 mm produced unreliable data due to low light). An 8-mm spatial filter was applied to the spatially-reconstructed data and the optical data were projected onto the axial (top) surface of a sample brain in Talairach space.

***Pulse Amplitude*.** To index cerebral vascular tone, pulse amplitude was defined as the mean AC amplitude in an interval between 384 and 538 ms after R wave onset for each phase of the BHT (Fabiani

et al., 2014b), an interval during which the peak of the systolic activity occurred in all subjects and for all regions of the brain. Given that the optical data were baselined to the period during which the diastolic peak occurred, pulse amplitude is essentially a measurement of the change in the light moving from sources to the detectors from the diastole to the systole. In order to quantify global changes, voxels on most of the axial surface (Talairach coordinates; X-axis: -45 to 45, Y-axis: -80 to 50) were averaged together prior to measuring pulse amplitude in each phase of the BHT.

***Breath-holding index*.** The BHI was derived by calculating the percent change in pulse amplitude from rest to the end of breath-holding, weighted by the length of breath-hold, paralleling the measurements done with transcranial Doppler (Markus & Harrison, 1992; Kassab et al., 2007; Silvestrini et al., 2000, Vernieri, Pasqualetti, Passarelli, Rossini & Silvestrini, 1999). The BHI was used to investigate the relationship between CVR, age, and general cognitive function (as indexed by the mMMSE).

***Heart and pulse rate*.** Heart and pulse rate were computed separately for each of the three phases of the BHT. We extended the duration of the rest and post-hold phases to 10 seconds in this analysis to accrue a sufficient number of beats to accurately calculate beats per minute. The heart rate was derived from the EKG by computing the inter-beat interval (IBI) from R-wave to R-wave and then converting it into beats per minute (bpm). Similarly, the optical pulse rate was derived by calculating the IBI from a peak systole to the next peak systole, and then converting it into pulses per minute.

Experiment 1: Results

Heart and Pulse Rate Changes. Grand average optical pulse waveforms across the whole head are presented in Figure 2.2, separately for each breath-holding period. These waveforms show the expected relationship between pulse amplitude and phase of the BHT. Figure 2.3 shows the average heart rate measures obtained with the EKG and optical pulse methods, separately for the three breath-holding periods.

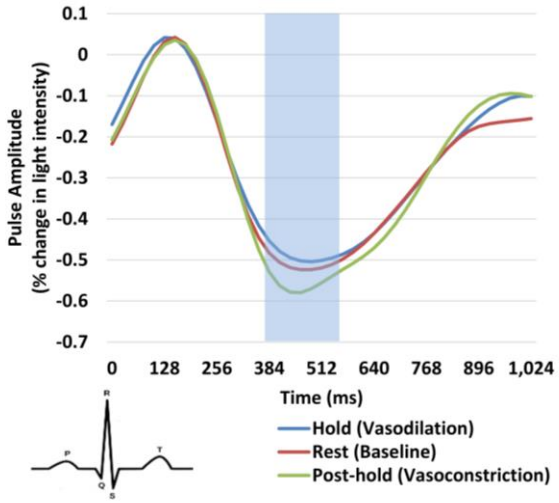

Figure 2.2. During breath holding arterioles vasodilate resulting in a reduction in blood pressure in large upstream arteries and in a corresponding decrease in pulse amplitude (blue line) compared to the resting baseline period (red line). During the post-hold period (green line) the opposite phenomena occur. The shaded blue area indicates the time range (384–538 ms) used to compute mean pulse amplitude.

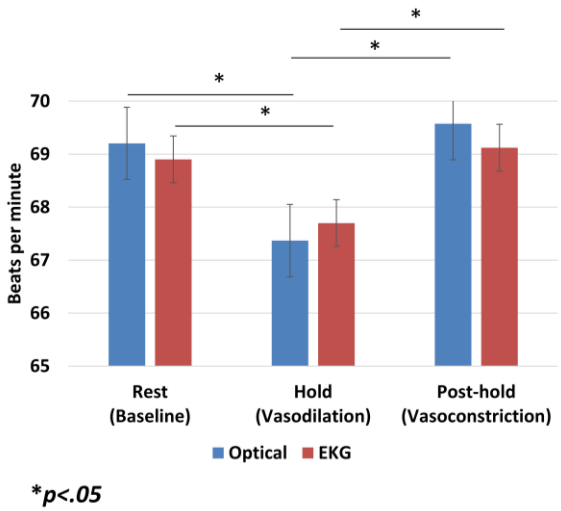

Figure 2.3. Changes in heart rate measured using optical and EKG methods. Both methods show a significant drop in beats per minute during the breath-hold and a subsequent increase post breath-hold.

There was a significant correlation between the heart rate measured by the EKG and the cerebral pulse rate measured optically for each of the 3 periods of the BHT; rest ($r(49) = .92$, $p < .001$), hold ($r(49) = .93$, $p < .001$) and post-hold ($r(49) = .88$, $p < .001$). This indicates a high correspondence between the two methods (one based on the average EKG IBI, and the other on the IBI of the average

optical waveforms). As can be seen in Figure 3, a repeated measures ANOVA determined that both heart and pulse rate differed significantly across the 3 BHT phases, $F(2, 100) = 11.2$, $p < .001$ and $F(2, 100) = 5.8$, $p < .001$, respectively. Planned comparisons showed that heart rate measured using EKG decreased significantly from rest (M = 68.9, SD = 9.8) to breath holding (M = 67.7, SD = 9.4), $t(50) = 3.59$, $p < .001$. Heart rate also increased from the hold phase to the post-hold phase (M = 69.1, SD = 9.0), $t(50) = -4.72$, $p < .001$. The optical pulse rate showed similar results, with the breath holding pulse rate (M = 67.4, SD = 9.3) lower than both the rest pulse rate (M = 69.2, SD = 8.9), $t(50) = 3.44$, $p < .001$ and the pulse rate during the post-hold phase (M = 69.6, SD = 8.2), $t(50) = -2.98$, $p = .004$. There was also a significant quadratic trend across the 3 phases for both EKG and optical measures, $F(1, 50) = 23.4$ and 15.3, respectively, p's < .001). These changes in heart rate were expected, as breath holding is considered a vagal activation task, and demonstrate that the participants were complying with the task.

Pulse Amplitude Changes. Two subjects were removed from this analysis due to being outliers (Z score >|2.5|) on pulse amplitude values collapsed across all 3 phases. Figure 2.4 shows pulse amplitude for the three phases of the BHT. Trend analysis revealed a significant quadratic trend across the three phases, $F(1,48) = 5.1$, $p = .029$, indicating that across the BHT, pulse amplitude decreased during hold (vasodilation) and increased post-hold (vasoconstriction).

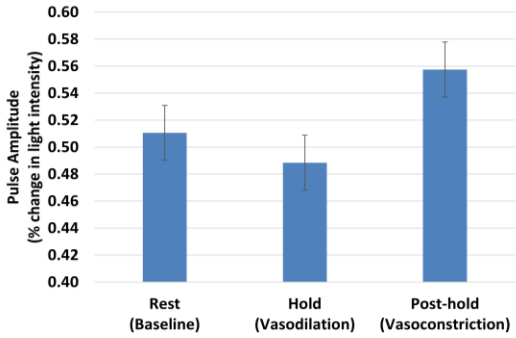

Figure 2.4. Changes in pulse amplitude across the 3 periods of the breath-holding task. The quadratic trend was statistically significant, indicating that pulse amplitude decreased (vasodilation) and increased (vasoconstriction) during the breath-hold and post-hold respectively

***BHI correlations with age and cognitive function*.** Three additional subjects were excluded from this analysis due to being outliers on BHI values (Z score >|2.5|). As shown in Figure 2.5, there was a significant negative correlation between BHI and age, $r(44) = -.32$, $p = .029$. Older participants had a lower BHI, indicating lower CVR with age. A lower BHI score was also associated with poorer performance on the mMMSE, $r(44) = .42$, $p = .004$. This correlation persisted even after partialing out the effects of age and education, $r(42) = .37$, $p = .014$.

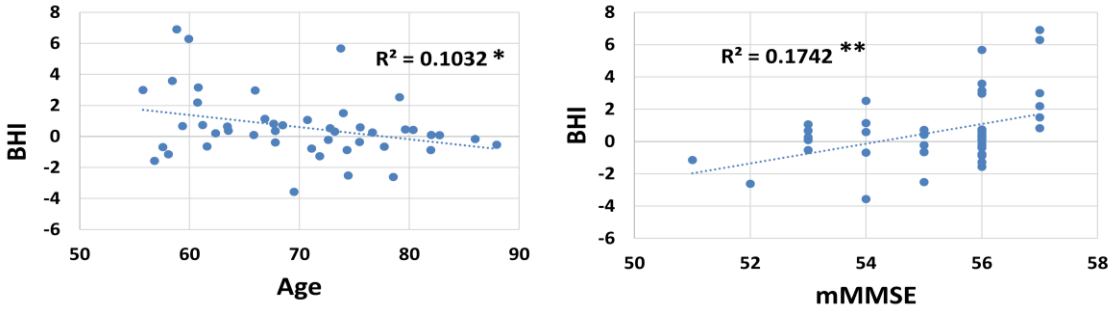

***p* = <.05, ****p* = <.01**

Figure 2.5. Correlations between cerebrovascular reactivity, as indexed by the BHI, age (left plot) and mMMSE (right plot).

Experiment 1: Discussion

Experiment 1 provides a validation of the use of an optically-recorded cerebral pulse amplitude to measure cerebral vascular tone by demonstrating that we can track cerebral vasodilation and vasoconstriction in response to changes in $PaCO_2$ during different periods of a BHT. Significant decreases in pulse beats per minute during the hold phase, and increases during the post-hold phase as measured by both EKG and optical methods indicate that subjects were performing the task correctly, providing a manipulation check.

The amplitude of the pulse was found to change systematically across the task, following a quadratic pattern decreasing with breath hold and increasing subsequent to the hold. As hypothesized, our measurement of CVR based on optically recorded pulse amplitudes correlated negatively with age

and positively with the mMMSE, a measure of general cognitive function. In sum, Experiment 1 provided evidence that the optical pulse amplitude measures can track global changes in vasodilation and vasoconstriction induced by a BHT. The validity of these measures is further supported by our finding that CVR calculated using pulse amplitudes also showed relevant correlations with age and cognitive performance.

EXPERIMENT 2: Sternberg Task

In this study we used a Sternberg memory task to investigate local changes in pulse amplitude in response to increases in memory load. Specifically, the primary aim of Experiment 2 was to demonstrate a reduction in pulse amplitude in task-relevant brain areas as a function of increased memory set sizes and but not in non-task relevant areas. Based on a large number of BOLD fMRI papers (Rypma, Berger, & D'Esposito, 2002; Rypma, Berger, Genova, Rebbechi, & D'Esposito, 2005; Schneider-Garces et al., 2010; Veltman, Rombouts, & Dolan, 2003).), we expect some regions of the brain but not others to show vasodilation effects (responsible for the increased blood flow in these regions evidenced by BOLD fMRI task-related activations), which would then be reflected by local changes in the pulse amplitude of the arteries feeding these regions. This would indicate that the optical pulse measures provide direct information about local cerebral vascular phenomena in addition to global phenomena.

Experiment 2: Methods

***Participants*.** The 54 participants who completed experiment 1 also completed experiment 2. Two subjects were removed from the analysis due to near chance accuracy (approximately 50%) on the Sternberg task. The final sample comprised 52 older adults (age range = 55-87 years, mean age = 69.8 years, mean education level = 16.8 years, 25 males). The demographic characteristics of the participants for experiment 2 are also summarized in Table 1.

***Sternberg Task*.** We implemented a modified version of Sternberg's memory search task (Sternberg, 1966), with memory set sizes two, four, six, and eight. All stimuli to be encoded by the

participants were uppercase letters, chosen from the set B, D, F, G, H, J, L, M, R, and T. Corresponding lowercase letters were used as probes in order to prevent a direct visual match (see Bunge et al., 2001; Schneider-Garces et al., 2010). The letters were selected due to their different shapes when presented in upper and lower case. Each letter subtended approximately 1.4° of visual angle in the diagonal on a computer monitor during the optical session.

Each trial was initiated by the presentation of a memory set of 2, 4, 6, or 8 letters distributed equally and equidistant above and below a central fixation cross. The memory set letters were presented simultaneously for 3 sec, followed by the fixation cross for 1 sec. Subsequently, a single probe letter was presented centrally (replacing the fixation cross) for 700 msec. The fixation cross reappeared for the 1.3 sec inter-trial interval. Once the probe letter was presented on screen, participants were asked to indicate whether or not the probe was part of the preceding memory set by pressing a button with the right or left hand. The response-hand assignments were counterbalanced across subjects. Each memory set was composed of letters chosen randomly from the set of letters listed above, with the constraint that no identical letters were allowed within the same memory set. The probe was part of the memory set on 50% of the trials.

A total of four runs were collected: each run consisted of four blocks of eight trials each, with a 20-sec fixation period preceding and following each block. A block of each set size was presented once in each run, with set size counterbalanced across runs and subjects using a modified balanced Latin Square design. This yielded a total of four task blocks (8 trials each) and four rest blocks per run, with a total of 32 trials per set size after all four runs.

All participants attended a training session 1 to 7 days prior to the experimental sessions. During the training session, participants received instructions, followed by at least 32 trials of set size 1 to familiarize them with the task. The first 12 trials were presented at a slower pace. Participants were then presented with 20 normal-paced set-size 1 trials until they reached a 90% accuracy. They then

practiced the task for an additional 32 trials (8 trials per set size for set sizes 2, 4, 6, and 8) in sequential blocks with feedback. Following that, they were given a final set of 32 trials without feedback. In total, each participant was trained for at least 96 trials.

Data acquisition and Preprocessing

***Electrocardiogram, Optical and Co-registration Procedures*.** These acquisition parameters were identical to Experiment 1.

***Optical Data Analysis*.** The optical data were preprocessed and the pulse waveforms extracted (time-locked to the R-wave) in the same manner as in Experiment 1. Pulse waveforms occurring during each task block were averaged separately for each set size, excluding the first trial of each task block (6 seconds), in order to account for the typical latency of the vasodilation (hemodynamic) response. For the purpose of comparing vasodilation under low and high cognitive load conditions, we only present results involving the comparison between set size 2 and set size 6 conditions. We did not use the set size 8 as the high load condition because previous findings in the lab using Cowan's K measures (Cowan, 2001; Cowan et al., 2005) suggested that, on average, older adult have difficulty maintaining more than four-to-six items in working memory (Schneider-Garces et al., 2010). Maximum Cowan's K data in the current sample were consistent with this finding (M = 4.4, SD = 1.1).

Source-detector distances included in the analysis were expanded to 2-6 cm, as cognitive tasks are less likely to induce localized superficial skin effects. We computed pulse amplitudes in five Brodmann's areas (BA7, BA8, BA9, BA10, BA17+18), where we expected to see differences between the 2 set sizes (Rypma, Berger, & D'Esposito, 2002; Rypma, Berger, Genova, Rebbechi, & D'Esposito, 2005; Schneider-Garces et al., 2010; Veltman, Rombouts, & Dolan, 2003). We also computed pulse amplitude effects in primary somatosensory cortex (BA1+2+3) and in auditory cortex (BA 41+42), where we did not expect to see differences as they are regions not relevant to the visual Sternberg memory task.

Experiment 2: Results

***Behavioral results*.** As expected, participants had greater accuracy and faster reaction times (RT) in the set size 2 condition compared to the set size 6 condition ($t(51) = 8.4$ and -18.3, respectively, p's < .001).

***Pulse Amplitude*.** Figure 2.6 depicts the difference in average pulse amplitude in each ROI between set sizes 2 and 6. Two-tailed paired t-tests were performed on each ROI (with positive values indicating greater pulse amplitude for set size 2 than set size 6, the predicted direction). Cerebral pulse amplitude decreased significantly between set size 2 and 6 in BA 7 ($t(51) = 2.56$, $p = .014$), BA 8 ($t(51) = 2.33$, $p = .024$), BA 9 ($t(51) = 2.28$, $p = .027$) and BA 10 ($t(51) = 2.10$, $p = .044$). BA17+18, however did not reach statistical significance ($t(51) = 1.35$, $p = .18$). As expected pulse amplitude did not differ significantly in BA1+2+3 ($t(51) = 1.75$, $p = .086$) and in BA41+42 ($t(51) = 0.38$, $p = .71$). As these were planned comparisons, no correction for multiple comparisons was made. In addition, two-tailed paired t-tests conducted on the averaged pulse amplitude across all task relevant regions revealed significant differences between set sizes ($t(51) = 2.96$, $p = .005$) but not across all non-task relevant regions, ($t(51) = .79$, $p = .43$). However, a repeated measures ANOVA did not reveal a significant interaction effect, $F(51,1) < 1$, $p = .45$.

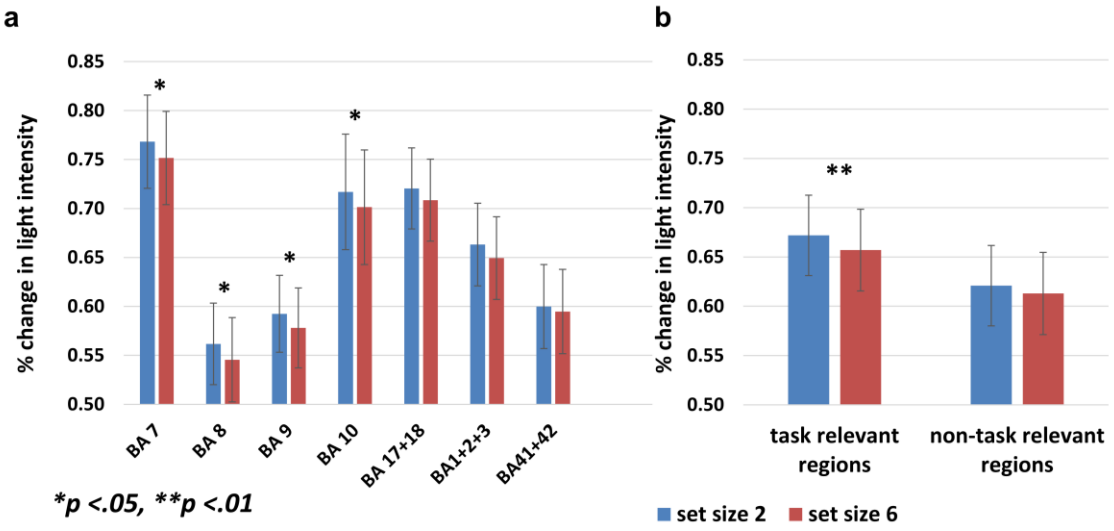

Figure 2.6. a) Differences in pulse amplitude between set-size 2 and set-size 6 for Brodmann areas (BA 7, 8, 9,10 and 17+18) involved in the Sternberg Task. Non-task-relevant legions (BA1+2+3, primary somatosensory cortex and BA41+BA42, auditory cortex) showed no differences in pulse amplitude. b) Averaged pulse amplitude in task-relevant regions was significantly different between set sizes 2 and 6 but not between non-task-relevant regions.

Experiment 2: Discussion

Pulse amplitude showed a significant decrease in frontal and parietal regions (BA7, BA8, BA9 and BA10) with increasing cognitive load (i.e. from set size 2 to 6), indicating that vasodilation has occurred in these areas. The effects in the visual cortex BA 17/18 did not reach statistical significance. This could be due to a combination of insufficient coverage in the posterior region of the optical montage and a general weaker effect in the optical measure's ability to detect vasodilation due to changes in the visual display. The absence of a set size effect in the primary somatosensory cortex (BA1+2+3) and both sides of the auditory cortex (BA 41+42) provides additional support to the claim that the pulse amplitude effects are regional, and isolated to brain regions involved in cognitive processing during the Sternberg memory task.

The results of Experiment 2 indicate that pulse amplitude measures using diffusive optical imaging demonstrate the occurrence of drops in pulse amplitude (and presumably pulse pressure) in

cortical regions exhibiting increased blood flow (presumably associated with vasodilation) based on typical fMRI results (Rypma, Berger, & D'Esposito, 2002; Rypma, Berger, Genova, Rebbechi, & D'Esposito, 2005; Schneider-Garces et al., 2010; Veltman, Rombouts, & Dolan, 2003).

General Discussion

Cerebral arterial pulse measures derived with diffuse optical imaging provide a new tool (and therefore a new perspective) for investigating the complex chain of cerebrovascular phenomena that are associated with various conditions, such as hypercapnia or neuronal activation. These include systemic changes (i.e., non-cerebral phenomena, such as changes in heart rate and peripheral blood pressure), large and medium-size cerebral artery phenomena (e.g., changes in local arterial blood pressure and pulse velocity), vasoconstriction and vasodilation at the level of the arterioles, and hyperhaemia/hypohaemia and changes in oxygenation at the level of the capillaries in the parenchyma. A critical role in this complex chain of events is played by the arterioles, whose constriction or dilation (enabled by the presence of smooth muscle fibers in their wall, paired with the relative thinness of the wall itself) leads to opposite effects at levels of the system occurring before and after them: vasoconstriction of the arterioles generates higher pressure in the large arteries and reduced blood flow reaching the capillaries. The opposite effects, of course, are obtained during arterioles' vasodilation. Both hypercapnia and neuronal activity induce vasodilation (generalized in the first case, and localized in the second). Diffuse optical measures of arterial pulse provide a tool for mapping large and medium-size cerebral arteries across extended areas of the cortex (in contrast with transcranial Doppler ultrasound measures, which are limited to a few points of specific cerebral arteries). In particular, the amplitude of the optical pulse in any particular region is determined by the blood pressure within the arteries of that region (assuming that the resistance of the arterial wall is relatively similar within the time course of the measurements). Therefore, the amplitude of the arterial pulse in a particular region will vary as a

function of the vasodilation or vasoconstriction occurring in the set of arterioles that are fed by the arteries that are studied. When considering vasodilation or vasoconstriction this way, however, it is important to also consider that spatial resolution will be limited by the fact that the same large and medium-size arteries will feed different arterioles.

The results of the two studies presented here are easily understood within this framework. In the two experiments we found evidence that pulse amplitude measures derived from diffuse optical methods can quantify changes in cerebrovascular tone both globally, using a physiological hypercapnia challenge, and locally in task-relevant areas during a cognitive Sternberg task. In experiment 1, we also demonstrated that the BHI derived from pulse amplitude measures and indexing CVR was associated with scores on the mMMSE in an older adults sample even after partialling out effects of age and education.

The framework presented above also provides a way of relating these novel diffuse optical pulse measures with other techniques for studying brain hemodynamic phenomena. The closest is transcranial Doppler ultrasound, which measures blood flow velocity. Although transcranial Doppler measurements are useful when investigating generalized effects induced by hypercapnia, their use is restricted to only a few major arteries such as the middle cerebral artery (MCA). This limitation and consequent lack of spatial information makes transcranial Doppler less suited for investigating *regional* effects as a function of cognitive manipulations than diffuse optical imaging methods. Whether generalized effects seen using whole-cortex measures from diffuse optical methods are comparable to MCA measurements using transcranial Doppler remains to be investigated. For practical applications, if the aim is to examine only generalized effects, transcranial Doppler is simpler in its implementation.

Both arterial spin labeling (ASL; e.g., Zimmerman et al., 2014) MRI and ^{15}O-PET can be used to quantify the flow of blood through cerebral arteries and arterioles into capillaries and parenchyma. Their advantage is the ability to provide absolute measures of flow with good spatial resolution.

However, (a) they provide a measure that summarizes the status of all the levels within the system rather than separating effects across different compartments (although see Yan et al., 2016, for an attempt to derive pulse measures from ASL-MRI); and (b) they are not easily adapted to follow rapid changes in hemodynamic phenomena, as their temporal resolution is of the order of several seconds (for ALS-MRI) or several minutes (for ^{15}O-PET).

The BOLD fMRI signal, as well as oxygenation signals obtained with functional near-infrared spectroscopy (fNIRS; Hoshi & Tamura, 1993; Murkin & Arango, 2009; Villringer & Chance, 1997), originate primarily from the capillaries/parenchyma, which are perfused by penetrating arterioles with a single layer of smooth muscle (Iadecola, 2004; see also Safonova et al., 2002). In this sense they provide complementary information to that obtained with measures of the optical pulse. Future experiments using simultaneous fMRI and optical imaging over the entire cortex, or in smaller regions such as the primary motor or visual cortex (e.g., Boas, Dale & Franceschini, 2004; Zhang et al., 2005), may further elucidate the similarities and differences between these two measures. Importantly, optical pulse measures are always available when fNIRS measures are recorded, at least when sampling rate is >5 Hz.

There are also both general limitations of diffuse optical methods for pulse analysis, and specific limitations concerning the paradigms used in the current study. The most important general limitation of diffuse optical imaging (independently of the specific physiological phenomenon studied) is the limited penetration of these methods. However, recent advancements in 3D reconstruction suggest that penetration can be pushed to 30-35 mm from the surface of the head, which may greatly expand the scope of the measures (Chiarelli et al., 2016).

Specific limitations of the current work include the use of a voluntary fixed-duration breath-holding task instead of a more controlled manipulation of $PaCO_2$ based on 5% CO_2 inhalation. Previous studies, however, have shown that fMRI-based measurements of CVR using voluntary BHT or CO_2 inhalation challenge provide comparable results (Kastrup, Krüger, Neumann-Haefelin & Moseley, 2001).

Measurements using more traditional transcranial Doppler methods also found that CVR measured using breath holding had good short-term reproducibility and was comparable to that obtained through CO_2 inhalation (Totaro, Marini, Baldassarre & Carolei, 1999). It should be noted, however, that these changes are but one of the many systemic hemodynamic phenomena associated with hypercapnia. In fact, hypercapnia generates changes in systemic blood pressure, cardiac stroke volume, and systolic time interval among others (Crystal, 2015; Kiely, Cargill, & Lipworth, 1996). Future studies can further compare the relative importance of cerebral and systemic autoregulatory mechanisms on cerebral blood pressure and CVR in order to gain a better understanding of the complex hemodynamic cascade induced by hypercapnia.

The effects seen in both studies reported here are relatively small and the quadratic trend seen in the BHT appears to be principally driven by vasoconstriction effects post-hold rather than by effects obtained during the hypercapnia period per se. This may reflect the complexity of the phenomena occurring during that period as discussed above. Although we see clear effects of cerebrovascular tone changes as a function of both the physiological and cognitive manipulations, these results could be bolstered by improved methodologies in the future. In particular, the use of a tomographic approach for localizing the effects, of stronger manipulations (such as increasing the length of the breath hold) and the implementation of other cognitive tasks that produce more localized brain effects may provide additional support for the use of optical imaging methods to quantify cerebral vascular tone.

In conclusion, the two experiments presented here demonstrate that changes in optical pulse amplitude generated by physiological and cognitive manipulations allow for making inferences about the current state of the cerebral arteries. This novel methodology provides another window into cerebrovascular phenomena, by not only looking at how arteries respond in a global manner during physiological stress but also how they differ regionally as a function of local variations in neuronal activity induced by cognitive load. Future work should further establish the reliability and validity of the

measure using a variety of physiological challenges and cognitive tasks to elucidate its relationship with information derived from other neuroimaging methods.

References

Abbott, D. F., Opdam, H. I., Briellmann, R. S., & Jackson, G. D. (2005). Brief breath holding may confound functional magnetic resonance imaging studies. *Human Brain Mapping, 24*(4), 284–290. http://doi.org/10.1002/hbm.20086

Ainslie, P. N., & Duffin, J. (2009). Integration of cerebrovascular CO2 reactivity and chemoreflex control of breathing: mechanisms of regulation, measurement, and interpretation. *American Journal of Physiology. Regulatory, Integrative and Comparative Physiology, 296*(5), R1473–1495. http://doi.org/10.1152/ajpregu.91008.2008

Altamura, M., Elvevåg, B., Blasi, G., Bertolino, A., Callicott, J. H., Weinberger, D. R., … Goldberg, T. E. (2007). Dissociating the effects of Sternberg working memory demands in prefrontal cortex. *Psychiatry Research: Neuroimaging, 154*(2), 103–114. http://doi.org/10.1016/j.pscychresns.2006.08.002

Beck, A. T., Steer, R. A., & Brown, G. K. (1996). *Manual for the Beck Depression Inventory* (2nd ed.). San Antonio, TX: The Psychological Corporation.

Boas, D. A., Dale, A. M., & Franceschini, M. A. (2004). Diffuse optical imaging of brain activation: approaches to optimizing image sensitivity, resolution, and accuracy. *NeuroImage, 23 Suppl 1*, S275–288. http://doi.org/10.1016/j.neuroimage.2004.07.011

Brandes, R. P., Fleming, I., & Busse, R. (2005). Endothelial aging. *Cardiovascular Research, 66*(2), 286–294. http://doi.org/10.1016/j.cardiores.2004.12.027

Bright, M. G., & Murphy, K. (2013). Reliable quantification of BOLD fMRI cerebrovascular reactivity despite poor breath-hold performance. *NeuroImage, 83*, 559–568. http://doi.org/10.1016/j.neuroimage.2013.07.007

Brown, A. D., McMorris, C. A., Longman, R. S., Leigh, R., Hill, M. D., Friedenreich, C. M., & Poulin, M. J. (2010). Effects of cardiorespiratory fitness and cerebral blood flow on cognitive outcomes in older

women. *Neurobiology of Aging, 31*(12), 2047–2057. http://doi.org/10.1016/j.neurobiolaging.2008.11.002

Bunge, S. A., Ochsner, K. N., Desmond, J. E., Glover, G. H., & Gabrieli, J. D. E. (2001). Prefrontal regions involved in keeping information in and out of mind. *Brain, 124*, 2074–2086.

Cantin, S., Villien, M., Moreaud, O., Tropres, I., Keignart, S., Chipon, E., … Krainik, A. (2011). Impaired cerebral vasoreactivity to CO2 in Alzheimer's disease using BOLD fMRI. NeuroImage, 58(2), 579–587. http://doi.org/10.1016/j.neuroimage.2011.06.070

Chang, T.-Y., Liu, H.-L., Lee, T.-H., Kuan, W.-C., Chang, C.-H., Wu, H.-C., … Chang, Y.-J. (2009). Change in cerebral perfusion after carotid angioplasty with stenting is related to cerebral vasoreactivity: a study using dynamic susceptibility-weighted contrast-enhanced MR imaging and functional MR imaging with a breath-holding paradigm. *American Journal of Neuroradiology, 30*(7), 1330–1336. http://doi.org/10.3174/ajnr.A1589

Chiarelli, A.M., Maclin, E.L., Fabiani, M. & Gratton, G. (2016). Combining energy and Laplacian regularization to accurately retrieve the depth of brain activity of diffuse optical tomographic data. *Journal of Biomedical Optics*, 21(3), 036008. doi:10.1117/1.JBO.21.3.036008

Chiarelli, A. M., Maclin, E. L., Low, K. A., Fabiani, M., & Gratton, G. (2015). Comparison of procedures for co-registering scalp-recording locations to anatomical magnetic resonance images. *Journal of Biomedical Optics, 20*(1), 016009. http://doi.org/10.1117/1.JBO.20.1.016009

Choi, J., Wolf, M., Toronov, V., Wolf, U., Polzonetti, C., Hueber, D., … Gratton, E. (2004). Noninvasive determination of the optical properties of adult brain: near-infrared spectroscopy approach. *Journal of Biomedical Optics, 9*(1), 221–229. http://doi.org/10.1117/1.1628242

Cipolla, M. J. (2009). *The Cerebral Circulation.* San Rafael (CA): Morgan & Claypool Life Sciences. Retrieved from http://www.ncbi.nlm.nih.gov/books/NBK53081/

Cohen, E. R., Ugurbil, K., & Kim, S.-G. (2002). Effect of basal conditions on the magnitude and dynamics of the blood oxygenation level-dependent fMRI response. *Journal of Cerebral Blood Flow and Metabolism: Official Journal of the International Society of Cerebral Blood Flow and Metabolism, 22*(9), 1042–1053. http://doi.org/10.1097/00004647-200209000-00002

Cowan, N. (2001). The magical number 4 in short-term memory: A reconsideration of mental storage capacity. *Behavioral and Brain Sciences, 24*, 87–114.

Cowan, N., Elliot, E. M., Scott-Saults, J., Moray, C. C., Mattox, S., Hismjatullina, A., & Conway, A. R. (2005). On the capacity of attention: Its estimation and its role in working memory and cognitive aptitudes. *Cognitive Psychology, 51*, 42–100.

Cox, R. W. (1996). AFNI: software for analysis and visualization of functional magnetic resonance neuroimages. *Computers and Biomedical Research, an International Journal, 29*(3), 162–173.

Crystal, G. J. (2015). Carbon Dioxide and the Heart: Physiology and Clinical Implications. *Anesthesia and Analgesia, 121*(3), 610–623. http://doi.org/10.1213/ANE.0000000000000820

D'Esposito, M., Postle, B. R., & Rypma, B. (2000). Prefrontal cortical contributions to working memory: evidence from event-related fMRI studies. *Experimental Brain Research, 133*(1), 3–11. http://doi.org/10.1007/s002210000395

Eifert, G. H., Zvolensky, M. J., Sorrell, J. T., Hopko, D. R., & Lejuez, C. W. (1999). Predictors of Self-Reported Anxiety and Panic Symptoms: An Evaluation of Anxiety Sensitivity, Suffocation Fear, Heart-Focused Anxiety, and Breath-Holding Duration. *Journal of Psychopathology and Behavioral Assessment, 21*(4), 293–305. http://doi.org/10.1023/A:1022116731279

Fabiani, M., Gordon, B. A., Maclin, E. L., Pearson, M. A., Brumback-Peltz, C. R., Low, K. A., … Gratton, G. (2014a). Neurovascular coupling in normal aging: a combined optical, ERP and fMRI study. *NeuroImage, 85* (Pt 1), 592–607. http://doi.org/10.1016/j.neuroimage.2013.04.113

Fabiani, M., Low, K. A., Tan, C.-H., Zimmerman, B., Fletcher, M. A., Schneider-Garces, N., … Gratton, G. (2014b). Taking the pulse of aging: mapping pulse pressure and elasticity in cerebral arteries with optical methods. *Psychophysiology, 51*(11), 1072–1088. http://doi.org/10.1111/psyp.12288

Gratton, G., & Corballis, P. M. (1995). Removing the heart from the brain: Compensation for the pulse artifact in the photon migration signal. *Psychophysiology, 32,* 292–299. doi: 10.1111/j.1469-8986.1995.tb02958.x

Gratton, G. & Fabiani, M. (2010). Fast optical imaging of human brain function. *Frontiers in Human Neuroscience, 4*(Art. 52), 1-9.

Gratton, G., & Fabiani, M. (2012). *Beyond ERP & fMRI: Other Imaging Techniques for Studying Human Brain Function*. In H. Cooper (Editor-in-Chief) APA Handbook of Research Methods in Psychology (Chapter 29, Vol. 2, pp. 567-580). APA Books: Washington, DC.

Gratton, G., Sarno, A., Maclin, E., Corballis, P. M., & Fabiani, M. (2000). Toward noninvasive 3-D imaging of the time course of cortical activity: investigation of the depth of the event-related optical signal. *NeuroImage, 11*(5 Pt 1), 491–504. http://doi.org/10.1006/nimg.2000.0565

Harper, A. M., & Glass, H. I. (1965). Effect of alterations in the arterial carbon dioxide tension on the blood flow through the cerebral cortex at normal and low arterial blood pressures. *Journal of Neurology, Neurosurgery, and Psychiatry, 28*(5), 449–452.

Hoshi, Y., & Tamura, M. (1993). Detection of dynamic changes in cerebral oxygenation coupled to neuronal function during mental work in man. *Neuroscience Letters, 150*(1), 5–8. http://doi.org/10.1016/0304-3940(93)90094-2

Iadecola, C. (2004). Neurovascular regulation in the normal brain and in Alzheimer's disease. *Nature Reviews. Neuroscience, 5*(5), 347–360. http://doi.org/10.1038/nrn1387

Kassab, M. Y., Majid, A., Farooq, M. U., Azhary, H., Hershey, L. A., Bednarczyk, E. M., … Johnson, M. D. (2007). Transcranial Doppler: An Introduction for Primary Care Physicians. *The Journal of the American Board of Family Medicine, 20*(1), 65–71. http://doi.org/10.3122/jabfm.2007.01.060128

Kastrup, A., Krüger, G., Glover, G. H., Neumann-Haefelin, T., & Moseley, M. E. (1999). Regional variability of cerebral blood oxygenation response to hypercapnia. *NeuroImage, 10*(6), 675–681. http://doi.org/10.1006/nimg.1999.0505

Kastrup, A., Krüger, G., Neumann-Haefelin, T., & Moseley, M. E. (2001). Assessment of cerebrovascular reactivity with functional magnetic resonance imaging: comparison of CO(2) and breath holding. *Magnetic Resonance Imaging, 19*(1), 13–20.

Kastrup, A., Li, T.-Q., Takahashi, A., Glover, G. H., & Moseley, M. E. (1998). Functional Magnetic Resonance Imaging of Regional Cerebral Blood Oxygenation Changes During Breath Holding. *Stroke, 29*(12), 2641–2645. http://doi.org/10.1161/01.STR.29.12.2641

Kiely, D. G., Cargill, R. I., & Lipworth, B. J. (1996). Effects of hypercapnia on hemodynamic, inotropic, lusitropic, and electrophysiologic indices in humans. *Chest, 109*(5), 1215–1221.

Leoni, R. F., Mazzetto-Betti, K. C., Silva, A. C., Santos, A. C. dos, de Araujo, D. B., Leite, J., … Pontes-Neto, O. M. (2012). Assessing Cerebrovascular Reactivity in Carotid Steno-Occlusive Disease Using MRI BOLD and ASL Techniques. *Radiology Research and Practice, e268483*. http://doi.org/10.1155/2012/268483

Logothetis, N. K. (2002). The neural basis of the blood-oxygen-level-dependent functional magnetic resonance imaging signal. *Philosophical Transactions of the Royal Society of London. Series B, Biological Sciences, 357*(1424), 1003–1037. http://doi.org/10.1098/rstb.2002.1114

Madden, J. A. (1993). The effect of carbon dioxide on cerebral arteries. *Pharmacology & Therapeutics, 59*(2), 229–250.

Magon, S., Basso, G., Farace, P., Ricciardi, G. K., Beltramello, A., & Sbarbati, A. (2009). Reproducibility of BOLD signal change induced by breath holding. *NeuroImage, 45*(3), 702–712. http://doi.org/10.1016/j.neuroimage.2008.12.059

Markus, H., & Cullinane, M. (2001). Severely impaired cerebrovascular reactivity predicts stroke and TIA risk in patients with carotid artery stenosis and occlusion. *Brain: A Journal of Neurology, 124*(Pt 3), 457–467.

Markus, H. S., & Harrison, M. J. (1992). Estimation of cerebrovascular reactivity using transcranial Doppler, including the use of breath-holding as the vasodilatory stimulus. *Stroke; a Journal of Cerebral Circulation, 23*(5), 668–673.

Mayeux, R., Stern, Y., Rosen, J., & Leventhal, J. (1981). Depression, intellectual impairment and Parkinson's disease. *Neurology, 31*, 645– 650.

Murkin, J. M., & Arango, M. (2009). Near-infrared spectroscopy as an index of brain and tissue oxygenation. *British Journal of Anaesthesia, 103 Suppl 1*, i3–13. http://doi.org/10.1093/bja/aep299

Ogawa, S., Lee, T. M., Kay, A. R., & Tank, D. W. (1990). Brain magnetic resonance imaging with contrast dependent on blood oxygenation. *Proceedings of the National Academy of Sciences of the United States of America, 87*(24), 9868–9872.

Oldfield, R. C. (1971). The assessment and analysis of handedness: the Edinburgh inventory. *Neuropsychologia, 9*(1), 97–113.

Peisker, T., Bartoš, A., Skoda, O., Ibrahim, I., & Kalvach, P. (2010). Impact of aging on cerebral vasoregulation and parenchymal integrity. *Journal of the Neurological Sciences, 299*(1-2), 112–115. http://doi.org/10.1016/j.jns.2010.08.064

Richiardi, J., Monsch, A., Haas, T., Barkhof, F., Van de Ville, D., Radü, E. W., … Haller, S. (2015). Altered cerebrovascular reactivity velocity in mild cognitive impairment and Alzheimer disease. *Neurobiology of Aging*, *36*(1), 33-41. http://doi.org/10.1016/j.neurobiolaging.2014.07.020

Riecker, A., Grodd, W., Klose, U., Schulz, J. B., Gröschel, K., Erb, M., … Kastrup, A. (2003). Relation between regional functional MRI activation and vascular reactivity to carbon dioxide during normal aging. *Journal of Cerebral Blood Flow and Metabolism, 23*(5), 565–573. http://doi.org/10.1097/01.WCB.0000056063.25434.04

Rypma, B., Berger, J. S., & D'Esposito, M. (2002). The influence of working-memory demand and subject performance on prefrontal cortical activity. *Journal of Cognitive Neuroscience, 14*(5), 721–731. http://doi.org/10.1162/08989290260138627

Rypma, B., Berger, J. S., Genova, H. M., Rebbechi, D., & D'Esposito, M. (2005). Dissociating age-related changes in cognitive strategy and neural efficiency using event-related fMRI. *Cortex; a Journal Devoted to the Study of the Nervous System and Behavior, 41*(4), 582–594.

Safonova, L. P., Michalos, A., Wolf, U., Wolf, M., Hueber, D. M., Choi, J. H., … Gratton, E. (2004). Age-correlated changes in cerebral hemodynamics assessed by near-infrared spectroscopy. Archives of Gerontology and Geriatrics, 39(3), 207–225. http://doi.org/10.1016/j.archger.2004.03.007

Schneider-Garces, N. J., Gordon, B. A., Brumback-Peltz, C. R., Shin, E., Lee, Y., Sutton, B. P., … Fabiani, M. (2010). Span, CRUNCH, and Beyond: Working Memory Capacity and the Aging Brain. *Journal of Cognitive Neuroscience, 22*(4), 655–669. http://doi.org/10.1162/jocn.2009.21230

Schneider, W., Eschman, A., & Zuccolotto, A. (2002). *Prime user's guide.* Pittsburgh, PA: Psychology Software Tools, Inc.

Silvestrini, M., Pasqualetti, P., Baruffaldi, R., Bartolini, M., Handouk, Y., Matteis, M., … Vernieri, F. (2006). Cerebrovascular reactivity and cognitive decline in patients with Alzheimer disease. *Stroke; a Journal of Cerebral Circulation, 37*(4), 1010–1015. http://doi.org/10.1161/01.STR.0000206439.62025.97

Silvestrini, M., Vernieri, F., Pasqualetti, P., Matteis, M., Passarelli, F., Troisi, E., & Caltagirone, C. (2000). Impaired cerebral vasoreactivity and risk of stroke in patients with asymptomatic carotid artery stenosis. *JAMA, 283*(16), 2122–2127.

Stefani, A., Sancesario, G., Pierantozzi, M., Leone, G., Galati, S., Hainsworth, A. H., & Diomedi, M. (2009). CSF biomarkers, impairment of cerebral hemodynamics and degree of cognitive decline in Alzheimer's and mixed dementia. *Journal of the Neurological Sciences, 283*(1-2), 109–115. http://doi.org/10.1016/j.jns.2009.02.343

Sternberg, S. (1966). High-Speed Scanning in Human Memory. *Science, 153*(3736), 652–654. http://doi.org/10.1126/science.153.3736.652

Thomason, M. E., Burrows, B. E., Gabrieli, J. D. E., & Glover, G. H. (2005). Breath holding reveals differences in fMRI BOLD signal in children and adults. *NeuroImage, 25*(3), 824–837. http://doi.org/10.1016/j.neuroimage.2004.12.026

Thomason, M. E., & Glover, G. H. (2008). Controlled inspiration depth reduces variance in breath-holding-induced BOLD signal. *NeuroImage, 39*(1), 206–214. http://doi.org/10.1016/j.neuroimage.2007.08.014

Totaro, R., Marini, C., Baldassarre, M., & Carolei, A. (1999). Cerebrovascular reactivity evaluated by transcranial Doppler: reproducibility of different methods. *Cerebrovascular Diseases, 9*(3), 142–145. http://doi.org/15943

van Beek, A. H., Claassen, J. A., Rikkert, M. G. O., & Jansen, R. W. (2008). Cerebral autoregulation: an overview of current concepts and methodology with special focus on the elderly. *Journal of Cerebral Blood Flow and Metabolism: Official Journal of the International Society of Cerebral Blood Flow and Metabolism, 28*(6), 1071–1085. http://doi.org/10.1038/jcbfm.2008.13

Veltman, D. J., Rombouts, S. A. R. B., & Dolan, R. J. (2003). Maintenance versus manipulation in verbal working memory revisited: an fMRI study. *NeuroImage, 18*(2), 247–256. http://doi.org/10.1016/S1053-8119(02)00049-6

Vernieri, F., Pasqualetti, P., Passarelli, F., Rossini, P. M., & Silvestrini, M. (1999). Outcome of carotid artery occlusion is predicted by cerebrovascular reactivity. *Stroke; a Journal of Cerebral Circulation, 30*(3), 593–598.

Villringer, A., & Chance, B. (1997). Non-invasive optical spectroscopy and imaging of human brain function. *Trends in Neurosciences, 20*(10), 435–442.

Whalen, C., Maclin, E. L., Fabiani, M., & Gratton, G. (2008). Validation of a method for coregistering scalp recording locations with 3D structural MR images. *Human Brain Mapping, 29*(11), 1288 – 1301.

Wolf, U., Wolf, M., Toronov, V., Michalos, A., Paunescu, L. A., & Gratton, E. (2000). Detecting cerebral functional slow and fast signals by frequency-domain near-infrared spectroscopy using two different sensors. *OSA Biomedical topical meeting, Technical digest,* 427-429.

Yan, L., Liu, C. Y., Smith, R. X., Jog, M., Langham, M., Krasileva, K., Chen, Y., Ringman, J.M., & Wange, D. J. J. (2016). Assessing intracranial vascular compliance using dynamic arterial spin labeling. *NeuroImage*, *124*, 433-441. http://doi.org/10.1016/j.neuroimage.2015.09.008

Zarahn, E., Rakitin, B., Abela, D., Flynn, J., & Stern, Y. (2007). Age-related changes in brain activation during a delayed item recognition task. *Neurobiology of Aging, 28*(5), 784–798. http://doi.org/10.1016/j.neurobiolaging.2006.03.002

Zhang, X., Toronov V. Y., Fabiani, M., Gratton, G. & Webb, A. G. (2005). The study of cerebral hemodynamic and neuronal response to visual stimulation using simultaneous NIR optical tomography and BOLD fMRI in humans. *Proceedings of the Society of Photo Optics Instrumentation and Engineering, 5686,* 566-572. http://doi.org/10.1117/12.593435

Zavoreo, I., & Demarin, V. (2010). Breath Holding Index and Arterial Stiffness as Markers of Vascular Aging. *Current Aging Science, 3*(1), 67–70. http://doi.org/10.2174/1874609811003010067

Zimmerman, B., Sutton, B. P., Low, K. A., Fletcher, M. A., Tan, C. H., Schneider-Garces, N., … Fabiani, M. (2014). Cardiorespiratory fitness mediates the effects of aging on cerebral blood flow. *Frontiers in Aging Neuroscience, 6*, 59. http://doi.org/10.3389/fnagi.2014.00059

CHAPTER 3

MAPPING CEREBRAL PULSE PRESSURE AND ARTERIAL COMPLIANCE OVER THE ADULT LIFESPAN WITH OPTICAL IMAGING

Many studies have demonstrated that vascular health plays an important role in both normal (pre-clinical) aging and in conditions that become more prevalent in aging, such as mild cognitive impairment (MCI) and Alzheimer's disease (AD). Systemic arterial stiffening contributes to negative neurological outcomes, including poorer cognitive function [1-6], greater brain atrophy in multiple regions [7], increased risk of degenerative disease states such as AD [8-11] as well as increased cardiovascular mortality rates [12-13].

In comparison, vascular health in younger adults has received more limited attention [14], despite evidence showing that arterial aging begins early in life [15-16] and that the negative consequences of arterial stiffness in relatively young populations are associated with poorer white matter health and reduced gray matter volume [17]. These adverse outcomes are also compounded by other known cardiovascular risk factors, such as low cardiorespiratory fitness (CRF) and poor dietary intake [18-20], emphasizing the need for control and intervention strategies at younger ages [21-22] for the prevention of age-related cognitive decline.

Fabiani and colleagues [23] recently introduced a novel, non-invasive method to derive indices of cerebrovascular health using diffuse optical imaging. This work was based on a body of research in humans and animals demonstrating that optical measures are sensitive to vascular phenomena due to changes in near-infrared (NIR) light absorption during arterial blood pulsation, as a function of the cardiac cycle. In the periphery, information about heart rate and oxygen saturation can be extracted from photoplethysmographic waveforms recorded by pulse oximeters [24]. For example, recording from neonatal pig brains, Themelis and colleagues [25] found that near-infrared spectroscopic (NIRS) methods for quantifying cerebral blood flow hemodynamics were highly correlated with well-established laser-Doppler flowmetry methods [26]. In clinical application, Ebihara and colleagues [27] analyzed the pulse

power spectrum using NIRS in patients with cerebral ischemia and found that pulse transmission in the ischemic cerebral hemisphere was smaller compared to the contralateral side, reflecting the reduced cerebral blood flow associated with ischemia.

Fabiani and colleagues [23] relied on diffuse optical methods and an extended recording montage to extract cerebral pulsatile waveforms from the adult human brain in a sample of middle age and older adults. From these waveforms, they quantified three indices reflective of different aspects of cerebrovascular health, namely, pulse amplitude, arterial compliance and pulse transit time. Pulse amplitude was conceptualized as a proxy measure of pulse pressure (systolic blood pressure minus diastolic blood pressure) in cerebral arteries, and this claim was supported by data showing that the two were highly correlated. Pulse amplitude measures were also positively correlated with age (as arterial stiffening induces an increase in the difference between systolic and diastolic pressure), but were not associated with eCRF, blood flow measured with arterial spin labeling (ASL; [28]), brain anatomy or cognitive function (as measured by neuropsychological tests).

Additional recent evidence from our laboratory supports the idea that optical pulse amplitude measures the temporary distension of the cerebral arteries caused by the movement of the pulse pressure wave across the vascular system. Tan and et al. [29] found that pulse amplitude measures can track both generalized and localized changes in cerebrovascular tone (vasodilation and vasoconstriction) as a function of voluntary breath-holding and a Sternberg memory task in a group of middle age and older adults. Further, estimates of cerebrovascular reactivity (CVR) derived from the pulse amplitude measures during the breath-holding task were also found to be negatively associated with age, and positively associated with performance on the modified mini-mental status examination (mMMSE; [30]). These data

suggest that the utility of cerebral pulse amplitude goes beyond simply indexing pulse pressure in the brain, but also provides information about the cerebrovascular system that is related to aging and CVR.

Fabiani and colleagues [23] also found that arterial compliance, measured with diffuse optical methods, was negatively associated with age and positively associated with eCRF, brain volumes (i.e., overall preservation of white and gray matter volumes) and cognitive flexibility. In addition, regional pulse transit time, also measured with diffuse optical methods, was associated with performance on distinct cognitive tasks. Specifically, they found evidence for a double dissociation, whereby slower pulse transit time (indicating higher arterial elasticity) in the left middle cerebral artery (IMCA, feeding Broca's area) was associated with higher performance on a verbal fluency task but not with performance in the operation span task (OSPAN, a test that provides an estimate of working memory capacity; [31]). The opposite relationship was found with pulse transit time in the superior portion of the precentral artery bilaterally (sPCA, feeding dorsolateral prefrontal cortex). The authors argued that this double dissociation reflects the functional specialization of the cortical areas fed by these two arteries. They concluded that these indices of cerebrovascular health provide complementary information about the arterial system to that obtained with other approaches such as magnetic resonance imaging (MRI) and Doppler ultrasound.

Fabiani and colleagues [23] also highlighted some limitations and areas of possible future improvements. Specifically, they suggested that the relatively low spatial resolution of the method could be improved by using a denser array of optodes. In addition, the utility of extracting regional estimates of arterial compliance on cognition remained largely unknown, even though the finding that arterial compliance was associated with pulse transit time is suggestive of a possible link to cognition.

The purpose of the current study is therefore two-fold; first, we seek to replicate and extend the initial findings (which were obtained in a sample of older adults aged 55 - 87 years) to an evenly distributed sample spanning a much broader age range (18 – 75 years). This will allow us to investigate how global measures of cerebrovascular health relate to eCRF, global brain volumetric indices and cognitive function, not only in older adults but also over the adult life span starting in the late teens.

Second, we increased the density of the optical recording montage from 384 to 1536 channels and increased recording time from 72 to 360 seconds, in order to increase the spatial resolution and reliability of the data. This allows us to not only replicate the previous findings but also to better explore relationships between regional measures of arterial compliance, age, and cognitive function.

Functional MRI studies have shown that both prefrontal and parietal regions are associated with performance on working memory tasks [32-37]. Other studies have shown that frontal and parietal regions are more prone to age-related volumetric losses than other regions such as the occipital cortex [38-39], that reductions in frontal and parietal lobe perfusion are associated with poorer cognitive performance [40-41] and that higher levels of CRF are associated with greater oxygenation in prefrontal regions [42] and more preserved prefrontal and parietal gray matter volumes [43-45]. Motivated by this fMRI- and sMRI-based evidence and by our initial findings that arterial compliance is associated with pulse transit time [23], here we investigated whether regional measures of arterial compliance in the frontoparietal cortex (Brodmann areas 9 and 7) would be more associated with performance on the OSPAN working memory task [31] compared to a global estimate of cerebral arterial compliance. Further, we also expected to find strong age-related reductions in arterial compliance in these regions but not in other regions such as visual cortex. Finally, we expected the association between eCRF and arterial

compliance to be more evident for frontoparietal regions than for visual cortex.

Taken together, the results presented in this paper should provide support for the utility of these newly developed optical cerebrovascular indices of arterial health during the adult lifespan, show their reliability, and validate their predictive value with respect to indices of volumetric and cognitive health. Finally, they should also show the utility of deriving regional measures of cerebrovascular health in addition to global cerebral and systemic measures.

Methods

Participants

Forty-eight adults (age range = 18-75 years, mean age = 47.8, 25 females) were recruited through advertisements in local newspapers, campus-wide emails and postings at area gyms, retirement homes and community centers in the Urbana-Champaign community. In order to ensure an even spread across ages, the age range was divided into six decades (18-27, 28-37, 38-47, 48-57, 58-67, and 68-77), and 8 subjects were recruited for each decade.

However, for the majority of analyses presented in this paper, age (in years) was used as a continuous variable. One subject (from an intermediate age group) had to be removed from all analyses involving pulse measures because we were unable to extract a suitable pulse trace from the optical data, possibly due to excessive movement, leaving a final sample count of 47 subjects. The demographic characteristics of the participants are summarized in Table 3.1. In this table, information is provided about the overall sample, as well as about three broad age groups (younger, middle-aged and older adults, each comprising two of the original decades used to generate the overall sample). This classification is provided to show that important variables such as years of education and IQ were consistent across the entire sample.

Table 3.1. Demographic characteristics of the participants

Variable	All (N=47) Mean (SD)	Young (N=16) Mean (SD)	Middle (N=15) Mean (SD)	Old (N=16) Mean (SD)
Age (years)	47.6 (17.5)	27.2 (6.1)	48.8 (6.2)	66.9 (5.0)
Education (years)	17.3 (2.2)	16.4 (2.3)	16.9 (1.8)	18.5 (2.2)
mMMSE	55.8 (1.2)	55.4 (1.2)	56.1 (1.1)	55.8 (1.3)
Shipley's Vocabulary Test	34.7 (3.7)	33.4 (2.7)	33.5 (4.1)	37.1 (3.0)
Beck's Depression Index	2.2 (2.5)	2.6 (2.2)	3.0 (3.0)	1.2 (2.1)
K-BIT2 (IQ)	116.4 (10.2)	116.3 (7.8)	113.1 (12.0)	119.6 (10.2)

Screening procedures

Participants were screened based on a number of health and cognitive criteria. Subjects with serious or chronic medical conditions or a history of major neurological or psychiatric disease or drug abuse were excluded from this study. Additionally, to be included in the study subjects had to score at least 51 on the mMMSE [30] and no more than 14 on the Beck's Depression Inventory [46]. Subjects who smoked more than half a pack of cigarettes and/or consumed more than two alcoholic drinks per day were also excluded. Three participants reported taking blood pressure medications (diuretics) and 2 others reported taking statins due to high cholesterol, which may indirectly affect blood pressure. All participants were right-handed (as assessed by the Edinburgh Handedness Inventory [47]), had normal or corrected-to normal vision, and were native speakers of English. All procedures described in this report were approved by the University of Illinois Institutional Review Board. Prior to participation, all participants signed informed consent documents.

Assessment of cognitive function

A battery of neuropsychological tests was administered to all participants, which included the Kaufmann Brief Intelligence Test Second Edition (K-BIT2 [48]) and the Raven's progressive matrices [49] to estimate crystallized and fluid IQ, the vocabulary sub-test of the Shipley-Institute of Living Scale [50] to measure vocabulary, the Wisconsin Card Sorting Test (WCST [51-52]), the Controlled Oral Word Association sub-test of the Multilingual Aphasia Examination (a measure of verbal fluency using the letters CFL [53]), the OSPAN task [32], the Trail Making Tests A and B [54], to measure working memory and executive function, and the Logical Memory I and II tasks from the Wechsler Memory Scale – Fourth Edition (WMS–IV [55]) to measure episodic memory. In addition, scores for forward and backward digit span were derived from the mMMSE.

Assessment of cardiorespiratory fitness

We estimated CRF with an equation that utilizes easily acquired parameters that are highly predictive of VO2max ($r \approx .7$ [56-57]). This measure is obtained from a linear combination of weighted variables, including gender, age, body mass index (BMI), resting heart rate, and a physical activity score, plus a numerical constant. This eCRF index, expressed in metabolic equivalents, was first developed in a large sample of men and women ($N > 40,000$) aged 20 to 70 years, which corresponds well to the age range of our participants. The validity of these CRF estimates has also been validated in samples of older adults [58-59]. In this study gender was partialed out from analyses involving eCRF to control for systematic differences in CRF between males and females, which are known to be present even when using VO2max to assess fitness [56], and would not be expected to reflect real variations in fitness or vascular health.

Experimental Procedures and Types of Measures

The data presented here were collected as a part of a much larger, multi-session project intended to investigate brain function using diffuse optical and magnetic resonance imaging (MRI) methods. Session 1 included neuropsychological assessments and familiarization to MRI scanning within a mock magnet. Session 2 included the collection of structural MRI data (used for anatomical co-registration and brain volume estimations). Session 3 included collection of optical imaging data from the visual cortex only, which are not included in this study. In session 4, we collected the optical imaging data and an electrophysiological measurement of the heartbeat for time-locking the arterial pulse. These are the data presented here. Participants' blood pressure was taken during sessions 2-4 and averaged to provide more stable estimates of their systolic and diastolic blood pressure.

Electrocardiogram Recording and Analysis

Lead I of the electrocardiogram (EKG, left wrist referenced to right wrist, impedance below 20 kOhm) was recorded with a Brain-Vision™ recorder and a Brain-Vision professional BrainAmp™

integrated amplifier system (Brain Products GmbH, Germany) with a sampling rate of 1000 Hz. The EKG data were extracted using EEGLab [60] and the optical pulse data were time-locked to the R-wave of the EKG. Each R-wave peak was found using an algorithm running on MATLAB R2014b (MathWorks, Natick, MA) that searches for peaks exceeding a certain voltage threshold (scaled for each subject) and discarding any points that fall outside the normal range of interbeat intervals. Manual visual inspection was also performed to ensure that any misidentifications of R-wave peak were discarded.

MRI acquisition and processing

Structural magnetic resonance images (sMRI) were collected for each participant using a 3T Siemens Trio full body scanner. A high resolution, 3D MPRAGE protocol was used, with flip angle = 9◦, TE = 2.32 ms, TR = 1900 ms, and inversion time = 900 ms. MR slices were obtained in the sagittal plane (192 slices, .9 mm slice thickness, voxel size .9 x .9 x .9 mm) having matrix dimensions of 192 x 256 x 256 (in-plane interpolated at acquisition to 192 x 512 x 512) and field of view of 172.8 x 230 x 230 mm. All images were visually examined by multiple researchers and no significant defects or distortions were discovered. Cortical reconstruction and volumetric segmentation were performed with the FreeSurfer© 5.3 image analysis suite (http://surfer.nmr.mgh.harvard.edu/; e.g., [61-65]. FreeSurfer morphometric procedures have been demonstrated to show good test-retest reliability across scanner manufacturers and across field strengths [65].

Optical Recording and Analysis

Recording. Optical data were recorded with six integrated frequency domain oxymeters (Imagent; ISS Inc., Champaign, IL). Data were collected from 24 detectors, each measuring light emitted by 16 time-multiplexed sources (384 channels), arranged in 4 different optical montages designed to cover the majority of the head. Sources and detectors were held flush to the participants' scalp using a custom-built, soft foam, adjustable cap (Figure 3.1a), giving rise to a total of 1536 channels (i.e., source-detector pairings; Figure 3.1b). This represents a fourfold increase in channels compared to what was

used by Fabiani et al. [23]. Laser diodes generated light at 830 and 690 nm (max amplitude: 10 mW, mean amplitude after multiplexing: 1 mW), modulated at 110 MHz. The light from the diodes was transmitted to the surface of the head by optic fibers (diameter = 400 µm; one fiber per emitter, with separate fibers carrying light at each of the two wavelengths, coupled at each location). Light was collected from the head using detector fiber bundles (diameter = 3 mm) connected to photomultiplier tubes (PMTs) fed with a current modulated at 110.003125 MHz, generating a 3.125 kHz cross-correlation frequency. A Fast Fourier Transform of the PMT output data was used to calculate DC (average) intensity, AC (amplitude), and relative phase, or photon, delay (in picoseconds). The analyses reported here are based on the AC intensity values. The arterial pulse is the largest phenomenon that can be measured using AC intensity, being easily visible on single trials [23]. Optical parameters were sampled at 39.0625 Hz (25.6 ms per sampling point).

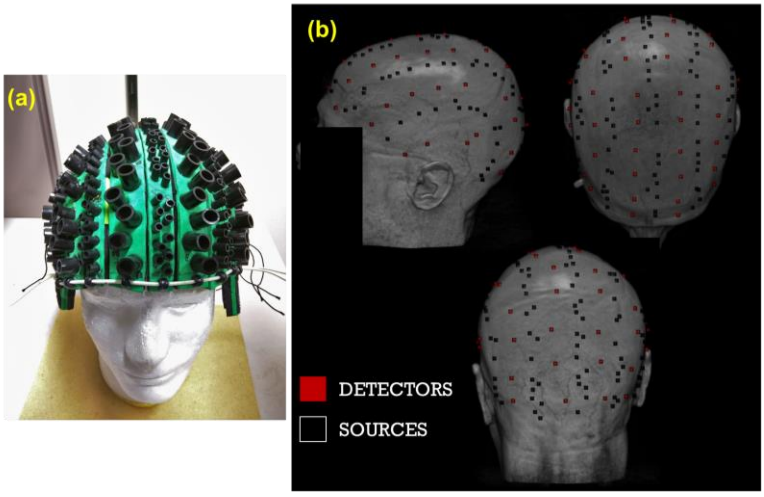

Figure 3.1. (a) Photograph of the soft foam, adjustable optical recording cap used in the study. Detectors were fitted into the larger tubes while sources were fitted into the smaller tubes. The cap was further secured to the subject's head by tightening an elastic band around its circumference of the cap and through the usage of a custom-built chin strap. (b) Locations of sources (black) and detectors (red) digitized in one representative participant, and plotted over the corresponding surface-rendered structural MRI (left, top and back views).

Co-registration with structural MRI. Using the nasion and preauricular points as references, the locations of individual optical sources and detectors were digitized using a Polhemus "3Space" FASTRAK

3D digitizer (Polhemus, Colchester, VT). T1-weighted structural magnetic resonance images were obtained for each subject. The Polhemus digitization points were then co-registered with the MR images first using the three fiducial markers and then surface fitting the entire set of digitized points to the estimated scalp surface based on a Levenberg-Marquardt algorithm (least-squares fit) using in-house software (Optical Coregistration Package, OCP [66]). Co-registration using this procedure has been shown to result in errors of less than 4 mm [66-67]. Figure 1b shows the digitized recording montage of one representative participant superimposed on the corresponding structural MRI. Measurement of pulse parameters.

Measurements were taken at rest for 8 blocks with each block lasting 6 minutes. Each of the 4 montages was recorded for a total of 2 blocks (12 minutes total recording time for each montage), with the sequence of 4 montages counterbalanced across subjects within each age sextile. The optical data were then normalized and a band-pass filter between 0.5-5Hz was applied. Pulse waveforms were then extracted from each channel by averaging AC light intensity, time-locked to the peak of the EKG R wave. Pulse epochs occurring during all blocks were then averaged together and baselined to the first peak diastole period occurring between 128-256 ms. In-house software, “Opt-3d” [68], was used to combine channels whose mean diffusion paths (modeled as a curved ellipsoid) intersected for a given brain volume [69]. Only source-detector distances between 2 and 6 cm were used in the analysis. Similar to Fabiani et al. [23], pulse amplitude was defined as the mean AC amplitude in an interval between 384 and 538 ms after R wave onset, an interval during which the peak systolic phase occurred in all subjects and for all brain regions. The arterial compliance measure was computed by calculating the area under the pulse waveform between the peak systole and the peak diastole, normalized by both time and amplitude and subtracted by a constant value of 0.5 (see [23]). Both pulse amplitude and arterial compliance data were extracted from an ROI comprising voxels covering most of the axial cortical surface (Talairach coordinates; X-axis: -45 to 45, Y-axis: -80 to 50). The denser optical array available in

this study provides a better signal-to-noise ratio with a two-point spatial resolution of <24 mm up to a depth of 30 mm [70]. It is now possible to compute arterial compliance on pulse waveforms in individual voxels and then average them, as opposed to computing it on a single waveform averaged over the axial surface (as it was done by [23]).

The global measurements of pulse amplitude and arterial compliance obtained in this manner were used for all analyses except when investigating regional effects of arterial compliance on OSPAN, where we extracted arterial compliance measurements from ROIs based on Brodmann area boundaries (as defined by [71-72]). For the reliability analyses, pulse amplitude and arterial compliance measures were extracted and compared between the block 1 and block 2 data that were collected for each of the 4 montages. For all other analyses, blocks were collapsed together.

General Analytic Approach

The analyses presented in this paper are designed to examine changes in cerebral pulse amplitude and arterial compliance as a function of age, first at the global level and then in some selected regions (regional analysis). Age was treated as a continuous variable for all statistical analyses. However, to create figures facilitating comparisons across age groups (Figure 3.1b), and for mapping age-related differences in pulse parameters on the brain (Figure 3.4b), subjects were divided into three age groups (as described in Table 1). Given that the goals of this paper were to replicate and extend the findings reported by Fabiani et al. [23] and to investigate known brain regions involved in the OSPAN task, one-tailed tests were used based on our a-priori directional hypotheses.

Results

Effects of Age and eCRF

Here we summarize data indicating that our sample exhibits the typical relationships between age, eCRF, cognitive function and neuroanatomy. As expected, age was negatively correlated with eCRF after partialing out gender, $r(44) = -.74$, $p < .001$. Controlling for estimated total intracranial volume

(eTIV), age also showed significant negative correlations with global brain volumetric measures, cortical white matter ($r(44) = -.43$, $p = .002$), cortical gray matter ($r(44) = -.82$, $p < .001$) and subcortical gray matter ($r(44) = -.76$, $p < .001$). Correlations with eCRF were similar, with higher eCRF being associated with greater cortical white matter ($r(43) = .29$, $p = .026$), cortical gray matter ($r(43) = .63$, $p < .001$) and subcortical gray matter ($r(43) = .56$, $p < .001$), controlling for both gender and eTIV. These results are in line (with respect to both magnitude and direction) with those reported by Fabiani et al. [23] and others (see [73] for a review). These results are also in agreement with findings showing that higher eCRF is associated with reduced atrophy in brain volumetric measures (e.g., [44-45], [74]; see [75] for a discussion of the overlap between the effects of age and fitness on regional brain anatomy).

Reliability of Pulse Parameters

We first set out to assess the reliability of pulse amplitude and arterial compliance measures by comparing the measures obtained in blocks 1 and 2, extracted from all 4 montages. Pulse amplitude measurements were highly reliable from block 1 to block 2, $r(45) = .99$, $p < .001$ (Figure 3.2a). Data from one additional subject were removed from the arterial compliance reliability analyses because they were statistical outliers, Z score > |2.5|. Arterial compliance was also highly reliable across blocks, $r(44) = .69$, $p < .001$ (see Figure 3.2b). This replicates our initial findings [23] that both measures show good reliability, with pulse amplitude being more stable than arterial compliance. The reliability of arterial compliance was higher in the current study, $r(44) = .69$ compared to our previous report, $r(51) = .56$, which may be due to a number of factors, including (a) the use of a denser optical array; (b) the increase in recording time from 72 to 360 s; and (3) the computation of arterial compliance on waveforms at the voxel level before averaging. For all other analyses, data from all blocks were combined.

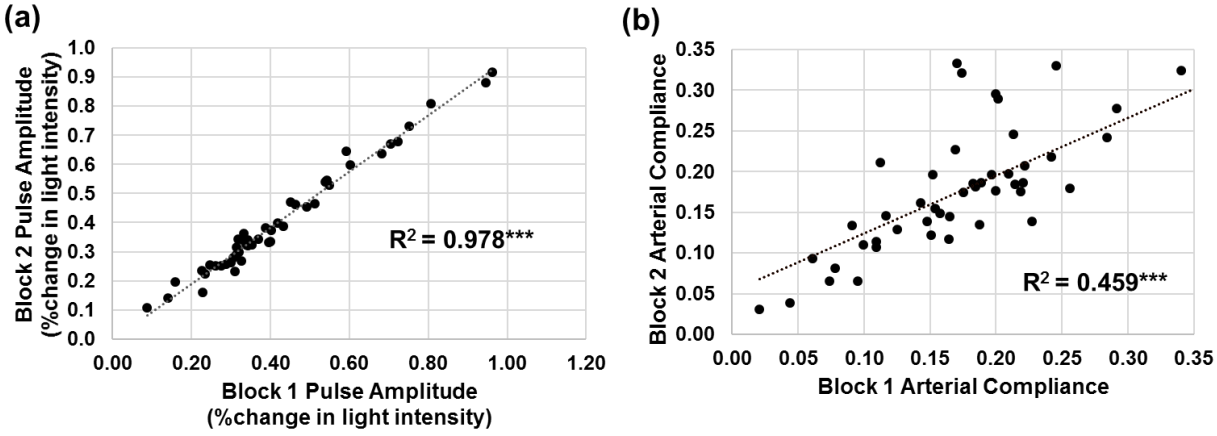

Figure 3.2. (a) Correlation between block 1 and 2 for pulse amplitude (expressed in percent change in light intensity). (b) Correlation between block 1 and 2 for arterial compliance (compliance is a dimensionless measure indicating the change of the shape of the diastolic section of the pulse from a straight line, with 0 indicating a straight, oblique line, and 0.5 indicating a flat line lasting the whole duration of the diastole followed by a vertical ascent).

Relationship between cerebral pulse amplitude and other variables

Of the 47 subjects, two were removed from the pulse amplitude analysis as they were outliers on the pulse amplitude measure (Z score > |2.5|) after combining data from all blocks together. Cerebral pulse amplitude was found to be positively correlated with pulse pressure measured at the arm ($r(43) = .36$, $p = .008$). As seen in Figure 3.3a, pulse amplitude was also significantly correlated with age, $r(43) = .31$, $p = .019$). This figure suggests the presence of increased pulse amplitude variability with age. In order to test whether this was indeed the case, we computed squared standardized residuals after regressing pulse amplitude on age. A correlation of these residuals with age confirmed that older age was associated with greater variance in pulse amplitude ($r(43) = .42$, $p = .002$). We further investigated whether this increase in variation with age was mediated by eCRF. After regressing age and gender from eCRF for the analysis, a 5000 bootstrap samples mediation analysis did not reveal a significant mediation effect of eCRF, 95% CI [-.0579, .0180]. Gold standard quantification of cardiorespiratory fitness using

VO2max measures may allow us to better explain the greater variation in pulse amplitude for older subjects in the future. Increase variation of pulse amplitude with age may also reflect the use of blood pressure medication in 3 older subjects. This may also reduce the correlations between pulse amplitude measures and other variables in the experiment. Figure 3.3b shows the cerebral pulse waveforms after dividing subjects into three age groups (see Table 3.1). The waveforms show a graded increase in pulse amplitude with age.

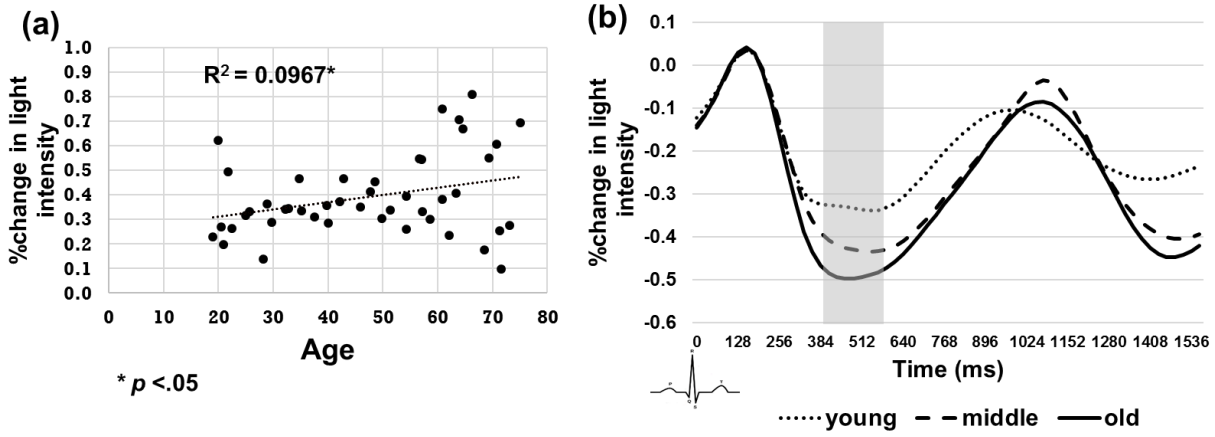

Figure 3.3 (a) Scatter plot showing that older age is associated with larger pulse amplitude (expressed as percent change in light intensity). (b) Average pulse waveforms split into age tertiles. The transparent gray bar indicates the time interval in which pulse amplitude values were extracted and averaged.

After controlling for gender, higher eCRF was not associated with lower pulse amplitude (r(42) = -.24, p = .056). Although this relationship was also not found by Fabiani et al. [23], the effect size in the current study was stronger in the predicted direction (r(42) = -.24 compared to r(50) = .083), which suggests that this association may be small but could become significant with greater sample size. Similar to Fabiani et al. [23], higher pulse amplitude was not associated with lower cortical white matter volume (r(42) = -.21, p = .091). However, we did find that higher pulse amplitude was associated with lower cortical gray matter volume (r(42) = -.33, p = .015) and subcortical gray matter volume (r(42) = -

.28, p = .035), controlling for eTIV. Similar to what was reported by Fabiani et al. [23], smaller pulse amplitude was not correlated with better performance on any neuropsychological tests.

Relationship between cerebral arterial compliance and other variables

Out of the sample of 47 subjects, one was removed from the arterial compliance analysis due to being a statistical outlier, Z score > |2.5|. Figure 3.4a shows that cerebral arterial compliance declines with age (r(44) = -.43, p < .001), replicating and extending previous findings. In addition, regional variations in arterial compliance are shown in Figure 3.4b for each of the three age groups. Unlike the pulse amplitude parameter, the variability in arterial compliance did not increase with age (r(44) = -.11, p = .24). This may reflect the fact that blood pressure medications (which may alter pulse amplitude estimates) may have little direct influence on arterial stiffness and arterial compliance (although they might produce a long term preventative effect). Greater eCRF was associated with higher arterial compliance (r(43) = .32, p = .017), controlling for gender.

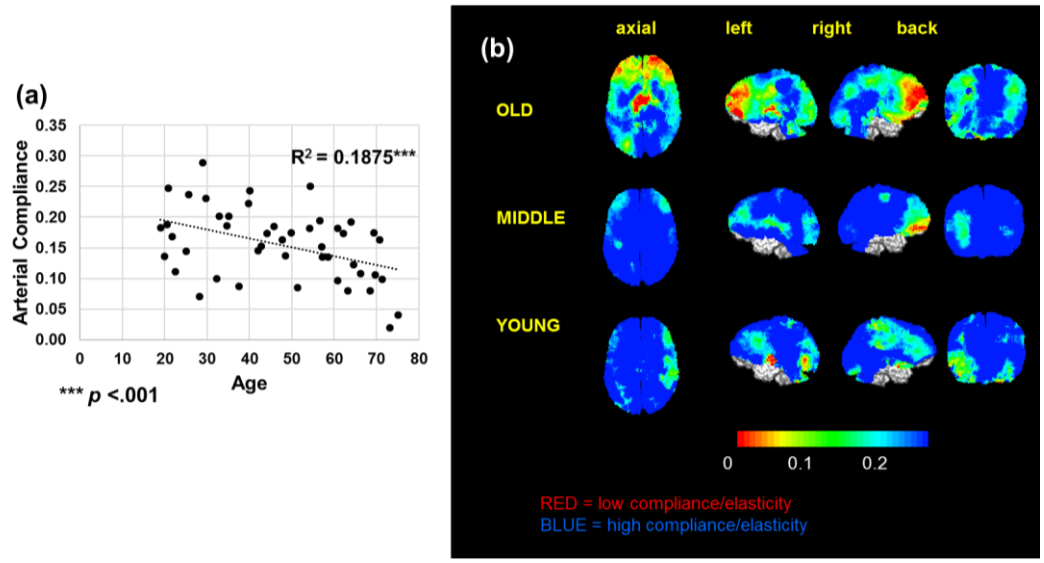

Figure 3.4 (a) Older age is associated with lower arterial compliance (i.e., greater arterial stiffness). b) Arterial compliance maps derived from age tertiles. Compared to younger subjects, older subjects appear to show poorer arterial compliance (red regions), especially in prefrontal areas.

Figure 3.5 shows 2 younger and 2 older representative subjects varying in fitness levels. In general, subjects who are younger and relatively fitter within their age group have higher arterial compliance. Better arterial compliance was also positively correlated with cortical white matter volume ($r(43) = .29$, $p = .028$), cortical gray matter ($r(43) = .35$, $p = .010$) and subcortical gray matter ($r(43) = .37$, $p = .007$), controlling for eTIV. Similar to data presented in Fabiani et al. [23], arterial compliance was also not correlated with pulse amplitude, ($r(42) = -.047$, $p = .76$), suggesting again that these are separate indices of brain arterial function.

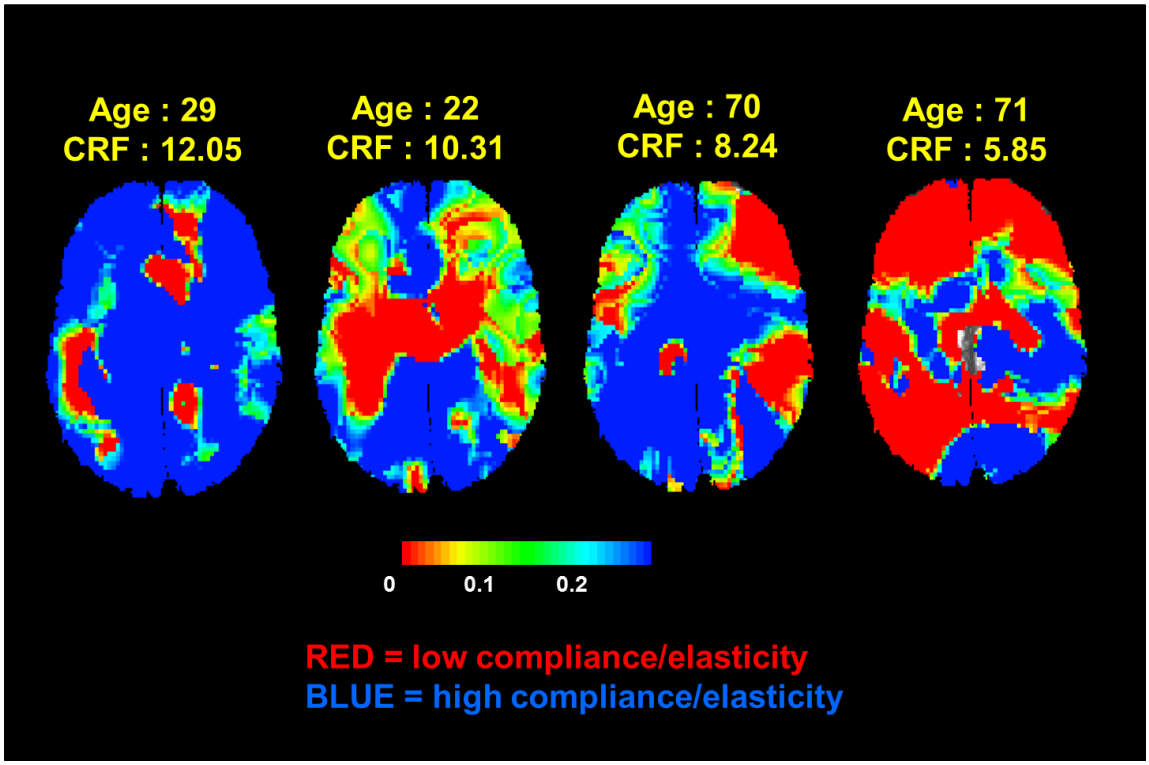

Figure 3.5. Maps of the arterial compliance estimate in four representative subjects varying in age and eCRF. In general, subjects who are younger and relatively fitter show greater arterial compliance (blue regions).

Two subjects did not complete the WCST. Higher global arterial compliance was associated with many components of the WCST, including total number of trials ($r(42) = .27$, $p = .037$), number of errors ($r(42) = -.33$, $p = .014$), number of perseverative responses ($r(42) = -.28$, $p = .032$), number of perseverative errors ($r(42) = -.31$, $p = .021$) and number of non-perseverative errors ($r(42) = -.32$, $p =$

.016), replicating previous findings that indicate that lower arterial compliance is associated with poorer cognitive flexibility.

Relationship between regional arterial compliance and other variables

One of the main advantages of these new optical methods is their potential to investigate not only the global effects of changes in cerebrovascular health, but also regional, localized effects that are not easily investigated with other means. Here we focused on specific regions that are known to support working memory function (for a review see [76]) and hypothesized that greater arterial compliance in these regions would be predictive of better performance in the OSPAN task. We extracted arterial compliance measures from frontoparietal regions (BA 9 and BA 7) and averaged them, and found the predicted association ($r(44) = .25$, $p = .045$, see Figure 3.6a). This relationship was not found when correlating OSPAN performance with global arterial compliance ($r(44) = .18$, $p = .11$). These data therefore provide evidence suggesting that there is added value in extracting regional measures of arterial compliance, permitting to examine relationships that might be washed out when global measures of arterial compliance are used. Further, as hypothesized, we found that arterial compliance in frontoparietal regions (BA 9 and BA 7) decreased with age ($r(44) = -.45$, $p < .001$) and increased with eCRF ($r(43) = .38$, $p = .004$) while arterial compliance in the visual cortex (BA 17 and BA 18) was not associated with age ($r(44) = -.17$, $p = .12$) or eCRF ($r(43) = .13$, $p = .19$), controlling for gender (Figs 3.6b and 3.6c). Taken together these results suggest that, similar to regional variations in age-related brain atrophy [38-39], hypoperfusion [40-41] and the neuroprotective benefits of fitness (see [44] for a review), reductions in arterial compliance in the brain also do not occur at similar rates in all regions, and that regional reductions in arterial compliance may have differential impact on cognition depending on where it occurs.

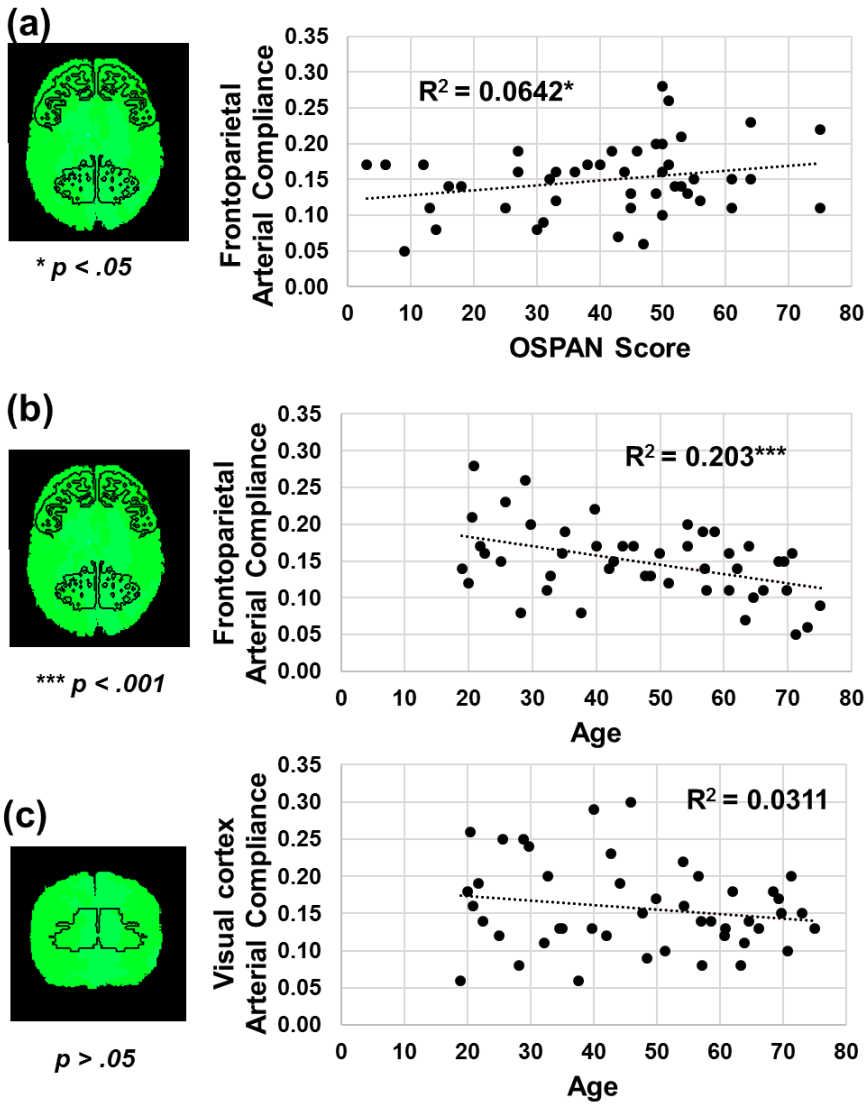

Figure 3.6. (a) Greater regional arterial compliance in frontoparietal regions (BA7 and BA9) was associated with performance on the OSPAN task. (b) Lower regional arterial compliance in frontoparietal regions (BA7 and BA9) was also associated with older age. c) Arterial compliance in the visual cortex (BA17 and BA18) was not associated with age.

Discussion

The results presented in the current paper represent evidence supporting the novel use of diffuse optical imaging methods to study cerebrovascular health and its functional consequences on cognitive decline over the course of life span development and aging. The importance of these findings

is underscored by growing evidence showing that disruptions in the microcirculatory processes in the brain's vasculature are closely linked to neurodegeneration in cognitive and brain aging [77-78]. In addition, a large scale study involving over 6000 autopsy reports found that patients with Alzheimer's disease had a significantly higher association with cerebrovascular disease and vascular pathology than other neurodegenerative diseases, suggesting that targeting cerebrovascular pathology for early intervention may help prevent or slow down the clinical manifestations of Alzheimer's disease [79]. Within this larger context, the results from the current study support the critical role of cerebrovascular health in brain and cognitive decline in the normal aging process. We have largely replicated the initial findings reported by Fabiani et al. [23] in a sample including only older adults, and extended them to a wider age range including much of the adult lifespan (18- 75).

For pulse amplitude, we replicated the positive correlations with age and pulse pressure reported by and colleagues [23]. We did not find any pulse amplitude associations with cortical white matter volume, eCRF and cognitive function. However, we found that larger pulse was associated with reduced cortical and subcortical gray matter volumes. This new evidence of associations between pulse amplitude and gray matter volume may be in part driven by the increase in signal-to-noise ratio (SNR) and the wider age-range available in the current study. These results are consistent with our original interpretation that, similarly to systemic pulse pressure measurements, pulse amplitude measures reflect both the long-term properties of the cerebrovascular system and also other factors such as the current state of the cerebrovascular tone (see also [29]).

For arterial compliance, we replicated our initial findings that greater arterial compliance is associated with younger age and higher eCRF, is predictive of global white and gray matter volume, as well as cognitive flexibility (as measured by the WCST). Many of the correlations between pulse amplitude and arterial compliance with age, eCRF, anatomy and cognitive function were very similar across both studies. These results suggest that we can reliably measure pulse amplitude and arterial

compliance both within and across studies. Maps of arterial compliance in the three age groups also showed clear differences, with older adults showing less compliance, especially in prefrontal regions. We empirically tested the functional consequences of the differences shown by the arterial compliance maps and found that arterial compliance in frontoparietal regions was associated with working memory performance indexed by the OSPAN task. Although global measures of arterial compliance can provide a quick overview of the general state of cerebral arterial health, our results suggest that regional arterial compliance may be more useful for investigating age and fitness-related declines in specific cognitive domains.

Other studies have used methodologies such as transcranial Doppler (TCD) ultrasound (see [79] for a review) and ASL [81-82] to investigate the relationship between cerebrovascular health and cognition. However, these measures lack the level of sensitivity to regional specificity afforded by diffuse optical imaging. TCD ultrasound relies on measuring blood flow velocity as an index of cerebral arterial compliance but is limited to the insonation of a few large arteries such as the middle cerebral artery (MCA). Likewise, although absolute measurements of cerebral blood flow using ASL can be derived, they are still limited by their intrinsically low SNR [83], which restricts ASL utility for examining regional relationships with domain-specific cognitive function associated with the OPSAN task and others.

The regional associations of arterial compliance and working memory performance index by the OSPAN task may provide an explanation for ceiling effects seen in blood-oxygen level dependent (BOLD) functional MRI studies on working memory. Schneider-Garces et al. [34] suggested that ceiling effects seen in both regional BOLD activity and performance at high memory loads may be due to either a limitation in working memory capacity (“cognitive” explanation) or a limitation in vascular supply (“energetic explanation”). Variation in regional compliance may provide some support for the “energetic explanation”. In other words, changes in regional neuronal activity as a function of cognitive load and its subsequent hemodynamic consequences may be both mediated by the physiological compliance of the

corresponding regional arterial supply. Future studies using concurrent fMRI and diffusive optical imaging may be able to further test this hypothesis.

In the current study we did not find an association between pulse amplitude and arterial compliance. This is consistent with data showing that systemic arterial compliance quantified using PWV measures is an independent predictor of vascular pathology and provides prognostic value over pulse pressure alone [84]. Cruickshank et al. [85] suggests that poor aortic arterial compliance reflects an integrated index of vascular damage over time, resulting in generalized “wear and tear” from repeated distension and recoil of blood vessels, and that multiple extraneous factors also contribute, such as smoking, lipidic dysfunction and glucose metabolism.

These results align with studies showing not only that arterial aging occurs early in life [15], but also that low physical activity in adolescents and young adults is independently associated with poorer arterial compliance [86]. In combination with studies showing that even modest increases in moderate-to-vigorous physical activity can improve systemic arterial stiffness measured using brachial-ankle pulse wave velocity (baPWV) in young adults [87], these studies provide converging evidence that although vascular risk factors accumulate from a young age, they are also amenable to change with adequate increase in physical activity. Although our results are consistent with these interpretations, whether increases in physical activity level can affect not only systemic arterial stiffness but also regional cerebral vascular stiffness, and whether it results in any improvement in cognitive function remain to be seen. Future studies should focus on using longitudinal intervention designs to elucidate these relationships.

Limitations of the current study include (a) the limited penetration of diffuse optical imaging, which precludes the examination of deep arteries and (b) the relatively low spatial resolution of the method. We have addressed the issue of low spatial resolution by using a much denser optical array in the current study, but this comes at the cost of an extended optical recording session which may limit its use in clinical settings. However, given that the associations between the pulse parameters and other

important variables are very similar in both the initial study and the current study, it may be the case that a relatively sparse recording array is sufficient to see these effects.

In summary, the results of the current study replicated and extended our initial findings that noninvasive measures derived from diffuse optical imaging can index cerebrovascular health. This is also the first study demonstrating the utility of regional arterial compliance measures in predicting working memory performance measured by the OSPAN task. This cumulative evidence supports the utility of optical imaging as a complementary method for assessing the status of the brain's arterial system and its consequences on cognition function and brain anatomy, in conjunction with other traditional methods such as MRI and Doppler ultrasound.

References

1. Elias, M. F., Robbins, M. A., Budge, M. M., Abhayaratna, W. P., Dore, G. A., & Elias, P. K.(2009). Arterial pulse wave velocity and cognition with advancing age. Hypertension, 53(4), 668–673. http://doi.org/10.1161/HYPERTENSIONAHA.108.126342

2. Singer, J., Trollor, J. N., Baune, B. T., Sachdev, P. S., & Smith, E. (2014). Arterial stiffness, the brain and cognition: A systematic review. Ageing Research Reviews, 15, 16–27. http://doi.org/10.1016/j.arr.2014.02.002

3. Scuteri, A., & Wang, H. (2014). Pulse wave velocity as a marker of cognitive impairment in the elderly. Journal of Alzheimer's Disease: JAD, 42 Suppl 4, S401–410. http://doi.org/10.3233/JAD-141416

4. Unverzagt, F. W., McClure, L. A., Wadley, V. G., Jenny, N. S., Go, R. C., Cushman, M., … Howard, G. (2011). Vascular risk factors and cognitive impairment in a stroke-free cohort. Neurology, 77(19), 1729–1736. http://doi.org/10.1212/WNL.0b013e318236ef23

5. Waldstein, S. R., Rice, S. C., Thayer, J. F., Najjar, S. S., Scuteri, A., & Zonderman, A. B. (2008). Pulse pressure and pulse wave velocity are related to cognitive decline in the Baltimore Longitudinal Study of Aging. Hypertension, 51(1), 99–104. http://doi.org/10.1161/HYPERTENSIONAHA.107.093674.

6. Zeki Al Hazzouri, A., Newman, A. B., Simonsick, E., Sink, K. M., Sutton Tyrrell, K., Watson, N., … Health ABC Study. (2013). Pulse wave velocity and cognitive decline in elders: the Health, Aging, and Body Composition study. Stroke; a Journal of Cerebral Circulation, 44(2), 388–393. http://doi.org/10.1161/STROKEAHA.112.673533

7. Beauchet, O., Celle, S., Roche, F., Bartha, R., Montero-Odasso, M., Allali, G., & Annweiler, C. (2013). Blood pressure levels and brain volume reduction: a systematic review and meta-analysis. Journal of Hypertension, 31(8), 1502–1516. http://doi.org/10.1097/HJH.0b013e32836184b5

8. Hughes, T. M., Craft, S., & Lopez, O. L. (2015). Review of “the potential role of arterial stiffness in the pathogenesis of Alzheimer”s disease’. Neurodegenerative Disease Management, 5(2), 121–135. http://doi.org/10.2217/nmt.14.53

9. Joas, E., Bäckman, K., Gustafson, D., Ostling, S., Waern, M., Guo, X., & Skoog, I. (2012). Blood pressure trajectories from midlife to late life in relation to dementia in women followed for 37 years. Hypertension, 59(4), 796–801. http://doi.org/10.1161/HYPERTENSIONAHA.111.182204

10. Kalaria, R. N., Akinyemi, R., & Ihara, M. (2012). Does vascular pathology contribute to Alzheimer changes? Journal of the Neurological Sciences, 322(1–2), 141–147. http://doi.org/10.1016/j.jns.2012.07.032

11. Rabkin, S. W. (2012). Arterial stiffness: detection and consequences in cognitive impairment and dementia of the elderly. Journal of Alzheimer’s Disease: JAD, 32(3), 541–549. http://doi.org/10.3233/JAD-2012-120757

12. Meaume, S., Benetos, A., Henry, O. F., Rudnichi, A., & Safar, M. E. (2001). Aortic pulse wave velocity predicts cardiovascular mortality in subjects >70 years of age. Arteriosclerosis, Thrombosis, and Vascular Biology, 21(12), 2046–2050.

13. Sutton-Tyrrell, K., Najjar, S. S., Boudreau, R. M., Venkitachalam, L., Kupelian, V., Simonsick, E. M., … Health ABC Study. (2005). Elevated aortic pulse wave velocity, a marker of arterial stiffness, predicts cardiovascular events in well-functioning older adults. Circulation, 111(25), 3384–3390. http://doi.org/10.1161/CIRCULATIONAHA.104.483628

14. Pizzi, O. L., Brandão, A. A., Pozzan, R., Magalhães, M. E. C., Campana, E. M. G., Fonseca, F. L., … Brandão, A. P. (2013). Pulse wave velocity, blood pressure and adipocytokines in young adults: the Rio de Janeiro study. Arquivos Brasileiros De Cardiologia, 100(1), 60– 66.

15. Nilsson, P. M., Lurbe, E., & Laurent, S. (2008). The early life origins of vascular ageing and cardiovascular risk: the EVA syndrome. Journal of Hypertension, 26(6), 1049–1057. http://doi.org/10.1097/HJH.0b013e3282f82c3e

16. Scuteri, A., & Lakatta, E. G. (2013). Bringing prevention in geriatrics: evidences from cardiovascular medicine supporting the new challenge. Experimental Gerontology, 48(1), 64–68. http://doi.org/10.1016/j.exger.2012.02.009

17. Maillard, P., Seshadri, S., Beiser, A., Himali, J. J., Au, R., Fletcher, E., … DeCarli, C. (2012). Effects of systolic blood pressure on white-matter integrity in young adults in the Framingham Heart Study: a cross-sectional study. Neurology, 11(12), 1039–1047. http://doi.org/10.1016/S1474-4422(12)70241-7

18. Fernhall, B., & Agiovlasitis, S. (2008). Arterial function in youth: window into cardiovascular risk. Journal of Applied Physiology, 105(1), 325–333. http://doi.org/10.1152/japplphysiol.00001.2008

19. Ferreira, I., Twisk, J. W. R., van Mechelen, W., Kemper, H. C. G., & Stehouwer, C. D. A. (2005). Development of fatness, fitness, and lifestyle from adolescence to the age of 36 years: determinants of the metabolic syndrome in young adults: the amsterdam growth and health longitudinal study. Archives of Internal Medicine, 165(1), 42–48. http://doi.org/10.1001/archinte.165.1.42

20. Scuteri, A., Najjar, S. S., Orru', M., Usala, G., Piras, M. G., Ferrucci, L., … Lakatta, E. G. (2010). The central arterial burden of the metabolic syndrome is similar in men and women: the SardiNIA Study. European Heart Journal, 31(5), 602–613. http://doi.org/10.1093/eurheartj/ehp491

21. Cruickshank, J. K., Rezailashkajani, M., & Goudot, G. (2009). Arterial stiffness, fatness, and physical fitness: ready for intervention in childhood and across the life course? Hypertension, 53(4), 602–604. http://doi.org/10.1161/HYPERTENSIONAHA.108.128033

22. Scuteri, A. (2012). Brain injury as end-organ damage in hypertension. The Lancet. Neurology, 11(12), 1015–1017. http://doi.org/10.1016/S1474-4422(12)70265-X

23. Fabiani, M., Low, K. A., Tan, C.H., Zimmerman, B., Fletcher, M. A., Schneider-Garces, N., … Gratton, G. (2014). Taking the pulse of aging: mapping pulse pressure and elasticity in cerebral arteries with optical methods. Psychophysiology, 51(11), 1072–1088. http://doi.org/10.1111/psyp.12288

24. Alian, A. A., & Shelley, K. H. (2014). Photoplethysmography: Analysis of the pulse oximeter waveform. In J. M. Ehrenfeld & M. Cannesson (Eds.), Monitoring technologies in acute care environments (pp. 165–178). New York, NY: Springer. doi: 10.1007/978-1- 4614-8557-5_19

25. Themelis, G., D'Arceuil, H., Diamond, S. G., Thaker, S., Huppert, T. J., Boas, D. A., & Franceschini, M. A. (2007). Near-infrared spectroscopy measurement of the pulsatile component of cerebral blood flow and volume from arterial oscillations. Journal of Biomedical Optics, 12, 014033. doi: 10.1117/1.2710250

26. Fabricius, M., Akgören, N., Dirnagl, U., & Lauritzen, M. (1997). Laminar analysis of cerebral blood flow in cortex of rats by laser-Doppler flowmetry: a pilot study. Journal of Cerebral Blood Flow and Metabolism:, 17(12), 1326–1336. http://doi.org/10.1097/00004647-199712000-00008

27. Ebihara, A., Tanaka, Y., Konno, T., Kawasaki, S., Fujiwara, M., & Watanabe, E. (2013). Detection of cerebral ischemia using the power spectrum of the pulse wave measured by near-infrared spectroscopy. Journal of Biomedical Optics, 18, 1–8. doi: 10.1117/1.JBO.18.10.106001

28. Zimmerman, B., Sutton, B.P., Low, K.A., Tan, C.H., Schneider-Garces, N., Fletcher, M.A., Li, Y., Ouyang, C., Maclin, E.L., Gratton, G., & Fabiani, M. (2014). Cardiorespiratory fitness mediates the effects of aging on cerebral blood flow. Frontiers in Aging Neuroscience, 8, 59. http:// dx.doi.org/10.3389/fnagi.2014.00059

29. Tan, C.H., Low, K. A., Schneider-Garces, N., Fletcher, M., Zimmerman, B., Maclin, E.L., Chiarelli, A. M., Gratton, G. & Fabiani, M. (inpress) Optical measures of changes in cerebral vascular tone during voluntary breath holding and a Sternberg memory task. Biological Psychology.

30. Mayeux, R., Stern, Y., Rosen, J., & Leventhal, J. (1981). Depression, intellectual impairment, and Parkinson disease. Neurology, 31(6), 645–650.

31. Unsworth, N., Heitz, R. P., Schrock, J. C., & Engle, R. W. (2005). An automated version of the operation span task. Behavior Research Methods, 37(3), 498–505.

32. Altamura, M., Elvevåg, B., Blasi, G., Bertolino, A., Callicott, J. H., Weinberger, D. R., … Goldberg, T. E. (2007). Dissociating the effects of Sternberg working memory demands in prefrontal cortex. Psychiatry Research, 154(2), 103–114. http://doi.org/10.1016/j.pscychresns.2006.08.002

33. D'Esposito, M., Postle, B. R., & Rypma, B. (2000). Prefrontal cortical contributions to working memory: evidence from event-related fMRI studies. Experimental Brain Research, 133(1), 3–11.

34. Schneider-Garces, N. J., Gordon, B. A., Brumback-Peltz, C. R., Shin, E., Lee, Y., Sutton, B. P., … Fabiani, M. (2010). Span, CRUNCH, and beyond: working memory capacity and the aging brain. Journal of Cognitive Neuroscience, 22(4), 655–669. http://doi.org/10.1162/jocn.2009.21230

35. Veltman, D. J., Rombouts, S. A. R. B., & Dolan, R. J. (2003). Maintenance versus manipulation in verbal working memory revisited: an fMRI study. NeuroImage, 18(2), 247–256.

36. Zarahn, E., Rakitin, B., Abela, D., Flynn, J., & Stern, Y. (2007). Age-related changes in brain activation during a delayed item recognition task. Neurobiology of Aging, 28(5), 784–798. http://doi.org/10.1016/j.neurobiolaging.2006.03.002

37. Fabiani, M. (2012). It was the best of times, it was the worst of times: A psychophysiologist's view of cognitive aging. Psychophysiology, 49, 293-304. http://dx.doi.org/10.1111/j.1469-8986.2011.01331.x

38. Raz, N., Gunning, F. M., Head, D., Dupuis, J. H., McQuain, J., Briggs, S. D., … Acker, J. D. (1997). Selective aging of the human cerebral cortex observed in vivo: differential vulnerability of the prefrontal gray matter. Cerebral Cortex, 7(3), 268–282.

39. Resnick, S. M., Pham, D. L., Kraut, M. A., Zonderman, A. B., & Davatzikos, C. (2003). Longitudinal magnetic resonance imaging studies of older adults: a shrinking brain. The Journal of Neuroscience, 23(8), 3295–3301.

40. Alosco, M. L., Gunstad, J., Jerskey, B. A., Xu, X., Clark, U. S., Hassenstab, J., … Sweet, L. H. (2013). The adverse effects of reduced cerebral perfusion on cognition and brain structure in older adults with cardiovascular disease. Brain and Behavior, 3(6), 626–636. http://doi.org/10.1002/brb3.171

41. Alsop, D. C., Detre, J. A., & Grossman, M. (2000). Assessment of cerebral blood flow in Alzheimer's disease by spin-labeled magnetic resonance imaging. Annals of Neurology, 47(1), 93–100.

42. Dupuy, O., Gauthier, C. J., Fraser, S. A., Desjardins-Crèpeau, L., Desjardins, M., Mekary, S., … Bherer, L. (2015). Higher levels of cardiovascular fitness are associated with better executive function and prefrontal oxygenation in younger and older women. Frontiers in Human Neuroscience, 9, 66. http://doi.org/10.3389/fnhum.2015.00066

43. Colcombe, S. J., Erickson, K. I., Raz, N., Webb, A. G., Cohen, N. J., McAuley, E., & Kramer, A. F. (2003). Aerobic fitness reduces brain tissue loss in aging humans. The Journals of Gerontology. Series A, Biological Sciences and Medical Sciences, 58(2), 176–180.

44. Erickson, K. I., Leckie, R. L., & Weinstein, A. M. (2014). Physical activity, fitness, and gray matter volume. Neurobiology of Aging, 35 Suppl 2, S20–28. http://doi.org/10.1016/j.neurobiolaging.2014.03.034

45. Gordon, B., Rykhlevskaia, E., Brumback, C. R., Lee, Y., Elavsky, S., Konopack, J. F., McAuley, E., Kramer, A. F., Colcombe, S., Gratton, G., & Fabiani, M. (2008). Anatomical correlates of aging,

cardiopulmonary fitness level, and education. Psychophysiology, 45(5), 825-838. http://dx.doi.org/10.1111/j.1469-8986.2008.00676.x

46. Beck, A. T., Steer, R. A., & Brown, G. K. (1996). Manual for the Beck Depression Inventory (2nd ed.). San Antonio, TX: The Psychological Corporation.

47. Oldfield, R. C. (1971). The assessment and analysis of handedness: the Edinburgh inventory. Neuropsychologia, 9(1), 97–113.

48. Kaufman, A. S., & Kaufman, N. L. (2004). Kaufman brief intelligence test (2nd ed.). San Antonio, TX: The Psychological Corporation.

49. Raven, J., Raven, J.C., & Court, J.H. (2003) Manual for Raven's Progressive Matrices and Vocabulary Scales. San Antonio, TX: Harcourt Assessment.

50. Shipley, W. C. (1940). A self-administering scale for measuring intellectual impairment and deterioration. Journal of Psychology, 9, 371–377.

51. Heaton, R. K. (1981). Wisconsin card sorting test manual, Odessa, FL: Psychological Assessment Resources, Inc.

52. Tien, A.Y., Spevack, T. V., Jones, D.W., Pearlson, G. D., Schlaepfer, T. E., & Strauss, M. E. (1996). Computerized Wisconsin card sorting test: Comparison with manual administration. Journal of Medical Sciences, 12, 479–485.

53. Benton, A. L., & Hamsher, K. (1989). Multilingual aphasia examination manual. Iowa City, IA: University of Iowa.

54. Corrigan, J. D., & Hinkeldey, N. S. (1987). Relationships between parts A and B of the Trail Making Test. Journal of Clinical Psychology, 43(4), 402–409.

55. Wechsler D. (2009) Wechsler Memory Scale–Fourth Edition. Pearson; San Antonio, TX.

56. Jurca, R., Jackson, A. S., LaMonte, M. J., Morrow, J. R, Jr., Blair, S. N., Wareham, N. J., . . . Laukkanen, R. (2005). Assessing cardiorespiratory fitness without performing exercise testing. American Journal of Preventive Medicine, 29, 185–193. doi: 10.1016/j.amepre.2005.06.004

57. Stamatakis, E., Hamer, M., O'Donovan, G., Batty, G. D., & Kivimaki, M. (2013). A nonexercise testing method for estimating cardiorespiratory fitness. European Heart Journal, 34, 750–758. doi: 10.1093/eurheartj/ ehs097.

58. Mailey, E. L., White, S. M., Wójcicki, T. R., Szabo, A. N., Kramer, A. F., & McAuley, E. (2010). Construct validation of a non-exercise measure of cardiorespiratory fitness in older adults. BMC Public Health, 10, 59. http://doi.org/10.1186/1471-2458-10-59

59. McAuley, E., Szabo, A. N., Mailey, E. L., Erickson, K. I., Voss, M., White, S. M., … Kramer, A. F. (2011). Non-Exercise Estimated Cardiorespiratory Fitness: Associations with Brain Structure, Cognition, and Memory Complaints in Older Adults. Mental Health and Physical Activity, 4(1), 5–11. http://doi.org/10.1016/j.mhpa.2011.01.001

60. Delorme, A., & Makeig, S. (2004). EEGLAB: An open source toolbox for analysis of singletrial EEG dynamics including independent component analysis. Journal of Neuroscience Methods, 134, 9–21. http://doi.org/10.1016/j.jneumeth.2003.10.009

61. Dale, A. M., Fischl, B., & Sereno, M. I. (1999). Cortical surface-based analysis. I. Segmentation and surface reconstruction. NeuroImage, 9(2), 179–194. http://doi.org/10.1006/nimg.1998.0395

62. Fischl, B., & Dale, A. M. (2000). Measuring the thickness of the human cerebral cortex from magnetic resonance images. Proceedings of the National Academy of Sciences of the United States of America, 97(20), 11050–11055. http://doi.org/10.1073/pnas.200033797

63. Fischl, B., Liu, A., & Dale, A. M. (2001). Automated manifold surgery: constructing geometrically accurate and topologically correct models of the human cerebral cortex. IEEE Transactions on Medical Imaging, 20(1), 70–80. http://doi.org/10.1109/42.906426

64. Fischl, B., Salat, D. H., Busa, E., Albert, M., Dieterich, M., Haselgrove, C., … Dale, A. M. (2002). Whole brain segmentation: automated labeling of neuroanatomical structures in the human brain. Neuron, 33(3), 341–355.

65. Han, X., Jovicich, J., Salat, D., van der Kouwe, A., Quinn, B., Czanner, S., … Fischl, B. (2006). Reliability of MRI-derived measurements of human cerebral cortical thickness: the effects of field strength, scanner upgrade and manufacturer. NeuroImage, 32(1), 180–194. http://doi.org/10.1016/j.neuroimage.2006.02.051

66. Chiarelli, A. M., Maclin, E. L., Low, K. A., Fabiani, M., & Gratton, G. (2015). Comparison of procedures for co-registering scalp-recording locations to anatomical magnetic resonance images. Journal of Biomedical Optics, 20(1), 016009. http://doi.org/10.1117/1.JBO.20.1.016009

67. Whalen, C., Maclin, E. L., Fabiani, M., & Gratton, G. (2008). Validation of a method for coregistering scalp recording locations with 3D structural MR images. Human Brain Mapping, 29(11), 1288–1301. http://doi.org/10.1002/hbm.20465

68. Gratton, G. (2000). “Opt-cont” and “Opt-3D”: a software suite for the analysis and 3D reconstruction of the event-related optical signal (EROS). Psychophysiology, 37, S44

69. Wolf, U., Wolf, M., Toronov, V., Michalos, A., Paunescu, L. A., & Gratton, E. (2000). Detecting cerebral functional slow and fast signals by frequency-domain near-infrared spectroscopy using two different sensors. OSA Biomedical Topical Meeting, Technical Digest (pp. 427–429).

70. Chiarelli, A. M., Maclin, E. L., Low, K. A., Mathewson, K. E., Fabiani, M., & Gratton, G. (2016). Combining energy and Laplacian regularization to accurately retrieve the depth of brain activity of diffuse optical tomographic data. Journal of Biomedical Optics, 21(3), 36008. http://doi.org/10.1117/1.JBO.21.3.036008

71. Lancaster J.L., Rainey L.H., Summerlin J.L., Freitas CS, Fox PT, Evans AC, Toga AW, Mazziotta JC. Automated labeling of the human brain: A preliminary report on the development and evaluation of a forward-transform method. Hum Brain Mapp 5, 238- 242, 1997.

72. Lancaster JL, Woldorff MG, Parsons LM, Liotti M, Freitas CS, Rainey L, Kochunov PV, Nickerson D, Mikiten SA, Fox PT, "Automated Talairach Atlas labels for functional brain mapping". Human Brain Mapping 10:120-131, 2000. DOI: 10.1002/1097- 0193(200007)10:3<120::AID-HBM30>3.0.CO;2-8

73. Raz, N., Lindenberger, U., Rodrigue, K. M., Kennedy, K. M., Head, D., Williamson, A., … Acker, J. D. (2005). Regional brain changes in aging healthy adults: general trends, individual differences and modifiers. Cerebral Cortex, 15(11), 1676–1689. http://doi.org/10.1093/cercor/bhi044

74. Zhu, N., Jacobs, D. R., Schreiner, P. J., Launer, L. J., Whitmer, R. A., Sidney, S., … Bryan, R. N. (2015). Cardiorespiratory fitness and brain volume and white matter integrity: The CARDIA Study. Neurology, 84(23), 2347–2353. http://doi.org/10.1212/WNL.0000000000001658

75. Fletcher, M.A., Low, K.A., Boyd, R., Zimmermam, B., Gordon, B.A., Tan, C.-H., Schneider- Garces, N., Sutton, B.P., Gratton, G., & Fabiani, M. (inpress) Comparing fitness and aging effects on brain anatomy. Frontiers in Aging Neuroscience.

76. Fabiani, M. Zimmerman, B., & Gratton, G. (2015). Chapter 11: Working memory and aging: A review. In P. Jolicoeur & C. Lefebvre, & J. Marinez-Trujillo (Eds.), Attention & Performance XXV: Mechanisms of sensory working memory (pp. 131-148). Elsevier. ISBN: 978-0-12-801371-7

77. Kalaria, R. N., & Ihara, M. (2013). Dementia: Vascular and neurodegenerative pathwayswill they meet? Nature Reviews. Neurology, 9(9), 487–488. http://doi.org/10.1038/nrneurol.2013.164

78. Zlokovic, B. V. (2011). Neurovascular pathways to neurodegeneration in Alzheimer's disease and other disorders. Nature Reviews. Neuroscience, 12(12), 723–738. http://doi.org/10.1038/nrn3114

79. Toledo, J. B., Arnold, S. E., Raible, K., Brettschneider, J., Xie, S. X., Grossman, M., … Trojanowski, J. Q. (2013). Contribution of cerebrovascular disease in autopsy confirmed neurodegenerative disease cases in the National Alzheimer's Coordinating Centre. Brain, 136(9), 2697–2706. http://doi.org/10.1093/brain/awt188

80. Keage, H. A. D., Churches, O. F., Kohler, M., Pomeroy, D., Luppino, R., Bartolo, M. L., & Elliott, S. (2012). Cerebrovascular function in aging and dementia: a systematic review of transcranial Doppler studies. Dementia and Geriatric Cognitive Disorders Extra, 2(1), 258–270. http://doi.org/000339234

81. Chao, L. L., Buckley, S. T., Kornak, J., Schuff, N., Madison, C., Yaffe, K., … Weiner, M. W. (2010). ASL perfusion MRI predicts cognitive decline and conversion from MCI to dementia. Alzheimer Disease and Associated Disorders, 24(1), 19–27. http://doi.org/10.1097/WAD.0b013e3181b4f736

82. Xekardaki, A., Rodriguez, C., Montandon, M.-L., Toma, S., Tombeur, E., Herrmann, F. R., … Haller, S. (2015). Arterial spin labeling may contribute to the prediction of cognitive deterioration in healthy elderly individuals. Radiology, 274(2), 490–499. http://doi.org/10.1148/radiol.14140680

83. Petersen, E. T., Zimine, I., Ho, Y.-C. L., & Golay, X. (2006). Non-invasive measurement of perfusion: a critical review of arterial spin labelling techniques. The British Journal of Radiology, 79(944), 688–701. http://doi.org/10.1259/bjr/67705974

84. Laurent, S. (2006). Arterial stiffness in arterial hypertension. Current Hypertension Reports, 8(3), 179–180.

85. Cruickshank, K., Riste, L., Anderson, S. G., Wright, J. S., Dunn, G., & Gosling, R. G. (2002). Aortic pulse-wave velocity and its relationship to mortality in diabetes and glucose intolerance: an integrated index of vascular function? Circulation, 106(16), 2085–2090.

86. Edwards, N. M., Daniels, S. R., Claytor, R. P., Khoury, P. R., Dolan, L. M., Kimball, T. R., & Urbina, E. M. (2012). Physical activity is independently associated with multiple measures of arterial stiffness in adolescents and young adults. Metabolism: Clinical and Experimental, 61(6), 869–872. http://doi.org/10.1016/j.metabol.2011.10.016

87. Hawkins, M., Gabriel, K. P., Cooper, J., Storti, K. L., Sutton-Tyrrell, K., & Kriska, A. (2014). The impact of change in physical activity on change in arterial stiffness in overweight or obese sedentary young adults. Vascular Medicine, 19(4), 257–263. http://doi.org/10.1177/1358863X14536630

CHAPTER 4

ASSOCIATIONS OF OPTICAL ARTERIAL COMPLIANCE WITH T1 WHITE MATTER LESION VOLUME AND WHITE MATTER MICROSTRUCTURE IN COGNITIVE AGING

The process of normal aging is associated with decreases in cognitive functions (Park & Reuter-Lorenz, 2009; Salthouse, 2010). These age-related declines in cognitive function have been found to be associated with degradation in white matter structure in the form of greater white matter lesion burden manifested as white matter signal abnormalities (WMSAs) appearing as hypointense on T1-weighted images or hyperintense on T2-weighted images (Brickman et al, 2011; Debette & Markus, 2010; Leritz et al., 2014; Wardlaw, 2015), and also changes in white matter microstructural properties, manifested as a reduction in measures from diffusion tensor imaging (DTI) such as fractional anisotropy (FA) or an increase in mean diffusivity (MD; Bennett & Madden, 2014; Burzynska et al., 2010).

Although the etiology underlying both greater WMSA lesion volume and alterations to normal appearing white matter (NAWM) microstructure is thought to be similar, there is also growing evidence that overt WMSA volume alone do not completely explain the association between older age and decreases in white matter microstructure tissue integrity (Leritz et al., 2014; Salat et al., 2014). These studies suggest that although the mechanism by which WMSAs and DTI measures are associated with cognitive decline in aging overlap to some extent, they are not equivalent. Greater WMSAs is due mostly to chronic ischemia associated with cerebral small vessel disease, as evidenced from both clinical and pathophysiological studies (Pantoni & Simons, 2013; Prins & Scheltens, 2015). On the other hand, FA and MD measures reflect mostly changes in multiple tissue properties such as axonal density and ordering, degree of myelination, membrane permeability and loss of oligodendrocytes, among others (Jones, Knösche & Turner, 2013; Stebbin & Murhy, 2009).

These findings are consistent with the theory that there are two separable vascular and neurodegenerative pathways in clinical diseases associated with cognitive decline such as dementia

(Kalaria & Ihara, 2013). Although both WMSAs and changes in white matter microstructure are associated with demyelination, studies comparing demyelination in vascular dementia (VaD) and Alzhiemer's disease (AD) suggest again that the mechanisms involved are partially different, with white matter tissue damage originating from hypoxic-ischemic conditions in VaD but secondary to axonal degeneration in AD (Ihara et al., 2010).

Studies supporting this relationship between cerebrovascular health and WMSA volume have found cross-sectional evidence that higher systemic blood pressure is associated with greater WMSA volume in older adults (Kennedy and Raz, 2009; Leritz et al., 2010; Salat et al., 2012). However, although accumulated evidence does indicate that poor cerebrovascular health results in greater WMSAs, the exact mechanism by which vascular pathology contributes to the changes that we see in cerebral white matter remains unknown. In addition, systemic measures of blood pressure only serve as an indirect proxy measure for cerebral vascular risk, as opposed to a direct measure of cerebral vascular health (Salat, 2014). Studies attempting to address this shortcoming have relied on extracting measurements of cerebral blood flow (CBF) using arterial spin labelling techniques (ASL) as a marker of cerebral vascular health. In general, they find that participants with greater WMSAs have lower CBF (Alosco et al., 2013; Fazekas et al., 1988; Hatazawa, Shimosegawa, Satoh, Toyoshima, & Okudera; 1997). These reductions in CBF and cerebrovascular reactivity have been also found to be localized within the WMSAs (Brickman at al., 2009; Marstrand et al., 2002). More recent attempts to extract pulsatile components using dynamic ASL as an index of vascular compliance (VC) have been developed but it is unknown if this marker of cerebrovascular health is associated with WMSA volume or dementia (Yan et al., 2016).

Fabiani et al. (2014) recently developed a novel way of directly estimating cerebral vascular health non-invasively with diffusive optical imaging in a group of older adults. The measurement of cerebral arterial compliance is of particular relevance to the current study. Fabiani et al (2014) found that greater arterial compliance was negatively associated with age, positively with CRF, global anatomy

measures (e.g. white and gray matter volume, hippocampal volume), and cognitive flexibility measured with the Wisconsin card sorting task (WCST). These results were replicated in a group of younger and older adults (Tan et al., *under review,* Chapter 2). The current study therefore aims to investigate and clarify the cerebrovascular mechanism by which greater age is associated with poorer cognitive function. Specifically, we hypothesized that given that cerebral arterial compliance is a measure of cerebrovascular health, it should predict WMSA volume over and above age and systemic pulse pressure. We also tested a mediation model to investigate whether the association between age and cognitive decline is mediated by arterial compliance and WMSA volume *sequentially*. The mediation model is motivated from accumulated evidence suggesting that WMSAs are a result of poor cerebrovascular health (Prins & Scheltens, 2015). Mediation analysis is particularly useful in this context as they allow us to test proposed mechanisms by which one factor influences another (Hayes, 2013).

In addition, we would expect that the associations between better arterial compliance and measurements of NAWM microstructure such as greater FA and lower MD to be smaller in comparison with WMSA volume. Also, we do not expect a sequential mediation effect of arterial compliance followed by FA or MD on the association between age and cognition, given that these alterations are likely due more to neurodegenerative, and not vascular mechanisms. However, there are also evidence suggesting that not all NAWM degenerates at the same rate as a function of aging. In particular, the fornix has gathered increasing interest with studies suggesting that damage to the fornix may precede brain atrophy in gray matter such as the hippocampus (Nowrangi & Rosenberg; 2015), and is predictive of conversion from mild cognitive impairment (MCI) to AD (Douaud et al., 2013; van Bruggen et al. 2012). These studies suggest a possible convergence of both vascular and neurodegenerative pathways in the fornix, whereby we would expect to see strong associations between arterial compliance, WMSA and regional FA and MD.

Methods

Participants

Forty-eight adults (age range = 18-75 years, mean age = 47.8, 25 females) were recruited through advertisements in local newspapers, campus-wide emails and postings at area gyms, retirement homes and community centers in the Urbana-Champaign community. In order to ensure an even spread across the age range, the age range was divided into sextiles, the age range was divided into six decades (18-27, 28-37, 38-47, 48-57, 58-67, and 68-77), and 8 subjects were recruited for each decade. For each sextile, at least 8 subjects were recruited. However, for the majority of analyses presented in this paper, age (in years) was used as a continuous variable. One subject had to be removed from all analyses involving the arterial compliance measure because we were unable to extract a suitable pulse trace from the optical data, possibly due to excessive movement, leaving a final sample of 47 participants. The demographic characteristics of the participants are summarized in Table 4.1. In this table, information is provided about the overall sample, as well as about 2 age groups (younger and older adults), derived by using a median split. This classification is provided to show that important variables such as years of education and IQ were consistent across the entire sample.

Table 4.1. Demographic characteristics of the participants (N = 47)

Variable	All (N=47) Mean (SD)	Young (N=24) Mean (SD)	Old (N=23) Mean (SD)
Age (years)	47.6 (17.5)	32.7 (9.6)	63.1 (7.3)
Education (years)	17.3 (2.2)	16.5 (1.9)	18.1 (2.3)
mMMSE	55.8 (1.2)	55.7 (1.3)	55.9 (1.1)
Shipley's Vocabulary Test	34.7 (3.7)	33.2 (3.5)	36.3 (3.2)
Beck's Depression Index	2.2 (2.5)	3.0 (2.7)	1.4 (2.1)
K-BIT2 (IQ)	116.4 (10.2)	114.5 (8.7)	118.3 (11.4)

Screening procedures

Participants were screened based on a number of health and cognitive criteria. Subjects with serious or chronic medical conditions or a history of major neurological or psychiatric disease or drug abuse were excluded from this study. Additionally, to be included in the study subjects had to score at least 51 on the mMMSE (Mayeux, Stern, Rosen & Leventhal, 1981) and no more than 14 on Beck's Depression Inventory (Beck, Steer & Brown, 1996). Subjects who smoked more than half a pack of cigarettes and/or consumed more than two alcoholic drinks per day were also excluded. All participants were right-handed (as assessed by the Edinburgh Handedness Inventory; Oldfield, 1971), had normal or corrected-to-normal vision, and were native speakers of English. All procedures described in this report were approved by the University of Illinois Institutional Review Board. Prior to participation, all participants signed informed consent documents.

Assessment of cognitive function

A battery of neuropsychological tests was administered, which included the Kaufmann Brief Intelligence Test Second Edition (K-BIT2; Kaufman & Kaufman, 2004) and Ravens progressive matrices (Raven, Raven & Court, 2003) to measure IQ, the vocabulary sub-test of the Shipley-Institute of Living Scale (Shipley, 1940) to measure vocabulary, the Wisconsin Card Sorting Test (WCST, Heaton, 1981; Tien et al., 1996), the Controlled Oral Word Association sub-test of the Multilingual Aphasia Examination (a measure of verbal fluency using the letters CFL; Benton & Hamsher, 1989), the operation-span task (OSPAN; Unsworth, Heitz, Schrock, & Engle, 2005), the Trail Making Tests A and B (Corrigan & Hinkeldey, 1987), to measure working memory and executive function, the Logical Memory I and II tasks from the Wechsler Memory Scale – Fourth Edition (WMS – IV, Wechsler, 2009) to measure episodic memory. In addition, scores for forward and backward digit span were derived from the mMMSE.

Experimental Procedures and Types of Measures

The data presented here were collected as a part of a much larger, multi-session project intended to investigate brain function using diffuse optical and magnetic resonance imaging (MRI) methods. Session 1 included neuropsychological assessments and familiarization to MRI scanning within a mock magnet. Session 2 included the collection of structural MRI data (used for anatomical co-registration and brain volume estimations). Session 3 included collection of optical imaging data from the visual cortex only, which are not included in this study. In session 4, we collected the optical imaging data and an electrophysiological measurement of the heartbeat for time-locking the arterial pulse. These are the data presented here.

Electrocardiogram Recording and Analysis

Lead I of the electrocardiogram (EKG, left wrist referenced to right wrist, impedance below 20 kOhm) was recorded with a Brain-Vision™ recorder and a Brain-Vision professional BrainAmp™ integrated amplifier system (Brain Products GmbH, Germany) with a sampling rate of 1000 Hz. The EKG data were extracted using EEGLab (Delorme & Makeig, 2004) and the optical pulse data were time-locked to the R-wave of the EKG. Each R-wave peak was found using an algorithm running on MATLAB R2014b (MathWorks, Natick, MA) that searches for peaks exceeding a certain voltage threshold (scaled for each subject) and discarding any points that fall outside the normal range of interbeat intervals. Manual visual inspection was also performed to ensure that any misidentifications of R-wave peak were discarded.

MRI Acquisition and Processing

Structural magnetic resonance images (sMRI) were collected for each participant using a 3T Siemens Trio full body scanner. A high resolution, 3D MPRAGE protocol was used, with a flip angle = 9◦,

TE = 2.32 ms, TR = 1900 ms, and inversion time = 900 ms. Slices were obtained in the sagittal plane (192 slices, .9 mm slice thickness, voxel size .9 x .9 x .9 mm) having matrix dimensions of 192 x 256 x 256 (in-plane interpolated at acquisition to 192x512x512) and field of view of 172.8 x 230 x 230 mm. All images were visually examined by multiple researcher personnel and no significant defects or distortions were discovered. Cortical reconstruction and volumetric segmentation were performed with the FreeSurfer© 5.3 image analysis suite (http://surfer.nmr.mgh.harvard.edu/; e.g., Dale, Fischl & Sereno, 1999; Fischl & Dale, 2000; Fischl, Liu, & Dale, 2001; Fischl et al., 2002; Han et al., 2006). FreeSurfer morphometric procedures have been demonstrated to show good test-retest reliability across scanner manufacturers and across field strengths (Han et al., 2006).

WMSA volume. WMSAs (appearing as hypointense on T1-weighted images) were labeled based on a probabilistic procedure (Fischi et al., 2002) and the automatic segmentation performed by FreeSurfer was extensively examined for errors. Any errors found were corrected according to the instructions found at http://surfer.nmr.mgh.harvard.edu/fswiki/FsTutorial/TroubleshootingData. WMSA volume computed from T1 hypointensities has previously been found to be highly correlated (r =0.8) with hyperintensities obtained using T2/FLAIR methods (Simon at al., 2000). Intraclass correlation between T1 WMSAs and manually segmented WMH has also been found to be as high as 0.91 (Smith et al., 2011). Other studies have also suggested that T1-weighting methods of quantifying WMSA volume may be more associated with clinical pathology (Bagnato, et al. 2010; Miller, et al. 1998; Sailer, et al. 2001). T1-weighted WMSA volume has also been used in studies investigating its role in cognitive aging (Leritz et al., 2014; Marquez et al., 2015; Salat et al., 2010).

Diffusion Tensor Imaging. DTI images were acquired using a spin echo single shot Echo Planar Imaging sequence consisting of a set of 30 non-collinear diffusion-weighted acquisitions with b-value =1000 s/mm^2 and one T2-weighted b-value = 0 s/mm^2 acquisition (TR/TE =10000/98 ms, 128x128 matrix, 1.9x1.9x2.0 mm voxel size, FA = 90, GRAPPA acceleration factor 2, and bandwidth of 1698 Hz/Px,

comprising 72 2-mm-thick slices). DTI provides information about WM microstructure in-vivo by measuring both the magnitude and direction of water diffusion present in brain tissue (Beaulieu, 2002). Visual inspection of the entire raw data did not reveal any artifact that warrants exclusion from analysis. DTI data were processed using the FSL Diffusion Toolbox v.3.0 (FDT: http://www.fmrib.ox.ac.uk/fsl) in a standard multistep procedure, including: (a) motion and eddy current correction of the images and corresponding b vectors, (b) removal of the skull and non-brain tissue using the Brain Extraction Tool (Smith, 2002), and (c) voxel-by-voxel calculation of the diffusion tensors. Using the diffusion tensor information, FA maps were computed using DTIFit within the FDT. The outputs from every step were visually inspected for errors.

We used TBSS (Smith et al., 2006), a toolbox within FSL v5.0.1, to create a representation of main white matter tracts common to all subjects (white matter "skeleton"). This included: (a) nonlinear alignment of each participant's FA volume to the 1 x 1 x 1 mm^3 standard Montreal Neurological Institute (MNI152) space via the FMRIB58_FA template using the FMRIB's Nonlinear Registration Tool (FNIRT, (Rueckert, 1999); http://www.doc.ic.ac.uk/~dr/software), (b) calculation of the mean of all aligned FA images, (c) creation of the white matter "skeleton" by perpendicular non-maximum-suppression of the mean FA image and setting the FA threshold to 0.25, and (d) perpendicular projection of the highest FA value (local center of the tract) onto the skeleton, separately for each subject. The TBSS analysis used here emphasizes normal appearing white matter due to the last step of using the highest FA value that is being projected on the white matter skeleton (Burzynska et al., 2013). Mean FA and MD values extracted from fornix ROIs used in Burzynska et al., (2013) and were identified based on the DTI white-matter atlas (Mori et al., 2005).

Optical Recording and Analysis

Recording. Optical data were recorded with six integrated frequency-domain oxymeters (Imagent; ISS, Inc., Champaign, IL). Data were collected from 24 detectors each measuring light emitted

by 16 time-multiplexed sources (384 channels) in 4 different optical montages designed to cover the majority of the head, giving rise to a total of 1536 channels. Laser diodes generated light at 830 and 690 nm (max amplitude: 10 mW, mean amplitude after multiplexing: 1 mW), modulated at 110 MHz. The light from the diodes was transmitted to the surface of the head using optical fibers (one per emitter, with separate fibers carrying light at each of the two wavelengths coupled at each location). Each optical fiber carrying the light to the surface of the head was 400 μm in diameter. Light was collected from the head using detector fiber bundles (diameter = 3mm) and connected to photomultiplier tubes (PMTs) fed with a current modulated at 110.003125 MHz, generating a 3.125 kHz cross-correlation frequency. Optical parameters were sampled at 39.0625 Hz (25.6 ms per sampling point). Sources and detectors were held flush with the participants' scalp using a lab-built helmet made of foam and plastic tubes held together by rubberized cords that can tightened or loosened to fit each individual's head as required (See Tan et al, under review, *Chapter 3*).

Coregistration with structural MRI. Using nasion and preauricular points as references, the locations of individual optical sources and detectors were digitized using a Polhemus "3Space" FASTRAK 3D digitizer (Polhemus, Colchester, VT). T1-weighted structural magnetic resonance images were obtained for each subject. The Polhemus digitization points were then co-registered with the MR images first using the three fiducial markers and then surface fitting the entire set of digitized points to the estimated scalp surface based on a Levenberg-Marquardt algorithm (least-squares fit) using in-house software Optical Coregistration Package (OCP; Chiarelli, Maclin, Low, Fabiani & Gratton, 2015). Coregistration using this procedure has been shown to result in errors of less than 4 mm (Chiarelli et al., 2015; Whalen, Maclin, Fabiani, & Gratton, 2008).

Analysis of optical data. Measurements were taken at rest for 8 blocks with each block lasting 6 minutes. Each of the 4 montages was recorded for a total of 2 blocks (12 minutes total recording time for each montage), with the sequence of 4 montages counterbalanced across subjects within each age

sextile. The optical data were normalized (by dividing them by their mean value), movement corrected (Chiarelli et al., 2015), and band-pass filtered between 0.5–5 Hz (Butterworth digital filter). DC light intensity data at 830nm of wavelength were used for pulse shape estimation. The longer 830nm wavelength has, in fact, higher sensitivity to pulse-related absorption changes due to its higher sensitivity to oxygenated hemoglobin, which are present in greater volume in the cerebral arteries compared to the shorter 690nm wavelength (Fabiani et al., 2014).

Pulse waveform for each channel was obtained by averaging the DC light intensity time-locked to the peak of the R wave of the EKG (signaling the depolarization of the ventricular myocardium, and ensuring that we were measuring the same pulse cycle at different locations) (Fabiani et al., 2014). Only channels above 25 mm of interoptode distance were used to increase sensitivity to deeper phenomena. Only channels within 70 mm of maximum interoptode distance were used to increase the overall signal to noise ratio of the measurements.

In order to estimate the pulse waveform in the head structures (relative changes in absorption related to the heart pulsation) a model of the light propagation in the head (forward model) and an inverse procedure were required (inverse model). The algorithms used were identical to the ones developed and applied in functional near-infrared spectroscopy (fNIRS) where the relative changes in absorption are caused by functional fluctuation of oxygenation in activated brain areas. Pulse propagation causes local changes in absorption up to few percentage points, which are very similar to the changes measured in the fNIRS studies. For image reconstruction purposes, the two procedures are treated similarly here.

Finite Element Method (FEM) applied to the diffusion equation (Ishimaru, 1989; Paulsen and Jiang, 1995) was used to estimate the forward model. The FEM software NIRFAST (Dehghani et al., 2009, Eggebrecht et al., 2014) was used to model the light propagation through the heterogeneous heads and to compute Jacobian matrices (sensitivity matrices) of DC light intensity to absorption changes. The

average Jacobian is displayed up to an attenuation of 60dB to its maximum value. “Fine” meshes (maximum tetrahedral volume = 2 mm^3) were generated for FEM using MATLAB R2014b (MathWorks, Natick, MA) function iso2mesh (Fang & Boas, 2009). The heterogeneous head geometries were evaluated from segmented T1-weighted 3D anatomical images. Segmentation of participants’ heads into skull and scalp, cerebrospinal fluid (CSF), white matter and grey matter was performed using SPM functions applied to T1 anatomical images (Penny et al., 2011). Baseline optical properties (absorption μa, reduced scattering coefficient μs’ and refraction index η of the tissues at the relevant wavelength were taken from Tian & Liu (2014) and Chiarelli et al., (2016). The optical values at the wavelength of interest (830 nm) were set to: scalp and skull: $\mu a = 0.014\ mm^{-1}$, $\mu s' = 0.84\ mm^{-1}$; CSF: $\mu a = 0.004\ mm^{-1}$, $\mu s' = 0.3\ mm^{-1}$; grey matter: $\mu a = 0.019\ mm^{-1}$, $\mu s' = 0.673\ mm^{-1}$; white matter: $\mu a = 0.021\ mm^{-1}$, $\mu s' = 1.01\ mm^{-1}$. The refraction index was set to $\eta=1.4$ for all the simulations and mediums.

In order to reconstruct the absorption changes based on channels’ signal recordings, an inverse procedure introduced by Chiarelli et al. (2016) was used. This inverse procedure allows for an unbiased localization of absorption fluctuations up to a depth of 30 mm from the scalp. Reconstructed optical pulse waves tomographic data (diffuse optical images of the pulse) were obtained in the same space of the structural MRI. Arterial compliance was estimated for each voxel within 30 mm from the scalp and with a maximum relative absorption change above 10^{-4} (that allowed us to disregard voxels close to the scalp but not covered by the optode montage). Arterial compliance was defined as the area under the pulse between the peak systole and the peak diastole normalized by both time and amplitude and subtracted by a constant value of 0.5 (Fabiani et al., 2014). The constant value was subtracted to compare the area of the pulse response measured to an area of a hypothetical pulse presenting a linear decay of its amplitude after the systolic period. As Freesurfer regions were identified on the original MR images whereas optical data were reconstructed based on resampled (1 mm isovoxel) images, the identified FreeSurfer ROI’s were mapped into the isovoxel images using a co-registration procedure

implemented in the software SPM (Friston et al., 1994). Average arterial compliance for each participant and each FreeSurfer segmented regions was extracted considering only voxel where compliance was computed (10% trimmed mean). By visual inspection 20 out of the 70 FreeSurfer regions were considered too deep for compliance estimation and not included in the analysis (Chiarelli et al., *in preparation*). The remaining 50 regions in each subject were averaged to compute the measure of generalized arterial compliance.

Results

Neuropsychology assessment and associations with age.

Based on the factor loadings of the various cognitive tasks, a total of 4 orthogonal factors with Eigen values >1 were derived by using factor analysis. They were putatively classified as episodic memory, working memory, fluid intelligence (IQ) and crystallized intelligence (IQ). Factors with >|0.5| loadings are bolded (see Table 4.2). Older subjects scored lower in fluid IQ, $r(45) = -.51$, $p < .001$ and higher in crystallized IQ, $r(45) = .38$, $p = .009$. Associations of age with episodic memory, $r(45) = -.21$, $p = .16$ and working memory, $r(45) = .21$, $p = .16$, did not reach statistical significance.

Table 4.2. Loadings of the 4 cognitive factors that were derived from factor analysis.

	Episodic Memory	Working Memory	Fluid Intelligence	Crystalized Intelligence
Modified Mini-Mental Status Exam	0.093	0.202	0.156	**0.535**
Forward Digit Span	-0.016	**0.772**	0.030	0.227
Backward Digit Span	-0.055	**0.769**	-0.234	0.227
Logical memory immediate A	**0.810**	0.028	0.158	0.202
Logical memory immediate B	**0.893**	0.105	0.147	0.034
Logical memory Delay A	**0.792**	-0.219	0.028	0.229
Logical memory Delay B	**0.908**	0.117	0.076	0.095
Raven's Progressive Matrices	0.206	-0.030	**0.828**	0.064
Verbal Fluency Test (CFL)	0.041	**0.683**	0.059	0.041
Trail making B-A	-0.009	0.066	**-0.716**	-0.040
Shipley	0.110	0.214	-0.118	**0.853**
OSPAN (letters)	0.356	**0.524**	**0.568**	0.094
KBIT2 IQ Composite	0.249	0.061	0.111	**0.854**

Relationship between arterial compliance and WMSA

Four subjects were excluded from the analysis: 3 were statistical outliers on the WMSAs measure and 1 on the arterial compliance measure, (Z score >|2.5|). WMSA volumes were log-transformed to adjust for skewing of the data, similar to procedures done in other studies (e.g. Atwood et al., 2004; Jefferson et al., 2007). Shapiro-Wilk's test was not significant (W = .97, *p* = .45), indicating that the log-transformed data were now normally distributed. As hypothesized, greater arterial compliance across the cortex was associated with lower WMSAs, r(41) = -.42, p = .002 (See Figure 1).

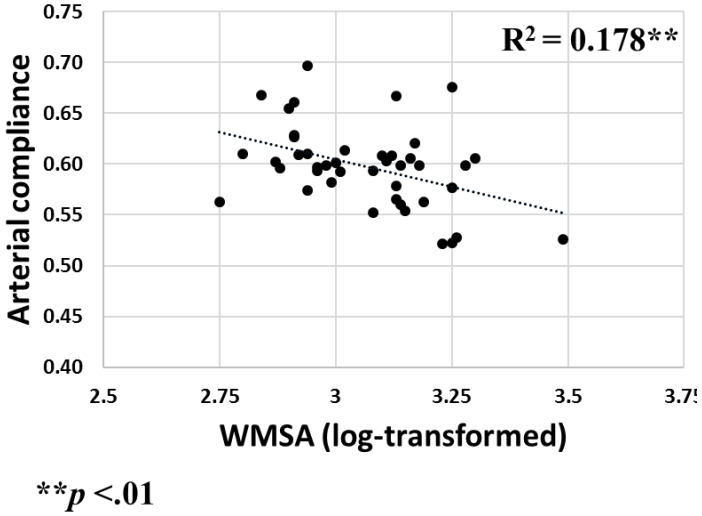

Figure 4.1. Greater arterial compliance was associated with lower WMSA volume (log-transformed).

We conducted a four-step hierarchical multiple regression with WMSAs as the dependent variable to investigate whether cerebral arterial compliance predicts the presence of WMSAs over and above the known predictors of age and systemic pulse pressure (difference between systolic and diastolic blood pressure). Estimated total intracranial volume (eTIV) was entered at stage one of the regression as a control variable. Age was entered at stage two, pulse pressure at stage three and arterial compliance at stage four. The hierarchical multiple regression revealed that at step one, eTIV did not contribute significantly to the regression model, *F* (1, 41) = .85, *p* = .18) and only accounted for 2.0% of

the variation in WMSAs. This is not surprising as eTIV was meant to serve simply as a control factor. Introducing age into the model explained an additional 17.0% of the variance and this change in R^2 was significant, F (1, 40) = 8.39, p = .003. This is consistent with the vast amount of literature showing that age is highly associated with white matter lesions in the brain (see Xiong & Mok, 2011 for a review). Adding systemic pulse pressure in step 3 explained an additional 5.6% of the variance but this change in R^2 was not significant, F (1, 39) = 2.92, p = .048). The final addition of arterial compliance into the model predicted an additional 7.9% of the variance in WMSAs and the change in R^2 was significant, F (1, 38) = 4.46, p = .021). These results are summarized in Table 4.3. Taken together, results from the hierarchical multiple regression suggest that cerebral arterial compliance is an independent predictor of WMSAs, explaining variance in WMSA volume over and above age and pulse pressure.

Table 4.3 Hierarchical regression models with different predictors.

	Beta	R^2	Δ R^2
Model 1		.02	.02
Intracranial Volume (eTIV)	.14		
Model 2		.19	.17**
Intracranial Volume (eTIV)	.24		
Age	.42**		
Model 3		.25	.056
Intracranial Volume (eTIV)	.14		
Age	.40**		
Pulse Pressure	.26		
Model 4		.33	.079*
Intracranial Volume (eTIV)	.16		
Age	.24		
Pulse Pressure	.25		
Arterial Compliance	-.32*		

Note. N = 43. Δ R^2 was significant in step 2 and 4, *p < .05, **p <.01. Dependent variable: WMSA volume

Serial multiple mediation analysis with arterial compliance and WMSAs

We employed PROCESS model 6 macro in SPSS (IBM, 2013) to examine serial mediation (Hayes, 2013) based on a series of ordinary least square (OLS) regression models method. Here we use age as

the predictor, arterial compliance as the first mediator, WMSA volume as the second sequential mediator and fluid IQ as the dependent variable. We focused on only fluid IQ due to its known relationship with WMSA (Raz et al., 2007). It should also be noted that WMSA has also been found to be associated with other cognitive domains such as executive functions (Cook et al., 2004; Kramer et al., 2007), that we did not assess in the current study. We employed serial multiple mediator analysis with the theoretical assumption that arterial compliance occurs before WMSAs appear. Specifically, we are testing for this indirect effect: age → arterial compliance → WMSAs → fluid IQ. eTIV was included in the model as a covariate. All variables were standardized prior to analysis.

We tested the indirect effect by using a bias-corrected bootstrapping procedure based on 5000 samples. The bias-corrected bootstrap procedure was chosen as it is considered the most trustworthy and provides more power given our relatively small sample size (Hayes & Scharkow, 2013). The relationship between age and fluid IQ was found to be mediated by arterial compliance and WMSA volume (Figure 4.2). The 95% confidence interval for the indirect effect did not include zero (-.2166, -.0026). Further, the finding that the relationship between age and fluid IQ remains significant after accounting for arterial compliance and WMSA volume is not surprising given the extant literature showing that the mechanism by which aging is associated with cognitive decline involves multiple mediators (Hedden et al., 2014).

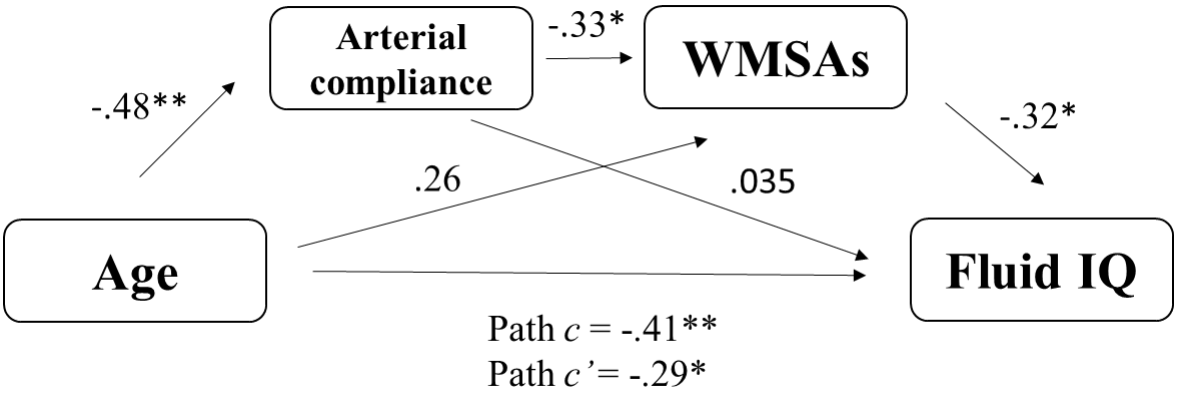

Figure 4.2. Schematic representation of the mediation analysis performed with age as the predictor, arterial compliance and WMSA as sequential mediators, and fluid IQ as the dependent variable. Values reported are standardized coefficients. Estimated total intracranial volume was included as covariate.

It is also possible that the relationship between arterial compliance and WMSA is bidirectional, whereby although initial reductions in arterial compliance and perfusion associated with aging may result in greater WMSA volumes, these focal lesions may then contribute to further degradation in arterial compliance. Given the correlational and cross-sectional nature of the study, we cannot explicit test this possibility. However, further analysis involving the switching of the temporal sequence of arterial compliance and WMSA did not revealed a significant indirect effect, 95% CI (-.0287, .0662). These results therefore suggest that the mediating effects of both arterial compliance and WMSAs on the relationship between greater age and lower fluid IQ is predominantly, through a sequential process of reduction in global arterial compliance and subsequent increase in WMSA volume.

Relationships between regional arterial compliance and WMSAs

Regional analyses revealed that greater arterial compliance measured in 35 brain regions was significantly associated with lower WMSA volume in the entire brain, all *ps* < .05 (see Figure 4.3a), controlling for eTIV. These associations were particularly strong in the frontal regions, consistent with literature demonstrating that frontal regions are more susceptible to age-related declines, using indices

such as regional volumes and cerebral blood flow (e.g. Alosco et al., 2013; Raz et al., 2997; Resnik et al., 2003). A median split based on the subjects' age revealed that these associations were mainly driven by the older subjects (see Figure 4.3b). In younger subjects none of the 50 regions showed a significant negative association with WMSAs. However, these data must be interpreted with caution as arterial compliance was computed from cortical structures and therefore does not share a direct overlap with the WMSAs found in white matter.

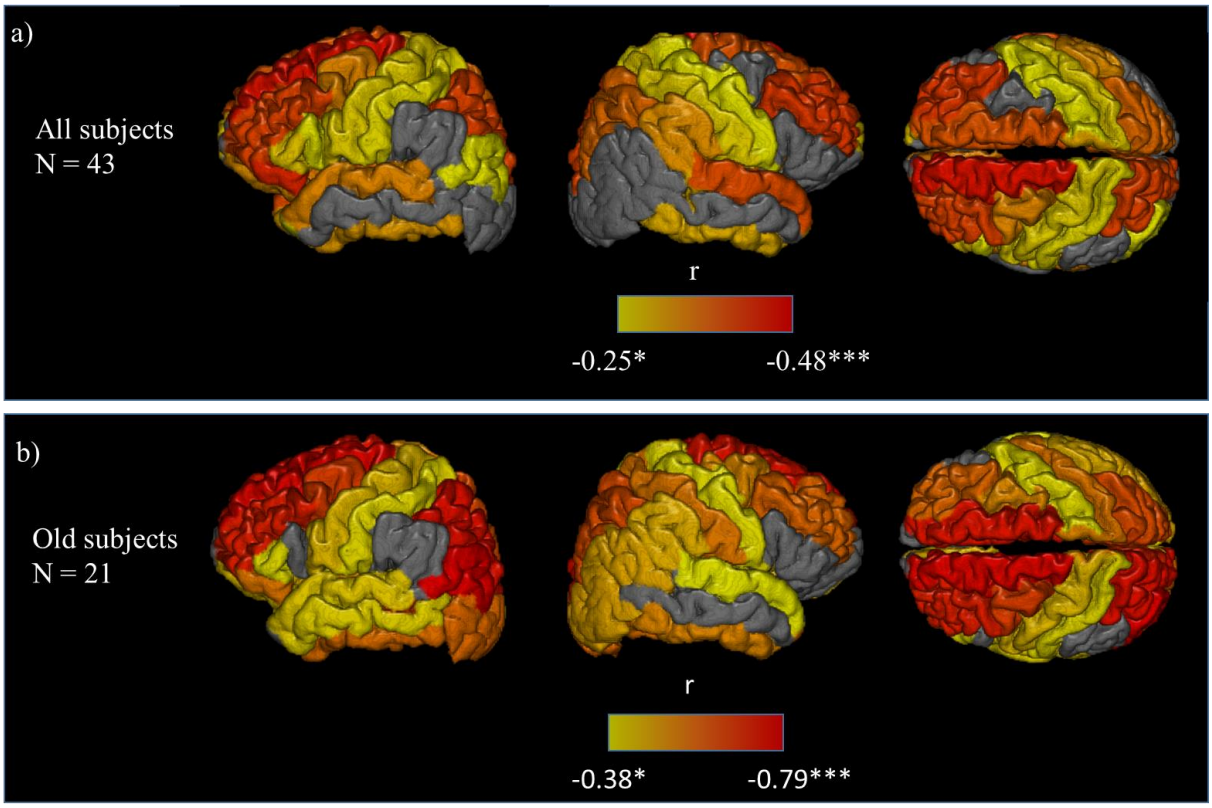

*Figure 4.3***.** a) Arterial compliance in 35 regions of the brain was found to be negatively associated with global WMSA volume. Regions in grey did not reach statistical significance. b) These regional associations were stronger in older subjects.

Arterial compliance and DTI indices

We expect that unlike WMSAs, the association between arterial compliance and FA and MD measures should be weaker or absent due to underlying differences pathological pathways. Out of the original 47 subjects, 3 were excluded for this analysis. Besides the 1 subject that was a statistical outlier

on the arterial compliance measure, we did not have DTI data for 2 subjects because they did not complete the scan. Consistent with established findings, greater age was associated with lower FA, $r(41) = -.42$, $p = .002$) and greater MD, $r(41) = .31$, $p = .021$), controlling for eTIV to avoid partial volume effects (Vos, Jones, Viergever & Leemans, 2011). As hypothesized, arterial compliance was not significantly associated with either global FA, $r(41) = .069$, $p = .33$ or global MD, $r(41) = -.045$, $p = .39$. Consistent with findings that age-related degeneration of white matter microstructure is associated with measures of fluid IQ (Ritchie et al., 2015), higher FA and lower MD were associated with higher fluid IQ ($r(41) = .30$, $p = .026$ and $r(41) = .-33$, $p = .015$ respectively). The relationship with fluid IQ was also stronger when investigating FA and MD in the fornix, ($r(41) = .51$, $p < .001$ and $r(41) = .-53$, $p = .001$, respectively). These data are consistent with research showing that microstructural degeneration in the fornix plays a role in the conversion from mild cognitive impairment (MCI) to AD (Douaud et al., 2013; van Bruggen et al. 2012).

We ran a similar mediation analysis to investigate if the relationship between age and fluid IQ was mediated in a sequential manner, first by arterial compliance, then FA or MD. We did not find a significant indirect effect using 5000 bias-corrected bootstrap sample when substituting WMSAs for FA (95% CI: -.0154, .1165) and MD (95% CI: -.0543, .0697). Taken together, the absence of a significant indirect effect and the lack of associations between arterial compliance with both FA and MD supports our hypothesis that degradation in NAWM microstructure is not primarily due to degradation of cerebrovascular health measured using diffusive optical imaging.

Association between arterial compliance, WMSA and regional FA and MD

As hypothesized, better arterial compliance was found to be associated with higher FA, $r(36) = .40$, $p = .005$, and lower MD, $r(36) = -.38$, $p = .008$, controlling for eTIV (See Figure 4.4). We also found that greater WMSA volume was associated with lower FA, $r(36) = -.49$, $p < .001$, and greater MD, $r(36) =$

.50, p <.001, controlling for eTIV. These results suggest that although globally, FA and MD measures are not associated with arterial compliance, accumulative damage from multiple risk factors of both vascular and neurodegenerative pathways may manifest themselves in alterations of white matter microstructure tissue in the fornix.

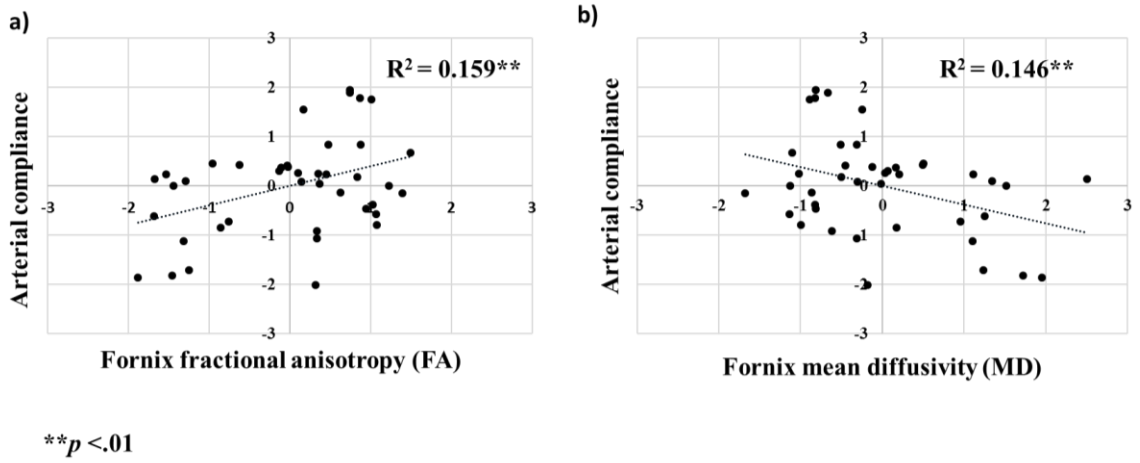

Figure. 4.4 a) Greater arterial compliance was positively associated with fractional anisotropy (FA) in the fornix. b) Greater arterial compliance was negatively associated with mean diffusivity (MD) in the fornix. Values plotted are standardized residuals after controlling for estimated total intracranial volume (eTIV).

Discussion

The results presented in the current paper support the role of diminished arterial compliance and subsequent cerebrovascular disease as mediators in age-related declines in fluid IQ. These data are consistent with a longitudinal clinical study showing that although the cerebrovascular diseases and neurodegeneration seen in Alzheimer's disease often occur in concert, the underlying metabolic dysfunctional pathways are likely to be independent (Haight et al., 2013). Specifically, they found that in converters from MCI to AD, greater white matter hyperintensities (vascular pathway) were associated with lower frontal but not temporo-parietal metabolism. The opposite was found for measurements of cerebrospinal fluid β-amyloid (neurodegeneration pathway), which were associated with lower

temporoparietal but not frontal metabolism. Within this dual-pathway framework (vascular and neurodegenerative) of progression towards AD (Kalaria & Ihara, 2013), the findings reported here provide indicate that cerebrovascular health measured using diffuse optical imaging plays a critical role in understanding the vascular pathway to age-related cognitive decline.

Specifically, we found that diffusive optical measure of cerebral arterial compliance predicted variance in WMSAs over and above age and pulse pressure. These results suggest that although central systemic indices of blood pressure have been found to be associated with WMSA volume (Kennedy and Raz, 2009; Leritz et al., 2010; Salat et al., 2012), they do not entirely predict WMSA volume, which is more strongly associated with down-stream damage in the peripheral cerebrovasculature. Diffusive optical methods of quantifying arterial compliance thus provide a more direct comparison of the state of cerebrovascular health than systemic measures. Our results showing that age-related declines in fluid IQ is mediated by both arterial compliance and WMSAs in a sequential manner is consistent with the general consensus that the emergence of WMSA lesions stems from cerebral vascular pathology that are exacerbated in the aging process (Salat, 2014). This mediation effect was no longer significant when the temporal sequence of arterial compliance and WMSA was swapped, indicating that the mediation is mostly due to effects of arterial compliance on down-stream WMSA volume as opposed to the other way around. These results thus suggest that poor cerebrovascular health in the aging process may result in adverse functional consequences on fluid IQ.

In contrast, the same mediation analysis substituting WMSA volume for indices of white matter microstructure (FA and MD) did not reach significance. These results add to the literature that although WMSAs and white matter microstructure may share some overlapping etiology, insofar as optical measures of arterial compliance tap on to the vascular pathway in cognitive aging, cerebrovascular health is the main driving factor of greater WMSA volume but not decreases in NAWM microstructure integrity. Our findings that arterial compliance was not associated with global FA and MD provides

further evidence that these alterations are not primarily due to underlying cerebrovascular dysfunction. However, these conclusions should also be considered in the context of evidence showing that cortical blood supply (measured using ASL) was associated with both FA and MD (Chen, Rosas & Salat; 2013). Fabiani et al., (2014) did not find an association between arterial compliance and ASL quantification of cerebral blood flow and they may reflect different cerebrovascular phenomena. However, the finding that FA and MD in the fornix are strongly associated with both arterial compliance and total WMSA volume suggests that cerebrovascular and neurodegenerative pathology may converge in deep subcortical regions of the brain that are most vulnerable to the effects of aging.

It must also be noted that in the sequential mediation analysis, after accounting for the effects of arterial compliance and WMSA volume, the relationship between older age and poorer fluid IQ remains significant. This is not surprising given findings that there are additional biomarkers such as glucose metabolism measured using positron emission tomography (PET) and brain volumetrics such as striatum volume that can serve as mediators of age-related declines in multiple domains of cognition such as processing speed and executive function (Hedden et al., 2014). Beyond these physiological factors, it is also possible that psychological factors such as increased stress may contribute to atherosclerotic burden by increasing intima thickness (Roepke at al., 2012), and work in conjunction with other biomarkers to amplify the adverse effects on cognition during the aging process. Given that in the current study, our primary goal was to demonstrate the role of optical measure of arterial compliance in the cerebrovascular pathway of cognitive decline, we did not further explore the relative contribution of different mediators. This was also partially constrained by our relatively small sample size which limits the statistical power available to explore more complex models with confidence.

Our regional analysis of arterial compliance with total WMSA volume also revealed that the strongest negative correlations were found in frontal regions, and were especially prominent in older adults. These findings parallel known regional variations in brain and cognitive degeneration (e.g. Raz et

al., 2003; Tan et al., *under review,* Chapter 3). Further, differences in the rate of cerebral atrophy in different neurodegenerative pathologies have been found and may reflect differences in underlying dysfunctions in cerebral protein biochemistry (Whitwell et al., 2007). In a similar vein, regional variations in associations between arterial compliance and WMSAs may also offer important information for distinguishing between different pathologies such as vascular dementia compared to frontotemporal dementia.

However, the interpretation of these findings must be couched in the inherent limitation of relatively short penetration distance of diffusive optical imaging, and hence, the regions where these measurements are taken do not map directly onto each other. Despite this shortcoming, the measurements used in the current study leverages on recent advancements in 3D reconstructions that has pushed the penetration distance to 30-35mm (Chiarelli et al., 2016) which provides the best estimation of arterial compliance possible given the current state of the technology. Regardless, our measurement of global arterial compliance should only be regarded an indicator of cerebrovascular health and does not provide us with sufficient penetration or spatial resolution to distinguish with specificity the cerebral arterial supply that feeds into specific focal or diffused WMSA seen on T1-images. Similar caveats must be considered when interpreting the arterial compliance and WMSA volume associations with white matter microstructural properties in the fornix. Although newer dynamic ASL methods of quantifying vascular compliance based on changes in cerebral blood volume and arterial pressure can be extracted from deep structures (Yan et al., 2016), they also suffer from lack of spatial resolution. Further, diffusive optical methods of quantifying arterial compliance and its association with a host of factors such as age, fitness, brain volume have been replicated (Fabiani et al., 2014, Tan et al; *under review,* chapter 3) and found to be robust. Whether dynamic ASL methods can serve as a mediator of age-related declines in cognition remains to be tested.

Other methodological considerations include findings that most WMSA tend to emerge only in older adults (Debette & Markus, 2010). Our current sample consisted of subjects over a large lifespan range of age 18-75 and WMSA volume observed in younger subjects are most likely inherited due to genetic deficiencies as opposed to acquired (Schiffmann & van der Knaap, 2009). Greater amount of periventricular white matter (PVWM) hyperintensities have also been found to be associated with shorter gestational age at birth (Panigraphy, 2001). Although the relative contribution of inherited compared to acquired WMSA on the effects we see here are unknown due to the cross-sectional nature of the current study, the mediation analysis remains significant (95% CI, -.6286, -.0022) even after selecting only subjects above the age of 40, paralleling the lower age limit used in the population described in Leritz et al., (2014). Taken together, our results suggest that arterial compliance and T1-weighted measures of WMSAs sequentially mediates the relationship between age and fluid IQ. Although the usage of T1-weighted WMSA as an index of white matter lesion has already been used in a number of studies to investigate its association with aging (Leritz et al., 2014; Marquez et al., 2015; Salat et al., 2010), whether these effects will be seen when using more commonly used T2-weight images should be further explored.

The current study also opens up the possibility of using arterial compliance as a target for intervention. Although vascular risk factors accumulate from a young age, they are amenable to changes by increasing physical activity (Hawkins et al., 2014). A recent review of studies investigating the association between white matter lesions and physical activity concluded that greater physical activity was associated with lower amount of lesions, but only in individuals without advanced disease (Torres et al., 2015). Given that the sequential multiple mediation analysis described in the current study suggest that WMSAs are secondary to reductions in arterial compliance, the early targeting of improving arterial compliance may slow or prevent progressive cerebral small vessel disease (SVD) from manifesting as WMSAs. This preventive approach is especially important given the general consensus that lesions in the

white matter are non-reversible, although revascularization surgery may help (Komatsu et al., 2016). Therefore, compared to using WMSAs as an indirect marker of cerebral SVD severity (Sachdev, Wen, Chen & Brodaty, 2007), arterial compliance may be a better alternative due to its precedence in the vascular pathway to AD. Further, of particular interest is the role of vascular endothelial derived growth factor (VEGF) involved in many of the neural benefits that comes with higher cardiorespiratory fitness (Cotman, Berchtold, & Christie, 2007; Voss, Vivar, Kramer, & van Praag, 2013). Intervention studies in the future can further clarify the role of increasing cardiorespiratory fitness and its associated cascade of neurotropic factor modulation in the cerebrovascular pathway in cognitive aging. In addition, the beneficial effects of increasing physical activity may be in part moderated by genetic factors (Bouchard, Rankinen & Timmons; 2011) and the extent by which genetic factors affects the modifiability of cerebral compliance remains to be investigated.

The results shown here is the first study demonstrating that cerebral arterial compliance measured using diffusive optical methods is predictive of total WMSA volume and that it mediates age-related declines in fluid IQ. It adds onto the growing literature that measures of cerebrovascular health using optical methods are associated with multiple measures of brain and cognitive aging. It is clear that the cerebrovascular pathway involved in age-related cognitive decline shown in the current study is but one of the many mediators and future large scale studies involving multiple measures of brain health such as measurements of CBF using ASL, glucose metabolism using PET, genetic assays and fitness intervention studies are required to distinguish the different contributors and pathways by which cognitive decline occur in the aging process.

References

Alosco, M. L., Gunstad, J., Jerskey, B. A., Xu, X., Clark, U. S., Hassenstab, J., … Sweet, L. H. (2013). The adverse effects of reduced cerebral perfusion on cognition and brain structure in older adults with cardiovascular disease. *Brain and Behavior, 3*(6), 626–636. http://doi.org/10.1002/brb3.171

Atwood, L. D., Wolf, P. A., Heard-Costa, N. L., Massaro, J. M., Beiser, A., D'Agostino, R. B., & DeCarli, C. (2004). Genetic variation in white matter hyperintensity volume in the Framingham Study. *Stroke; a Journal of Cerebral Circulation, 35*(7), 1609–1613. http://doi.org/10.1161/01.STR.0000129643.77045.10

Bagnato, F., Salman, Z., Kane, R., Auh, S., Cantor, F. K., Ehrmantraut, M., … McFarland, H. F. (2010). T1 cortical hypointensities and their association with cognitive disability in multiple sclerosis. *Multiple Sclerosis, 16*(10), 1203–1212. http://doi.org/10.1177/1352458510377223

Beck, A. T., Steer, R. A., & Brown, G. K. (1996). *Manual for the Beck Depression Inventory (2nd ed.).* San Antonio, TX: The Psychological Corporation.

Benedict, R. H. B., Weinstock-Guttman, B., Fishman, I., Sharma, J., Tjoa, C. W., & Bakshi, R. (2004). Prediction of neuropsychological impairment in multiple sclerosis: comparison of conventional magnetic resonance imaging measures of atrophy and lesion burden. *Archives of Neurology, 61*(2), 226–230. http://doi.org/10.1001/archneur.61.2.226

Bennett, I. J., & Madden, D. J. (2014). Disconnected aging: cerebral white matter integrity and age-related differences in cognition. *Neuroscience, 276*, 187–205. http://doi.org/10.1016/j.neuroscience.2013.11.026

Bouchard, C., Rankinen, T., & Timmons, J. A. (2011). Genomics and genetics in the biology of adaptation to exercise. *Comprehensive Physiology, 1*(3), 1603–1648. http://doi.org/10.1002/cphy.c100059

Brickman, A. M., Siedlecki, K. L., Muraskin, J., Manly, J. J., Luchsinger, J. A., Yeung, L.-K., … Stern, Y. (2011). White matter hyperintensities and cognition: testing the reserve hypothesis. *Neurobiology of Aging, 32*(9), 1588–1598. http://doi.org/10.1016/j.neurobiolaging.2009.10.013

Brickman, A. M., Zahra, A., Muraskin, J., Steffener, J., Holland, C. M., Habeck, C., … Stern, Y. (2009). Reduction in cerebral blood flow in areas appearing as white matter hyperintensities on magnetic resonance imaging. *Psychiatry Research, 172*(2), 117–120. http://doi.org/10.1016/j.pscychresns.2008.11.006

Burzynska, A. Z., Garrett, D. D., Preuschhof, C., Nagel, I. E., Li, S.-C., Bäckman, L., … Lindenberger, U. (2013). A scaffold for efficiency in the human brain. *The Journal of Neuroscience: The Official Journal of the Society for Neuroscience, 33(*43), 17150–17159. http://doi.org/10.1523/JNEUROSCI.1426-13.2013

Burzynska, A. Z., Preuschhof, C., Bäckman, L., Nyberg, L., Li, S.-C., Lindenberger, U., & Heekeren, H. R. (2010). Age-related differences in white matter microstructure: region-specific patterns of diffusivity. *NeuroImage, 49*(3), 2104–2112. http://doi.org/10.1016/j.neuroimage.2009.09.041

Chiarelli, A. M., Maclin, E. L., Low, K. A., Fabiani, M., & Gratton, G. (2015). Comparison of procedures for co-registering scalp-recording locations to anatomical magnetic resonance images. *Journal of Biomedical Optics, 20*(1), 16009. http://doi.org/10.1117/1.JBO.20.1.016009

Chiarelli, A. M., Maclin, E. L., Low, K. A., Mathewson, K. E., Fabiani, M., & Gratton, G. (2016). Combining energy and Laplacian regularization to accurately retrieve the depth of brain activity of diffuse optical tomographic data. *Journal of Biomedical Optics, 21*(3), 36008. http://doi.org/10.1117/1.JBO.21.3.036008

Cook, I. A., Leuchter, A. F., Morgan, M. L., Dunkin, J. J., Witte, E., David, S., … Rosenberg, S. (2004). Longitudinal progression of subclinical structural brain disease in normal aging. *The American*

Journal of Geriatric Psychiatry: Official Journal of the American Association for Geriatric Psychiatry, 12(2), 190–200.

Corrigan, J. D., & Hinkeldey, N. S. (1987). Relationships between parts A and B of the Trail Making Test. *Journal of Clinical Psychology, 43*(4), 402–409.

Cotman, C. W., Berchtold, N. C., & Christie, L.-A. (2007). Exercise builds brain health: key roles of growth factor cascades and inflammation. *Trends in Neurosciences, 30*(9), 464–472. http://doi.org/10.1016/j.tins.2007.06.011

Dale, A. M., Fischl, B., & Sereno, M. I. (1999). Cortical surface-based analysis. I. Segmentation and surface reconstruction. *NeuroImage, 9*(2), 179–194. http://doi.org/10.1006/nimg.1998.0395

Debette, S., & Markus, H. S. (2010). The clinical importance of white matter hyperintensities on brain magnetic resonance imaging: systematic review and meta-analysis. *BMJ (Clinical Research Ed.), 341*, c3666.

Dehghani, H., White, B. R., Zeff, B. W., Tizzard, A., & Culver, J. P. (2009). Depth sensitivity and image reconstruction analysis of dense imaging arrays for mapping brain function with diffuse optical tomography. *Applied Optics, 48*(10), D137-143.

Delorme, A., & Makeig, S. (2004). EEGLAB: an open source toolbox for analysis of single-trial EEG dynamics including independent component analysis. *Journal of Neuroscience Methods, 134*(1), 9–21. http://doi.org/10.1016/j.jneumeth.2003.10.009

Douaud, G., Menke, R. A. L., Gass, A., Monsch, A. U., Rao, A., Whitcher, B., … Smith, S. (2013). Brain microstructure reveals early abnormalities more than two years prior to clinical progression from mild cognitive impairment to Alzheimer's disease. *The Journal of Neuroscience: The Official Journal of the Society for Neuroscience, 33*(5), 2147–2155. http://doi.org/10.1523/JNEUROSCI.4437-12.2013

Eggebrecht, A. T., Ferradal, S. L., Robichaux-Viehoever, A., Hassanpour, M. S., Dehghani, H., Snyder, A. Z., … Culver, J. P. (2014). Mapping distributed brain function and networks with diffuse optical tomography. *Nature Photonics, 8*(6), 448–454. http://doi.org/10.1038/nphoton.2014.107

Fabiani, M., Low, K. A., Tan, C.-H., Zimmerman, B., Fletcher, M. A., Schneider-Garces, N., … Gratton, G. (2014). Taking the pulse of aging: mapping pulse pressure and elasticity in cerebral arteries with optical methods. *Psychophysiology, 51*(11), 1072–1088. http://doi.org/10.1111/psyp.12288

Fang, Q., & Boas, D. A. (2009). Monte Carlo simulation of photon migration in 3D turbid media accelerated by graphics processing units. *Optics Express, 17*(22), 20178–20190.

Fazekas, F., Offenbacher, H., Fuchs, S., Schmidt, R., Niederkorn, K., Horner, S., & Lechner, H. (1988). Criteria for an increased specificity of MRI interpretation in elderly subjects with suspected multiple sclerosis. *Neurology, 38*(12), 1822–1825.

Fischl, B., & Dale, A. M. (2000). Measuring the thickness of the human cerebral cortex from magnetic resonance images. *Proceedings of the National Academy of Sciences of the United States of America, 97*(20), 11050–11055. http://doi.org/10.1073/pnas.200033797

Fischl, B., Liu, A., & Dale, A. M. (2001). Automated manifold surgery: constructing geometrically accurate and topologically correct models of the human cerebral cortex*. IEEE Transactions on Medical Imaging, 20*(1), 70–80. http://doi.org/10.1109/42.906426

Fischl, B., Salat, D. H., Busa, E., Albert, M., Dieterich, M., Haselgrove, C., … Dale, A. M. (2002). Whole brain segmentation: automated labeling of neuroanatomical structures in the human brain. *Neuron, 33*(3), 341–355.

Friston, K.J., Holmes, A.P., Worsley, K.J., Poline, J.P., Frith, C.D., Frackowiak, R.S.J. (1994) Statistical parametric maps in functional imaging: A general linear approach. *Human Brain Mapping, 2*:189-210.

Han, X., Jovicich, J., Salat, D., van der Kouwe, A., Quinn, B., Czanner, S., … Fischl, B. (2006). Reliability of MRI-derived measurements of human cerebral cortical thickness: the effects of field strength, scanner upgrade and manufacturer. *NeuroImage, 32*(1), 180–194. http://doi.org/10.1016/j.neuroimage.2006.02.051

Hatazawa, J., Shimosegawa, E., Satoh, T., Toyoshima, H., & Okudera, T. (1997). Subcortical hypoperfusion associated with asymptomatic white matter lesions on magnetic resonance imaging. *Stroke; a Journal of Cerebral Circulation, 28*(10), 1944–1947.

Hawkins, M., Gabriel, K. P., Cooper, J., Storti, K. L., Sutton-Tyrrell, K., & Kriska, A. (2014). The impact of change in physical activity on change in arterial stiffness in overweight or obese sedentary young adults. *Vascular Medicine, 19*(4), 257–263. http://doi.org/10.1177/1358863X14536630

Hayes, A. F. (2013). *An introduction to mediation, moderation, and conditional process analysis: A regression-based approach*. New York, NY: Guilford Press.

Hayes, A. F., & Scharkow, M. (2013). The relative trustworthiness of inferential tests of the indirect effect in statistical mediation analysis: does method really matter? *Psychological Science, 24*(10), 1918–1927. http://doi.org/10.1177/0956797613480187

Heaton, R. K. (1981). *Wisconsin card sorting test manual*, Odessa, FL: Psychological Assessment Resources, Inc.

Hedden, T., Schultz, A. P., Rieckmann, A., Mormino, E. C., Johnson, K. A., Sperling, R. A., & Buckner, R. L. (2014). Multiple Brain Markers are Linked to Age-Related Variation in Cognition. Cerebral *Cortex, 238*. http://doi.org/10.1093/cercor/bhu238

Ihara, M., Polvikoski, T. M., Hall, R., Slade, J. Y., Perry, R. H., Oakley, A. E., … Kalaria, R. N. (2010). Quantification of myelin loss in frontal lobe white matter in vascular dementia, Alzheimer's disease, and dementia with Lewy bodies. *Acta Neuropathologica, 119*(5), 579–589. http://doi.org/10.1007/s00401-009-0635-8

Ishimaru, A. (1989). Diffusion of light in turbid material. *Applied Optics, 28*(12), 2210–2215.

Jefferson, A. L., Tate, D. F., Poppas, A., Brickman, A. M., Paul, R. H., Gunstad, J., & Cohen, R. A. (2007). Lower cardiac output is associated with greater white matter hyperintensities in older adults with cardiovascular disease. *Journal of the American Geriatrics Society, 55*(7), 1044–1048. http://doi.org/10.1111/j.1532-5415.2007.01226.x

Jones, D. K., Knösche, T. R., & Turner, R. (2013). White matter integrity, fiber count, and other fallacies: the do's and don'ts of diffusion MRI. *NeuroImage, 73,* 239–254. http://doi.org/10.1016/j.neuroimage.2012.06.081

Kalaria, R. N., & Ihara, M. (2013). Dementia: Vascular and neurodegenerative pathways-will they meet? Nature Reviews. *Neurology, 9*(9), 487–488. http://doi.org/10.1038/nrneurol.2013.164

Kaufman, A. S., & Kaufman, N. L. (2004). *Kaufman brief intelligence test (2nd ed.).* San Antonio, TX: The Psychological Corporation.

Kennedy, K. M., & Raz, N. (2009). Aging White Matter and Cognition: Differential Effects of Regional Variations in Diffusion Properties on Memory, Executive Functions, and Speed. *Neuropsychologia, 47*(3), 916–927. http://doi.org/10.1016/j.neuropsychologia.2009.01.001

Komatsu, K., Mikami, T., Noshiro, S., Miyata, K., Wanibuchi, M., & Mikuni, N. (2016). Reversibility of White Matter Hyperintensity by Revascularization Surgery in Moyamoya Disease. *Journal of Stroke and Cerebrovascular Diseases, 25*(6), 1495–1502. http://doi.org/10.1016/j.jstrokecerebrovasdis.2016.02.035

Kramer, J. H., Mungas, D., Reed, B. R., Wetzel, M. E., Burnett, M. M., Miller, B. L., … Chui, H. C. (2007). Longitudinal MRI and cognitive change in healthy elderly. *Neuropsychology, 21*(4), 412–418. http://doi.org/10.1037/0894-4105.21.4.412

Kuperberg, G. R., Broome, M. R., McGuire, P. K., David, A. S., Eddy, M., Ozawa, F., … Fischl, B. (2003). Regionally localized thinning of the cerebral cortex in schizophrenia. *Archives of General Psychiatry, 60*(9), 878–888. http://doi.org/10.1001/archpsyc.60.9.878

Leritz, E. C., Shepel, J., Williams, V. J., Lipsitz, L. A., McGlinchey, R. E., Milberg, W. P., & Salat, D. H. (2014). Associations between T1 white matter lesion volume and regional white matter microstructure in aging. *Human Brain Mapping, 35*(3), 1085–1100. http://doi.org/10.1002/hbm.22236

Marques, P. C. G., Soares, J. M. M., Magalhães, R. J. da S., Santos, N. C., & Sousa, N. J. C. (2016). Macro- and micro-structural white matter differences correlate with cognitive performance in healthy aging. *Brain Imaging and Behavior, 10*(1), 168–181. http://doi.org/10.1007/s11682-015-9378-4

Marstrand, J. R., Garde, E., Rostrup, E., Ring, P., Rosenbaum, S., Mortensen, E. L., & Larsson, H. B. W. (2002). Cerebral perfusion and cerebrovascular reactivity are reduced in white matter hyperintensities. *Stroke; a Journal of Cerebral Circulation, 33*(4), 972–976.

Mayeux, R., Stern, Y., Rosen, J., & Leventhal, J. (1981). Depression, intellectual impairment, and Parkinson disease. *Neurology, 31*(6), 645–650.

Miller, D. H., Grossman, R. I., Reingold, S. C., & McFarland, H. F. (1998). The role of magnetic resonance techniques in understanding and managing multiple sclerosis. *Brain: A Journal of Neurology, 121* (Pt 1), 3–24.

Mori S, Wakana S, Nagae-Poetscher LM, van Zijl PCM (2005) *MRI atlas of human white matter.* Amsterdam: Elsevier Science.

Nowrangi, M. A., & Rosenberg, P. B. (2015). The fornix in mild cognitive impairment and Alzheimer's disease. *Frontiers in Aging Neuroscience, 7*, 1. http://doi.org/10.3389/fnagi.2015.00001

Oldfield, R. C. (1971). The assessment and analysis of handedness: the Edinburgh inventory. *Neuropsychologia, 9*(1), 97–113.

Panigrahy, A., Barnes, P. D., Robertson, R. L., Back, S. A., Sleeper, L. A., Sayre, J. W., … Volpe, J. J. (2001). Volumetric brain differences in children with periventricular T2-signal hyperintensities: a grouping by gestational age at birth. *AJR. American Journal of Roentgenology, 177(*3), 695–702. http://doi.org/10.2214/ajr.177.3.1770695

Pantoni, L., & Simoni, M. (2003). Pathophysiology of cerebral small vessels in vascular cognitive impairment*. International Psychogeriatrics / IPA, 15* Suppl 1, 59–65. http://doi.org/10.1017/S1041610203008974

Park, D. C., & Reuter-Lorenz, P. (2009). The adaptive brain: aging and neurocognitive scaffolding. *Annual Review of Psychology, 60,* 173–196. http://doi.org/10.1146/annurev.psych.59.103006.093656

Paulsen, K. D., & Jiang, H. (1995). Spatially varying optical property reconstruction using a finite element diffusion equation approximation*. Medical Physics, 22*(6), 691–701. http://doi.org/10.1118/1.597488

Penny, W.D., Friston, K.J., Ashburner, J.T., Kiebel, S.J., Nichols, T.E. (2011) *Statistical parametric mapping: the analysis of functional brain images: the analysis of functional brain images.* Academic press.

Prins, N. D., & Scheltens, P. (2013). Treating Alzheimer's disease with monoclonal antibodies: current status and outlook for the future. *Alzheimer's Research & Therapy, 5*(6), 56. http://doi.org/10.1186/alzrt220

Raven, J., Raven, J.C., & Court, J.H. (2003) *Manual for Raven's Progressive Matrices and Vocabulary Scales*. San Antonio, TX: Harcourt Assessment.

Raz, N., Gunning, F. M., Head, D., Dupuis, J. H., McQuain, J., Briggs, S. D., … Acker, J. D. (1997). Selective aging of the human cerebral cortex observed in vivo: differential vulnerability of the prefrontal gray matter. Cerebral Cortex, 7(3), 268–282.

Raz, N., Rodrigue, K. M., Kennedy, K. M., & Acker, J. D. (2007). Vascular health and longitudinal changes in brain and cognition in middle-aged and older adults. *Neuropsychology, 21*(2), 149–157. http://doi.org/10.1037/0894-4105.21.2.149

Resnick, S. M., Pham, D. L., Kraut, M. A., Zonderman, A. B., & Davatzikos, C. (2003). Longitudinal magnetic resonance imaging studies of older adults: a shrinking brain. The Journal of Neuroscience, 23(8), 3295–3301.

Rosas, H. D., Liu, A. K., Hersch, S., Glessner, M., Ferrante, R. J., Salat, D. H., … Fischl, B. (2002). Regional and progressive thinning of the cortical ribbon in Huntington's disease. *Neurology, 58*(5), 695–701.

Rovaris, M., Comi, G., Rocca, M. A., Cercignani, M., Colombo, B., Santuccio, G., & Filippi, M. (1999). Relevance of hypointense lesions on fast fluid-attenuated inversion recovery MR images as a marker of disease severity in cases of multiple sclerosis. *AJNR. American Journal of Neuroradiology, 20*(5), 813–820.

Sachdev, P., Wen, W., Chen, X., & Brodaty, H. (2007). Progression of white matter hyperintensities in elderly individuals over 3 years. *Neurology, 68*(3), 214–222. http://doi.org/10.1212/01.wnl.0000251302.55202.73

Sailer, M., Losseff, N. A., Wang, L., Gawne-Cain, M. L., Thompson, A. J., & Miller, D. H. (2001). T1 lesion load and cerebral atrophy as a marker for clinical progression in patients with multiple sclerosis. A prospective 18 months follow-up study. *European Journal of Neurology, 8*(1), 37–42.

Salat, D. H. (2014). Imaging small vessel-associated white matter changes in aging. *Neuroscience, 276,* 174–186. http://doi.org/10.1016/j.neuroscience.2013.11.041

Salat, D. H., Tuch, D. S., van der Kouwe, A. J. W., Greve, D. N., Pappu, V., Lee, S. Y., … Rosas, H. D. (2010). White matter pathology isolates the hippocampal formation in Alzheimer's disease. *Neurobiology of Aging, 31*(2), 244–256. http://doi.org/10.1016/j.neurobiolaging.2008.03.013

Salat, D. H., Williams, V. J., Leritz, E. C., Schnyer, D. M., Rudolph, J. L., Lipsitz, L. A., … Milberg, W. P. (2012). Inter-individual variation in blood pressure is associated with regional white matter integrity in generally healthy older adults. *NeuroImage, 59*(1), 181–192. http://doi.org/10.1016/j.neuroimage.2011.07.033

Salthouse, T. A. (2010). Selective review of cognitive aging. *Journal of the International Neuropsychological Society : JINS, 16*(5), 754–760. http://doi.org/10.1017/S1355617710000706

Schiffmann, R., & van der Knaap, M. S. (2009). Invited Article: An MRI-based approach to the diagnosis of white matter disorders. *Neurology, 72*(8), 750–759. http://doi.org/10.1212/01.wnl.0000343049.00540.c8

Shipley, W. C. (1940). A self-administering scale for measuring intellectual impairment and deterioration. *Journal of Psychology, 9*, 371–377.

Simon, J. H., Lull, J., Jacobs, L. D., Rudick, R. A., Cookfair, D. L., Herndon, R. M., … Munschauer, F. E. (2000). A longitudinal study of T1 hypointense lesions in relapsing MS: MSCRG trial of interferon beta-1a. Multiple Sclerosis Collaborative Research Group. *Neurology, 55*(2), 185–192.

Smith, E. E., Salat, D. H., Jeng, J., McCreary, C. R., Fischl, B., Schmahmann, J. D., … Greenberg, S. M. (2011). Correlations between MRI white matter lesion location and executive function and episodic memory. *Neurology, 76*(17), 1492–1499. http://doi.org/10.1212/WNL.0b013e318217e7c8

Smith, S. M., Jenkinson, M., Johansen-Berg, H., Rueckert, D., Nichols, T. E., Mackay, C. E., … Behrens, T. E. J. (2006). Tract-based spatial statistics: voxelwise analysis of multi-subject diffusion data. *NeuroImage, 31*(4), 1487–1505. http://doi.org/10.1016/j.neuroimage.2006.02.024

Stebbins, G. T., & Murphy, C. M. (2009). Diffusion tensor imaging in Alzheimer's disease and mild cognitive impairment. *Behavioural Neurology, 21*(1), 39–49. http://doi.org/10.3233/BEN-2009-0234

Tian, F., & Liu, H. (2014). Depth-compensated diffuse optical tomography enhanced by general linear model analysis and an anatomical atlas of human head. *NeuroImage, 85* Pt 1, 166–180. http://doi.org/10.1016/j.neuroimage.2013.07.016

Tien, A.Y., Spevack, T. V., Jones, D.W., Pearlson, G. D., Schlaepfer, T. E., & Strauss, M. E. (1996). Computerized Wisconsin card sorting test: Comparison with manual administration. *Journal of Medical Sciences, 12*, 479–485.

Unsworth, N., Heitz, R. P., Schrock, J. C., & Engle, R. W. (2005). An automated version of the operation span task. *Behavior Research Methods, 37*(3), 498–505.

van Bruggen, T., Stieltjes, B., Thomann, P. A., Parzer, P., Meinzer, H.-P., & Fritzsche, K. H. (2012). Do Alzheimer-specific microstructural changes in mild cognitive impairment predict conversion? *Psychiatry Research, 203*(2–3), 184–193. http://doi.org/10.1016/j.pscychresns.2011.12.003

Voss, M. W., Vivar, C., Kramer, A. F., & van Praag, H. (2013). Bridging animal and human models of exercise-induced brain plasticity. *Trends in Cognitive Sciences, 17*(10), 525–544. http://doi.org/10.1016/j.tics.2013.08.001

Wardlaw, J. M., Valdés Hernández, M. C., & Muñoz-Maniega, S. (2015). What are White Matter Hyperintensities Made of? *Journal of the American Heart Association: Cardiovascular and Cerebrovascular Disease, 4*(6). http://doi.org/10.1161/JAHA.114.001140

Wechsler D. (2009) *Wechsler Memory Scale–Fourth Edition.* Pearson; San Antonio, TX.

Whalen, C., Maclin, E. L., Fabiani, M., & Gratton, G. (2008). Validation of a method for coregistering scalp recording locations with 3D structural MR images. *Human Brain Mapping, 29*(11), 1288–1301. http://doi.org/10.1002/hbm.20465

Whitwell, J. L., Jack, C. R., Parisi, J. E., Knopman, D. S., Boeve, B. F., Petersen, R. C., … Josephs, K. A. (2007). Rates of cerebral atrophy differ in different degenerative pathologies. *Brain: A Journal of Neurology, 130*(Pt 4), 1148–1158. http://doi.org/10.1093/brain/awm021

Xiong, Y. Y., & Mok, V. (2011). Age-Related White Matter Changes. *Journal of Aging Research,* http://doi.org/10.4061/2011/617927

Yan, L., Liu, C. Y., Smith, R. X., Jog, M., Langham, M., Krasileva, K., … Wang, D. J. J. (2016). Assessing intracranial vascular compliance using dynamic arterial spin labeling. *NeuroImage, 124(*Pt A), 433–441. http://doi.org/10.1016/j.neuroimage.2015.09.008

CHAPTER 5

GENERAL CONCLUSIONS

"A brain is as old as its arteries."
Chin Hong Tan, Ph.D.

The series of studies described in this thesis highlights the potential of using recently developed diffuse optical imaging methods to quantify indices associated with cerebrovascular health in the context of cognitive and brain aging. Although the cerebral pulse obtained from diffuse optical imaging was once regarded as an artifact that must be eliminated when measuring hemodynamic measures of brain function (Gratton & Corballis, 1995), it is now clear that these pulsatile parameters contain valuable information about the state of the cerebrovasculature. These findings were first reported by Fabiani et al. (2014). The results reported in this thesis represent incremental evidence demonstrating the robustness of the initial findings, and also provide a glimpse into the wide array of studies that can be investigated using these parameters.

Specifically, in Chapter 2, we employed two well-studied paradigms to investigate changes in cerebral pulse pressure in a physiological and cognitive task. We demonstrated that cerebrovascular tone changes in the hypothesized direction as a function of vagal response during breath holding and also as a function of cognitive load during a Sternberg task. In addition, we showed that greater cerebrovascular reactivity derived from pulse amplitude measures was associated with younger age and better cognitive function as measured by the mMMSE. Given the novelty of these cerebrovascular measures, in Chapter 3 we replicated our initial findings, originally obtained in middle-aged and older adults (Fabiani et al., 2014) to a new sample including people spanning much of the adult lifespan (from 18-75 years). Further, we also demonstrated that both the pulse amplitude and arterial compliance measures are highly reliable, by comparing these measures across experimental blocks. We also showed that associations with age, CRF, brain volumes and cognitive function are generally robust across these

two studies. New regional analyses of arterial compliance also suggest that, similar to many other indices of brain aging, arterial compliance in frontal regions appears to be especially vulnerable to the effects of aging and cognitive decline while that in visual cortex is relatively spared.

Much of the initial work described in Chapters 2 and 3 has focused on demonstrating the validity and reliability of these measures of cerebrovascular health using well-established paradigms (e.g. breath-holding task, Sternberg memory task). Moving forward, the aim would be to go beyond looking at simple associations of these cerebrovascular measures with other indices of brain health, and to further elucidate their role as mediators or moderators in the complex cascade of events that result in age-related cognitive decline.

Given this aim, In Chapter 4, we found evidence that arterial compliance predicts variance in WMSAs over and above age and systemic pulse pressure. Further, arterial compliance serves as a mediator in age-related cognitive decline associated with cerebrovascular small vessel disease in the white matter. Importantly, this mediation analysis was not significant when substituting WMSAs for global measures of FA and MD. This is in accordance to prevailing theories that that are two independent pathways (vascular and neurodegenerative) leading to age-related cognitive decline in AD (Kalaria et al., 2013). Preliminary findings suggesting that these two pathways may converge first in the fornix deserves further investigation in the future. It is also clear that given that DTI measures tap mostly on NAWM, they may not be as indicative or predictive of future degradation in cognitive function during the aging process. Information from other imaging modalities such as amyloid and tau positron emission imaging (PET) can provide a better picture of the mediators involves in the neurodegenerative pathway seen in clinical manifestations of AD.

From a preventive perspective towards mitigating the adverse effects seen in age-related cognitive decline, it is of paramount importance to identify and target early markers of future neural and

vascular degeneration before the progression of disease reaches a state of no return. de la Torre (2000) proposed the critically attained threshold of cerebral hypoperfusion (CATCH) theory, suggesting that once cerebrovascular degeneration advances in severity past a certain threshold, it will result in a cascade of events that eventually cumulates in the expression of neurodegeneration symptoms seen in AD. Insofar as the theory is correct, measures of cerebrovascular health derived using diffusive optical imaging may provide early warning signals and act as a call for intervention before the threshold of cerebral hypoperfusion is reached.

However, as mentioned throughout the series of studies presented in this thesis, the use of diffuse optical imaging to quantify cerebrovascular health is not without its shortcomings. Notably, the relative short penetration into the brain limits the interrogation of cerebral arterial health to cortical areas. It is clear that although the technique provides valuable information with regards to signals arising from cortical cerebral arteries, it would be best used in conjunction with other imaging modalities such as ASL, TCD in order to derive a more complete picture of the underlying cerebrovascular system. That is to say, the data presented here do not imply that diffuse optical imaging of cerebrovascular health aims to supplant other imaging modalities, but to provide converging evidence on the importance of cerebrovascular health in ameliorating age-related cognitive decline. Another caveat that must be noted is that these studies were conducted in normal aging populations. Although the cerebrovascular antecedents to cognitive decline may be similar and deferring only in severity in normal aging populations compared to clinical populations, only longitudinal studies investigating the onset of MCI and subsequent conversion to AD can provide a definitive answer to whether they may differ in the early stages of subclinical cognitive decline.

In summary, the cumulative evidence presented in the thesis points to the immense utility in extracting indices of cerebrovascular health with diffusive optical imaging to understand the

cerebrovascular pathway age-related cognitive decline. In conjunction with a plurality of imaging modalities, we may be able to truly understand the interactions between different pathways to AD.

References

de la Torre JC (2000) Critically attained threshold of cerebral hypoperfusion (CATCH): Can it cause Alzheimer's disease? *Ann NY Acad Sci 903*, 424-436.

Fabiani, M., Low, K. A., Tan, C.-H., Zimmerman, B., Fletcher, M. A., Schneider-Garces, N., … Gratton, G. (2014). Taking the pulse of aging: mapping pulse pressure and elasticity in cerebral arteries with optical methods. *Psychophysiology, 51*(11), 1072–1088. http://doi.org/10.1111/psyp.12288

Gratton, G., & Corballis, P. M. (1995). Removing the heart from the brain: Compensation for the pulse artifact in the photon migration signal. *Psychophysiology*, *32*, 292–299. doi: 10.1111/j.1469-8986.1995.tb02958.x

Kalaria, R. N., & Ihara, M. (2013). Dementia: Vascular and neurodegenerative pathways-will they meet? Nature Reviews. Neurology, 9(9), 487–488. http://doi.org/10.1038/nrneurol.2013.164